

**Integration of Ozone and Ultrasound Activated Sludge Pre-Treatments
into a Wastewater Treatment Whole-Plant Simulator**

by

Jonathan Musser

A thesis

presented to the University of Waterloo

in fulfillment of the

thesis requirement for the degree of

Master of Applied Science

in

Civil Engineering

Waterloo, Ontario, Canada, 2010

© Jonathan Musser 2010

AUTHOR'S DECLARATION FOR ELECTRONIC SUBMISSION OF A THESIS

I hereby declare that I am the sole author of this thesis. This is a true copy of the thesis, including any required final revisions, as accepted by my examiners.

I understand that my thesis may be made electronically available to the public.

Abstract

Modern wastewater treatment provides great benefit to society by reducing the transmission of disease. In recent years computer simulation of whole plants has allowed for improved design and more economical consideration of alternatives. One new alternative for wastewater treatment is the pre-treatment of sludges, although this technology has not yet been adapted for computer simulation. This thesis describes research which was conducted to describe pre-treatments in terms appropriate for whole-plant computer models.

Pre-treatment shows promise in terms of reducing sludge, a waste product the disposal of which can be costly depending on the applicable regulations. At the same time pre-treatment can improve the generation of biogas, which is readily converted to heat and/or electricity and can help to offset treatment energy requirements. Pre-treatments can be broadly categorized as physical, chemical, or thermal. For this study, ultrasound was selected as a model physical pre-treatment and ozone as a model chemical pre-treatment. The range of doses to be tested was obtained by reviewing earlier literature.

Waste activated sludge was obtained from pilot reactors treating screened municipal wastewater. This sludge was subjected to a range of doses in batch reactors. Conventional laboratory analyses were used to determine the effects of pre-treatment on such parameters as chemical oxidant demand, solids, and various nitrogen fractions. As well, respirometry was utilized to estimate the biologically active and bioavailable fractions. A novel technique for analysis of respirometric data was developed, which consisted of fitting synthetic oxygen uptake rate curves to the measured data.

Both ultrasound and ozone were observed to decrease the amount of active biomass present while increasing the amount of biodegradable material. The conversions between these fractions were modeled using simple functions of pre-treatment dose. For ultrasound, a conversion which exponentially decayed with respect to increasing ultrasound dose was used to relate these fractions. For ozone, the conversion from active biomass to slowly degradable material occurred more slowly than the conversion to rapidly degradable material; as such two conversions were modeled, each exponentially decaying with respect to dose but with different dose constants.

The observed conversions were added to a whole-plant model and the implications of the models were considered for one simple wastewater treatment plant. Both pre-treatments showed a decrease in total sludge production and an increase in biogas production, as predicted by earlier research. Published full-scale results were not reported with sufficient detail to be replicated, and so a quantitative comparison was not possible.

Acknowledgements

The research described in this paper would not have been possible without the financial support of the Natural Sciences and Engineering Research Council of Canada and the Ontario Centres of Excellence. Generous in-kind contributions from EnviroSim Associates facilitated certain key stages. The technical guidance of Dr. Wayne J. Parker was helpful throughout the project.

Table of Contents

List of Tables	vii
List of Figures	viii
1. Introduction.....	1
2. Earlier research	3
2.1. Waste Activated Sludge Pre-treatment.....	4
2.2. Sonication	5
2.2.1. Introduction.....	5
2.2.2. Mechanisms	5
2.2.3. Doses	6
2.2.4. Results	7
2.3. Ozonation	8
2.3.1. Introduction.....	8
2.3.2. Mechanisms	8
2.3.3. Doses	9
2.3.4. Results	10
2.4. Respirometry	11
3. Materials and methods	13
3.1. Activated Sludge Source: Pilot Sequencing Batch Reactors.....	13
3.2. Batch Pre-treatments	15
3.2.1. Ultrasound reactor	15
3.2.2. Ultrasound efficiency	16
3.2.3. Ozone reactor.....	16
3.3. Analytical Methods.....	19
4. Collection and Analysis of Respirometric data	21
4.1. Respirometer and test setups	21
4.2. Respirometric model	23
4.3. Examples.....	28
5. Sonication results.....	32
5.1. Sonication efficiency.....	33
5.2. COD and BOD responses	35
5.2.1. Total COD.....	36
5.2.2. Soluble COD.....	37
5.2.3. Colloidal COD.....	38
5.2.4. Particulate COD	40
5.2.5. Heterotrophic organisms	40
5.2.6. Slowly biodegradable COD	42

5.2.7. Readily biodegradable COD.....	43
5.3. Nitrogen responses.....	45
5.4. pH response.....	47
6. Ozonation results.....	48
6.1. Ozone transfer efficiency.....	49
6.2. COD and BOD responses	51
6.2.1. Total COD.....	51
6.2.2. Soluble and colloidal COD	52
6.2.3. Heterotrophic biomass.....	54
6.2.4. Biodegradable COD	55
6.3. Nitrogen responses.....	57
6.3.1. N ^{III-} : Ammonia and organic nitrogen	58
6.3.2. N ^{III+} : Nitrite.....	59
6.3.3. N ^{V+} : Nitrate	60
6.4. pH response.....	63
7. Whole-plant modeling approaches.....	64
7.1. BioWin Integration	67
7.2. Sonication modeling approach.....	68
7.3. Ozone modeling approach	70
7.4. Modeling approach comparison: physical vs. chemical pre-treatments	72
8. Whole-plant modeling results	73
8.1. Sonication results	73
8.2. Ozone results	79
8.3. Comparison of modeling results.....	81
9. Recommendations	82
References	84
Appendix A – BioWin Model	88
Appendix B – Standard Operating Procedures	89
Appendix C – Visual basic source code for interpretation of respirometry	99
Appendix D – Measured data.....	111

List of Tables

Table 2.1: Ultrasound doses reported by other researchers to degrade RAS/WAS.....	6
Table 2.2: Ozone doses reported by other researchers to degrade RAS/WAS	9
Table 3.1: Operational parameters for experimental SBRs	14
Table 4.1. Cell contents for respirometric tests.....	22
Table 4.2. Model employed for interpretation of respirometric data: stoichiometry and kinetics.....	24
Table 7.1. Model plant parameters.....	66
Table 7.2. Ultrasound conversion processes	70

List of Figures

Figure 2.1. Diagram showing interactions targeted in this reseach	3
Figure 3.1. Pilot sequencing batch reactors.....	13
Figure 3.2. Ultrasound apparatus.....	15
Figure 3.3. Ozone pre-treatment apparatus.....	18
Figure 4.1. Challenge Technology respirometer	22
Figure 4.2. COD fractions predicted by simplified ASM over time	25
Figure 4.3. Sample OUR curve using simplified ASM1	26
Figure 4.4. Dynamically dimensioned search algorithm [after <i>Tolson and Shoemaker, 2007</i>]	27
Figure 4.5. Example of decay-dominated respirometric response.....	28
Figure 4.6. Example of complex respirometric response (good fit).....	29
Figure 4.7. Example of complex respirometric response (poor fit)	30
Figure 4.8. Typical oxygen uptake curve following high ozone dose.....	31
Figure 5.1. Appearance of sample following sonication	32
Figure 5.2. Un-moderated temperature curves due to sonication.....	33
Figure 5.3. Sonication efficiency model results	35
Figure 5.4. Change in total COD during sonication	36
Figure 5.5. ffCOD fraction following pretreatment.....	37
Figure 5.6. Glass filtered fraction following pretreatment	39
Figure 5.7. Inactivation of heterotrophic organisms	41
Figure 5.8. Conversion of heterotrophs to degradable substrate	42
Figure 5.9. Formation of readily degradable substrate from heterotrophs and slowly degradable substrate	44
Figure 5.10. Change in total nitrogen during sonication	45
Figure 5.11. Change in organic nitrogen during ultrasound pre-treatment.....	46
Figure 5.12. Change in inorganic nitrogen species during ultrasound pre-treatment	46
Figure 5.13. pH effects of ultrasound pre-treatment	47
Figure 6.1. Illustration of the decrease in colour following ozonation.....	49
Figure 6.2. Ozone transfer efficiencies.....	50
Figure 6.3. Change in total COD following ozonation	51
Figure 6.4. Change in filtered COD following ozonation.....	53
Figure 6.5. Change in heterotroph concentrations as a function of ozone dose	54
Figure 6.6. Biodegradable substrate produced on inactivation of heterotrophs.....	55
Figure 6.7. Slowly and readily biodegradable COD released by ozonation with speculative trendlines	56
Figure 6.8. Change in total nitrogen during ozonation	58
Figure 6.9. Change in TKN and sTKN due to ozonation.....	59

Figure 6.10. Change in nitrite during ozonation	60
Figure 6.11. Nitrate & nitrite produced by ozonation	61
Figure 6.12. Ozone conversion model for nitrite and nitrate	61
Figure 6.13. Change in nitrate & nitrite relative to change in TKN	62
Figure 6.14. pH before and after ozonation.....	63
Figure 7.1. Wastewater fraction conversions for pre-treatment	65
Figure 7.2. Model plant for consideration of pre-treatment responses.....	66
Figure 7.3. Modeled fate of heterotrophs following sonication.....	69
Figure 7.4. Modeled fate of heterotrophs after ozonation	71
Figure 8.1. Model plant with ultrasound on return sludge line.....	73
Figure 8.2. Sludge production for various ultrasound doses with fixed SRT	74
Figure 8.3. Changes to MLVSS concentrations due to sonication of RAS	74
Figure 8.4. Digester gas production as a function of ultrasound dose	75
Figure 8.5. Sludge production for various ultrasound doses with fixed MLVSS	76
Figure 8.6. BioWin model for WAS pre-treatment with ultrasound.....	77
Figure 8.7. Sludge production for various WAS pre-treatment ultrasound doses	77
Figure 8.8. Gas production for various WAS pre-treatment ultrasound doses	78
Figure 8.9. Comparison of gas production for RAS vs. WAS pre-treatment.....	79
Figure 8.10. Sludge production for various WAS pre-treatment ozone doses	80
Figure 8.11. Gas production for various WAS pre-treatment ozone doses.....	80

1. Introduction

This project was conceived to connect two significant technologies: the modeling of wastewater treatment and the pre-treatment of wastewater sludges. The first, modeling of wastewater treatment, is widely used in the design of wastewater treatment facilities and is a key component of sanitation practices in the developed world. Modern sanitation practices greatly reduce the spread of communicable disease. The treatment of human waste can largely eliminate the fecal-oral pathway, lowering disease transmission rates dramatically. Along with purified water, this treatment produces sludge which has value as it may be used to produce biogas or as a fertilizer, but there are also difficulties such as ensuring sufficient pathogen inactivation. Other options for disposal are often expensive or otherwise undesirable.

Wastewater treatment is most often achieved using some type of activated sludge process, for which computer modeling has been increasingly seen as an essential design tool. In these processes, bacteria capable of metabolizing a wide variety of materials are retained in an engineered system and used to purify the waste stream. Since a large variety of configurations are possible, accurate modeling allows for a cost-effective evaluation of various options. The earliest model was simply called the Activated Sludge Model 1 (ASM1) and was proposed in 1987. This was followed by several more complex ASM models as well as the related Anaerobic Digestion Models (ADMs). A number of commercially-available whole-plant models are based on these, including GPS-X (Hydromantis, Ontario, Canada) and Pro2D (CH2M Hill, Colorado, USA). For this project, BioWin (EnviroSim, Ontario, Canada) was used.

Several relatively new processes had been proposed as enhancements of the activated sludge process but had not yet been modeled. They could be broadly categorized as thermal, chemical, mechanical, or biological, with some technologies falling under more than one category. To evaluate properly the potential benefits of these pre-treatments, the effects of pre-treatment needed to be expressed in terms of the parameters employed in whole-plant models.

This project aimed to develop a methodology for evaluating pre-treatments and modeling them. Ozonation was selected as a representative chemical technology and ultrasound as a physical one. At the time of this writing each of these technologies had a small number of full-scale installations as well as vendors actively promoting the technology. These pre-treatments had not previously been modeled, and so this project was intended to produce the simplest possible model which accurately reflected the pre-treatment effects. Published results were compared to the model results, but a complete validation of the model and assessment of the implications were beyond the scope of this project.

2. Earlier research

The primary waste product of modern activated sludge wastewater treatment is waste activated sludge (WAS). The cost to dispose of this sludge often represents half of the operating budget of wastewater treatment [Stensel and Strand, 2004] or even more [Paul et al., 2006]. To reduce and/or offset the cost of disposal, research has been conducted into pre-treatment processes. This research has focused on processes that reduce the quantity of WAS, either directly or by increasing the degradability of WAS so that downstream processes can reduce the quantity. At the same time, these technologies had variously claimed to improve settling, dewaterability, and biogas production. Figure 2.1 shows, in very general terms, an activated sludge process with some important inputs and outputs in black, the addition of a pre-treatment process in blue, and the poorly defined interactions which the current research was targeted to understanding in red.

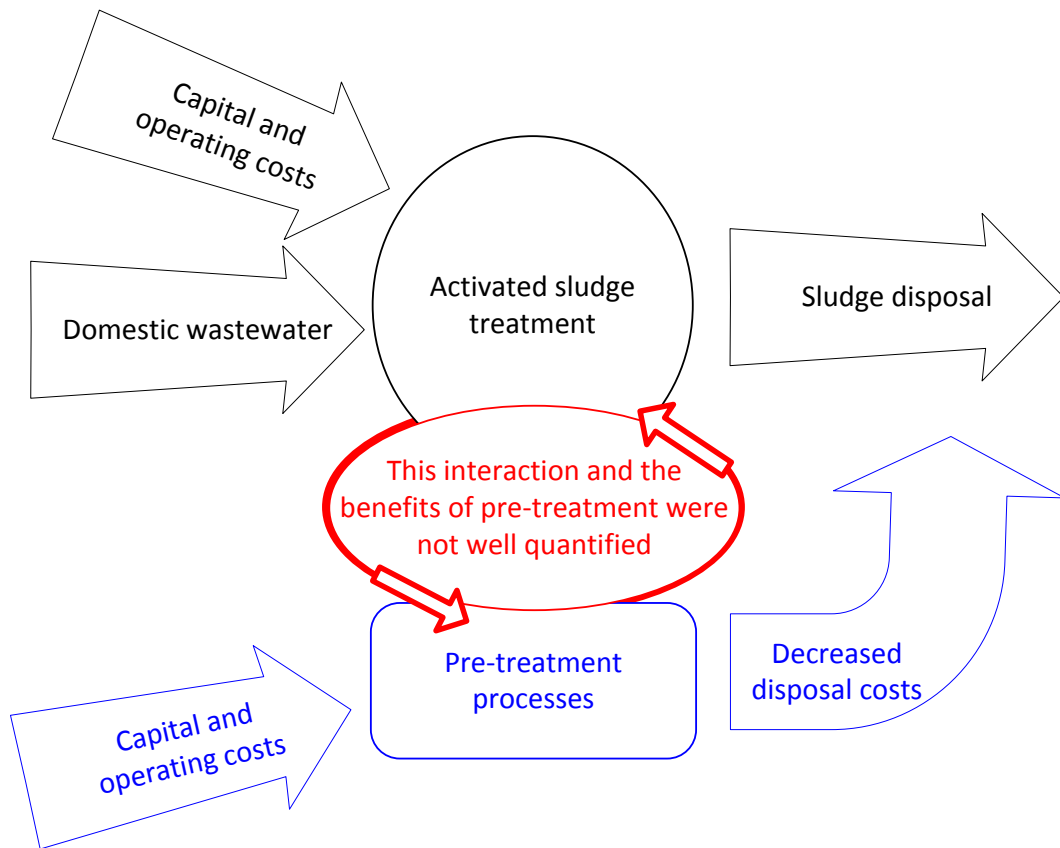


Figure 2.1. Diagram showing interactions targeted in this research

A number of sludge pre-treatment technologies have been suggested and tested, including thermal, chemical, mechanical, and biological processes [Stensel and Strand, 2004; Müller,

2000]. Various full-scale process implementations have been evaluated and found beneficial for both municipal and industrial wastewaters [Paul *et al.*, 2006; Sievers *et al.*, 2004, Elliott and Mahmood, 2007]. Whether a particular pre-treatment is cost-effective or not depends on the capital and operational costs for implementing pre-treatment, but even more importantly the cost-effectiveness depends on the disposal costs of sludge, which must be high in order to justify pre-treatments.

The various whole-plant simulators mentioned in Section 1 use different techniques to integrate the aerobic and anaerobic environments modeled by ASM and ADM respectively. The BioWin model used for this project uses the same variables for the various chemical environments present, and is described in further detail in Appendix A. By describing sludge pre-treatment in terms of the BioWin model parameters, a variety of scenarios for estimating the costs and benefits of sludge pre-treatment can be evaluated in a rapid and cost-effective manner. By realistically evaluating options using software modeling, only the most promising technologies can be subjected to further testing and implementation, thereby reducing costs and speeding progress.

2.1. Waste Activated Sludge Pre-treatment

Sludge pre-treatment has been considered by a large number of researchers as a method of decreasing WAS production and increasing WAS usability, but often the applicability of the results of these studies to waste streams different from the one used in the original research is difficult to determine [Scheminski *et al.*, 1999]. In large part, this difficulty is probably due to differences in domestic wastewater composition and in the operation of treatment facilities. For example, variation in activated sludge treatment solids retention times (SRTs) leads to further differences in the waste sludge that can be impossible to ascertain from routine analyses such as solids and biochemical oxygen demand (BOD) tests.

In addition to the uncertainties surrounding the waste sludge to be treated, some pre-treatment dosages are difficult to quantify precisely. Applied doses and transfer efficiencies of harsh chemical, physical, and mechanical treatments can be difficult to measure, and these harsh treatments are often exactly those treatments which seem to be effective as sludge pre-treatments. At the time of this writing, site specific pilot studies were needed to accurately estimate the effects of a full-scale application of pre-treatment technologies.

One common problem in pre-treatment studies is the link between sludge reduction and increased SRTs. The functional definition of SRT is given in Equation 2.1 and it can be seen that a decrease in the rate of sludge leaving the system will increase the SRT. Since the rate of sludge leaving the system decreases with pre-treatment, the system SRT increases.

$$\text{Solids Residence Time} = \frac{\text{Mass of solids in the system}}{\text{Mass flow rate of solids leaving the system}}$$

Equation 2.1

Since increased SRT has also been proposed as an effective sludge reduction technology, modeling is helpful for understanding the interactions of these two effects. Some earlier studies have not considered the effect of increased SRT. For example, Cao *et al.* [2006] operated a control system at an SRT of 6 days but for a system with ultrasound pre-treatment report that “no excess sludge was removed from the system” during the test.

To estimate the effectiveness of sludge pre-treatment a rapid method for estimating the effects of such treatment is desirable and this project was designed to test such a method using two typical pre-treatment technologies: ultrasound and ozone. Ultrasound was selected as a typical physical pre-treatment which is readily applied at bench scale, with a sizeable body of existing research. Ozone, likewise, is a common chemical pre-treatment which has been researched for many years and can be tested at laboratory scale. The methodology used for testing and quantifying the effects of these two pre-treatments is intended to be easily applied to other types of pre-treatments.

2.2. Sonication

2.2.1. Introduction

High-frequency sound has a wide variety of uses including imaging for medical or nondestructive testing, measurement of distances, and when applied at high intensity, breaking down of cellular materials. The breaking down of cellular materials using ultrasound can be used in a wastewater treatment system to enhance the degradability of biomass. Ultrasound is also referred to using the term sonication.

2.2.2. Mechanisms

During sonication, high amplitude sound energy is added to the sludge, resulting in localized regions of extremely high pressure and temperature. Suslick [1990] noted that this application of energy has been shown to generate free radicals. The combination of extreme pressure and temperature with free radicals means that a wide variety of reactions are possible, and some degradation of biological matter is likely even at very low levels of sonication.

When sonicating at low ultrasound densities, a significant portion of the energy applied to the sludge ends up as heat energy. Wang *et al.* [2006] found the temperature of samples increased by 64°C at the highest dose tested. This heat may provide a synergistic inactivation of biomass, and decrease the heating requirements for subsequent anaerobic digestion, but

it is not clear whether it aids in solubilization of chemical oxidant demand (COD). Peer reviewed literature has shown that the temperature increase is important for sludge solubilization [Chu *et al.*, 2001]. Other such literature has shown the opposite [Wang *et al.*, 2006]. Clearly, this issue remains to be resolved.

2.2.3. Doses

The amount of ultrasound applied can be considered in two ways: relative to the amount of liquid present or relative to the amount of solids present. Both of these measurements are important, since the amount of energy supplied per unit of solids is a good measure of the potential for useful work while the energy per unit of liquid is related to the potential for absorbance of ultrasonic energy by the water. While a universally accepted nomenclature does not exist in the literature, the most common terms are used herein; ultrasound **dose** refers to the energy supplied per unit of solids while ultrasound **density** refers to the energy supplied per unit of liquids. Some researchers only supply one or the other of these measures, complicating comparison of various studies.

Table 2.1 illustrates the wide range of doses and densities considered for ultrasound pre-treatments of sludge. In most cases, the ultrasound density used was determined by the electrical and liquid capacities of the apparatus used. The ultrasound doses shown in Table 2.1 are reported variously as a function of suspended solids (SS), dissolved solids (DS), or total solids (TS).

Table 2.1: Ultrasound doses reported by other researchers to degrade RAS/WAS

Author	Ultrasound dose (kJ/g SS)	Ultrasound density (kW/L)
Akin [2008]	0.36 – 40.75	2.07 – 3.05
Braguglia <i>et al.</i> [2008]	2.5, 5.0 ¹	Not reported
Cao <i>et al.</i> [2006]	Not reported	0.25 - 0.50
Chu <i>et al.</i> [2001]	Not reported	0.11 – 0.44
Grönroos <i>et al.</i> [2005]	0.5 – 15	0.05 – 0.3
Rai <i>et al.</i> [2004]	6.9 – 64	Not reported
Show <i>et al.</i> [2007]	Up to 340 ¹	0.18 – 0.52
Strünkmann <i>et al.</i> [2006]	2 – 47	Not reported
Wang <i>et al.</i> [2005]	Not reported	0.096 – 0.72
Wang <i>et al.</i> [2006]	Up to 135 ²	0.528 – 1.44

¹kJ/g DS

²kJ/g TS

The body of research summarized in Table 2.1 suggests that the most effective ultrasound dose for effective pre-treatment is below 20 kJ/g TS. Although some studies considered much higher doses, the effects of sonication were much greater per unit energy input at doses below 20 kJ/g TS.

During sonication, some ultrasonic energy is converted to heat. Since heating of water provides an alternate pathway for the consumption of ultrasonic energy, the ultrasound density affects the amount of ultrasonic energy passed to solids. Show *et al.* [2007] found that the highest ultrasound density tested provided the most effective solubilization of sludge. Chu *et al.* [2001] found very little effect using low density treatment, with much more than 4 times the effect when density was quadrupled. These results suggest that a high power system may be more effective than a low power system for the same total energy input. Chu *et al.* [2001] also found that treating sludge at 3% total solids was more effective than treating either higher or lower sludge solids concentration, although no explanation for this optimal concentration was attempted.

The frequency of ultrasound used has been found not have a significant effect, over the typical range used in sonication [Grönroos *et al.*, 2005]. This may be a result of the large differences in scale between ultrasonic wavelength in water (a few centimetres) and the size of biomass cells (a few micrometres).

2.2.4. Results

Many researchers have considered the effect of sonication primarily in terms of solubilization of COD, but for understanding of pretreatment effects, biodegradability is at least equally important. Enhanced biodegradability due to sonication has not been well studied. Sonication has been shown to solubilize volatile suspended solids (VSS) preferentially, decreasing the ratio of VSS to total suspended solids (TSS) [Cao *et al.*, 2006]. Strünkmann *et al.* [2006] found no degradation of effluent soluble COD quality in a system when ultrasound pre-treatment was added, but found that a high sludge age system received the greatest benefit from ultrasonic pre-treatment. This result suggests that most of the solubilized COD was biodegradable, but perhaps only slowly. COD solubility following sonication did not appear closely correlated with COD biodegradability.

In one study, anaerobic batch tests showed no clear improvement in terms of methane production due to sonication, though some weak correlation was found between soluble COD (sCOD) following treatment and methane potential [Grönroos *et al.*, 2005]. Braguglia *et al.* [2008] found an increase in biogas production following sonication, but no change in the biogas production per gram of solids destroyed.

Previous research has found that the settling characteristics of sludge treated with ultrasound changed significantly, with sludge volume index (SVI) decreasing for all treatment conditions. For the highest density tested, Cao *et al.* [2006] found the settled density of pretreated sludge was twice that of untreated sludge. Changes to the settling characteristics of sludge are outside of the scope of this project, but such improvements to settling would be of benefit in practice. For instance, a plant with settlers at or near capacity might be able to benefit from this effect of sonication.

Some research has stressed the importance of careful ultrasonic reactor design [Grönroos *et al.*, 2005]. Some variables which will determine the efficiency of a given reactor are the solids content of the sludge, temperature, polymer concentration (if applicable), and ultrasonic delivery device. The optimum solids concentration may depend on the ultrasound reactor used, and the specific sludges being tested.

2.3. Ozonation

2.3.1. Introduction

Ozone (triatomic oxygen or O₃) is the most powerful oxidant in common use for municipal water and wastewater treatment. Oxidation may occur by direct reaction with molecular ozone or following the generation of free radicals, and both reaction pathways are important. The oxidative properties of ozone can be employed to convert biomass to degradable components, to inactivate pathogens, or to completely oxidize all organic materials present. The progression through these oxidation effects takes place sequentially, depending upon the amount of ozone transferred and consumed relative to the amount of oxidisable material present. For pathogen inactivation accepted models are available, and the scope of this project is limited to the conversion of biomass. This study focuses on these sludge reduction applications in the context of whole-plant modeling since this scenario is complex, with recycle streams and interactions in both directions between the pre-treatment and other processes.

2.3.2. Mechanisms

There are at least two mechanisms by which biomass yield is decreased due to ozonation. By breaking up the structure of the biomass and freeing the assimilable components for use as substrate, the overall amount of substrate converted to unbiodegradable particulate matter is increased. At the same time, damaged biomass consumes additional substrate to repair cellular structure. In considering these two mechanisms, one paper suggests that ozonation would most effectively be applied to digested sludge, and focus on releasing matter bound by organisms rather than on stressing biomass [Scheminski *et al.*, 1999].

2.3.3. Doses

In practice, ozonation has been used in a wide variety of ways in municipal wastewater treatment, but the most promising areas of current research are as a pre-treatment for the reduction of sludge production. Ozone doses which some other researchers have investigated for the purposes of improving activated sludge degradability are summarized in Table 2.2.

Table 2.2: Ozone doses reported by other researchers to degrade RAS/WAS

Author	Doses tested (mg O ₃ /mg SS)
Chiavola <i>et al.</i> [2007]	0.025, 0.05, 0.07, 0.37
Dytczak <i>et al.</i> [2006; 2007]	0.016 – 0.08
Huysmans <i>et al.</i> [2001]	0.01 – 0.03
Nagare <i>et al.</i> [2008]	0.17 – 0.41
Paul and Debellefontaine [2007]	0.01, 0.034
Sakai <i>et al.</i> [1997]	0.02, 0.04
Saktaywin <i>et al.</i> [2006]	0.03, 0.04
Scheminski, Krull, and Hempel [1999]	0.3 – 0.5 ¹
Sievers, Ried, and Koll [2004]	0 – 0.15
Weemaes <i>et al.</i> [2000]	0.05, 0.1, 0.2
Yasui and Shibata [1994]	0.05, 0.1, 0.2
Yeom <i>et al.</i> [2002]	0.02 – 2
Zhao <i>et al.</i> [2008]	0.005 – 0.028

¹mg O₃/mg VSS

Table 2.2 illustrates the range of ozone doses used, and shows the majority of research on biomass degradation using ozone has been performed using doses in the range between 0.01 to 0.2 $\frac{mg O_3}{mg SS}$, with some researchers considering doses outside of this range. One recent US Patent suggests that useful doses may be even lower than 0.01 $\frac{mg O_3}{mg SS}$ [Fabiyyi and Novak, 2007].

Adding some confusion to the comparison of doses between studies is the fact that accurately measuring the ozone dose consumed by reductants is difficult. As a result, ozone dose is often poorly quantified. Both the transfer from gaseous to aqueous phase and the reduction of ozone must be measured indirectly. Some authors have reported the ozone dose simply in terms of the ozone supplied to the reactor, implicitly assuming complete transfer efficiency [Zhao *et al.*, 2008; Müller *et al.*, 1998]. Other researchers reported efficiency greater than 90% [Sakai *et al.*, 1997], while Weemaes *et al.* [2000] reported ozone

transfer efficiencies between 76 and 92%, with efficiency decreasing as applied ozone increases.

2.3.4. Results

The conversion of wastewater components as a function of ozone dose has not been adequately quantified for modeling. In some cases, this has been due to a focus on the structure of WAS before and after solubilization where degradability was not the primary focus [for examples see *Scheminski et al.*, 1999; *Dytczak et al.*, 2006]. This approach can provide hints of the mechanisms at work, but be difficult to translate to a prediction for operating plants since the starting conditions are not known in terms of the appropriate model parameters. Other work has considered generic bulk parameters [for example *Nagare et al.*, 2008], but results vary between research groups, and adequate generalization has not progressed to a point that is useful for prediction.

Most published literature shows that ozone is effective at reducing quantities of waste sludge. The earliest published literature on WAS ozonation described a bench-scale experiment using synthetic wastewater as substrate. In this experiment, WAS production was reduced to near-zero levels when ozone was applied to a portion of the RAS stream [*Yasui and Shibata*, 1994]. It was hypothesized that the heterotrophic biomass was able to consume the ozonation products.

The same process was later tested at full scale using an oxidation ditch activated sludge plant treating domestic wastewater located in central Japan [*Sakai et al.*, 1997]. Over a nine month period, RAS ozonation was found to be effective at reducing overall solids production. Unfortunately, the overall effectiveness of this treatment technique was difficult to quantify due to differences between the control and ozone treatment trains.

Again at the bench scale, *Scheminski et al.* [1999] found that following ozonation overall gas yield in anaerobic digesters was increased, with consequent reduction in the volatile solids in the digester effluent. A reduction in the initial rate of biogas production was attributed to the need for anaerobic organisms to acclimate to the ozonated sludge. This concept may be important in consideration of ozonated sludges but has not been adequately addressed by research to date. At the highest ozone dose considered of 0.201 g O₃/g organic dry matter (ODM), the gas yield decreased slightly compared to 0.115 g O₃/g ODM.

Some more recent research describes a minimum or threshold value of ozone required for any observable release of degradation components [*Zhao et al.*, 2008]. Following the threshold, *Zhao et al.* [2008] found a nearly linear decrease in biomass activity and increase in soluble COD with increasing ozone dose, and a non-linear reduction in solids. Other research

shows that high doses of ozone oxidize the released components, making them unavailable for further biomass growth [Yeom *et al.*, 2002].

The bulk of the literature reviewed suggests that the most useful ozone dose for conversion of biomass to useable substrate should be in the range of 0.01 to 0.1 $\frac{mg\ O_3}{mg\ SS}$. Lower doses may not produce large enough effects, while high doses may oxidize rather than improving biodegradability.

Finally, variation in the effectiveness of ozonation has been observed. The amount of WAS generated for one lab scale trial was observed to vary by 30% over a two year period [Paul *et al.*, 2006]. Whether this variation can be attributed to variation in sludge composition is unclear.

The production of a layer of foam above the liquid sludge phase is commonly reported by researchers applying ozone to pre-treat WAS at the bench scale [Yeom *et al.*, 2002; Zhao *et al.*, 2008]. Weemaes *et al.* [2000] attributed the high ozone transfer efficiencies measured to the foaming, since the foam allows for much higher contact times than the liquid phase alone. Foaming may make dose control difficult and must be considered in design of any ozonation apparatus.

The settling and dewaterability of ozonated sludges varies depending on the source of the sludge and the dose of ozone used. Park *et al.* [2003] found that dewaterability deteriorated slightly at low ozone doses but improved significantly at higher doses. Other studies have found that ozonation resulted in good settling characteristics regardless of dose [Paul and Debellefontaine, 2007], or conversely that ozonated sludge was more difficult to dewater than control sludge [Scheminski *et al.*, 1999]. While such changes in settling characteristics are beyond the scope of this project, they are important to consider and should be incorporated into whole-plant models at some future date.

2.4. Respirometry

Respirometry is the estimation of biological activity by measurement of respiration rate. This measurement can be carried out for any organism or population of organisms to determine metabolic activity, if a device of appropriate capacity and sensitivity is used. Using an accepted model for various metabolic pathways, biological activity can be inferred.

Respirometry is typically conducted over a fixed time period or volume of gas consumed. For example, in a biochemical oxygen demand (BOD) test, a fixed duration of 5 or 7 days is commonly used. Higher rates can be measured by monitoring the oxygen depletion corresponding to a fixed volume of oxygen.

By conducting respirometric tests over time, various responses can be found. As an example, if the respiration rate of a bacterial culture increases over time then it is accepted that the bacteria are growing or reproducing. In this way, estimates of the various biological and bioavailable COD fractions may be obtained. When considered in combination with the results of more common analyses such as COD and solids, these estimates can be used as measures of the constituent fractions of a wastewater or sludge. The conventional analyses provide information about physical and chemical characteristics while respirometry provides information about bioavailability of COD and activity of biomass. Respirometry has been used to ascertain parameters for biological systems for several decades, but a standard testing method is elusive since the information available depends on the sample characteristics as well as the test conditions.

Interpretation of respirometric results depends on the model which is proposed for the system. While BioWin and other whole-plant models are convenient for modeling complex interactions and dynamic loadings, a simpler model is appropriate for a batch test such as the respirometry conducted for this project. The first activated sludge model of the International Association of Water Quality, known as ASM1, was published in 1987 [Henze *et al.*]. This was the first widely accepted model to describe wastewater in terms of its components, and within a few years respirometry conducted under carefully controlled conditions was used with this model to estimate quantitatively the kinetic parameters and fractionation of activated sludge biomass [Kappeler and Gujer, 1992; Spanjers and Vanrolleghem, 1995]. At the same time, respirometry was used to estimate the various fractions of wastewater [Henze, 1992]. Short-term respirometric tests have been found to be very effective for determining readily biodegradable COD [Çokgör *et al.*, 1998].

Determining the impact and effectiveness of WAS pre-treatments by respirometry is an obvious extension of earlier work characterizing activated sludge properties. Andreottola and Foladori [2006] used respirometry to determine the readily degradable COD concentration, combined with COD analyses to assess the effectiveness of sonication and alkaline thermolytic treatment.

Since respirometry depends on the biological activity of samples, storage conditions and time are very important considerations. In one study, storage of 48 hours was found to result in significant degradation of the sample while storage of less than 24 hours had no significant impact [Spérandio and Etienne, 2000].

3. Materials and methods

Sludges of various solids residence times were treated using ultrasound and ozone pre-treatments. Sludge was obtained from sequencing batch reactors (SBRs) with known SRTs. Batch pre-treatments were conducted, and the effects of these pre-treatments were quantified in terms of biology and chemistry using common laboratory analyses as well as respirometric techniques.

3.1. Activated Sludge Source: Pilot Sequencing Batch Reactors

Sludges were obtained from four SBRs operated by the University of Waterloo at the wastewater treatment plant in New Hamburg, Ontario. These SBRs received screened municipal waste from New Hamburg and the surrounding area, and cycled 4 times per day. Each of the four reactors was designed to operate at the same hydraulic residence time but waste a different amount of sludge each cycle. In this way, the reactors were identical except for solids residence time. The reactors are pictured in Figure 3.1 below.

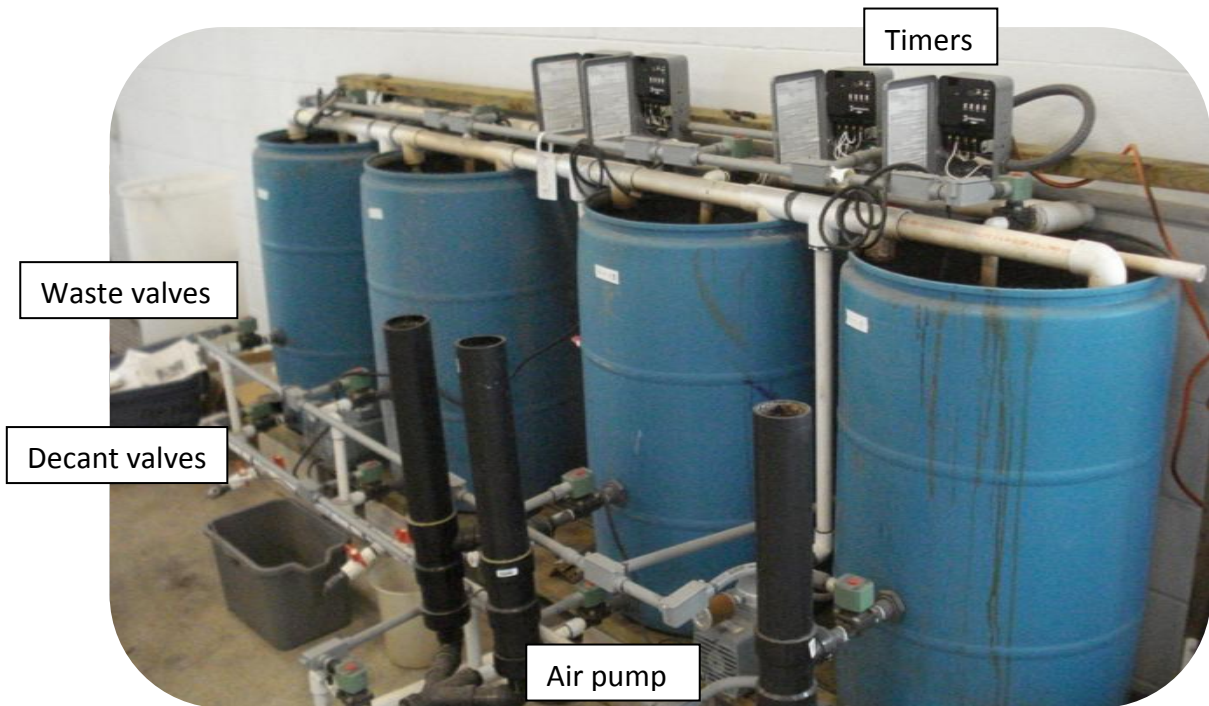


Figure 3.1. Pilot sequencing batch reactors

The sequencing batch reactors provided similar sludge to that of a conventional activated sludge process, but with highly controlled SRT. All four reactors were operated from a

common set of timers so that cycle times were the same between reactors. Each 6 hour cycle consisted of 5 hours and 15 minutes of aeration, 30 minutes of settling, and 15 minutes of decant. During the last 15 minutes of aeration, a fixed volume of mixed liquor was wasted according to the desired SRT for each reactor. The time required to fill the reactors was typically only about 2 minutes, so this phase has been included in the react time. Aeration was applied throughout the react or aeration phase, and so these reactors were not operated to provide any denitrification.

During the experimental period, the operational parameters of the four reactors were measured twice. As Table 3.1 shows, the hydraulic residence times (HRTs) were very similar between reactors. The differences in performance between reactors were primarily due to the different SRTs. The measured volumes of waste and decant were very similar on replicate measurements, demonstrating that the SBRs do in fact operate with stable SRTs.

Table 3.1: Operational parameters for experimental SBRs

Reactor #	Full Volume (L)	Cycle time (h)	Waste (L/cycle)	Decant (L/cycle)	HRT (h)	SRT (d)
1	183	6.0	39	92	8.3	1.1
2	186	6.0	34	107	8.1	1.4
3	181	6.0	6.8	128	8.0	6.7
4	173	6.0	2.8	119	8.5	15.7

The full-scale plant that served as a host for the experimental SBRs was one of the newest plants operated by the Region of Waterloo. The plant had excess capacity and the nearest residential area was located nearly 1 km away, resulting in very few odour complaints. As a result, during the experimental period the feed to the SBRs in New Hamburg sometimes received significant amounts of non-typical wastewater which was difficult for the operating authority to handle at other plants. This included a significant amount of septage as well as leachate from the municipal solid waste facility. Data regarding the amounts and makeup of these streams and the timing of their introduction to the plant were not available. This variability in influent which was not taken into account likely increased the variability of results for this study.

3.2. Batch Pre-treatments

Each of the pre-treatments considered was carried out in batch using well mixed reactors. Sample sizes and target solids concentrations were selected to improve the efficiency of pre-treatments: For ultrasound a higher solids concentration and a smaller volume reduced the proportion of the energy which heated the water, while for ozone a larger total volume was required in order to obtain an appropriate depth for gas-liquid transfer.

3.2.1. Ultrasound reactor

The ultrasound apparatus consisted of a Branson Sonifier 250 ultrasound generator equipped with a micro tip (Branson Ultrasonics Corp, Danbury, CT), a 250 mL beaker inside a ice-filled crystallizing dish as cooling jacket, and a magnetic stir plate for mixing. The apparatus is pictured in Figure 3.2 below.

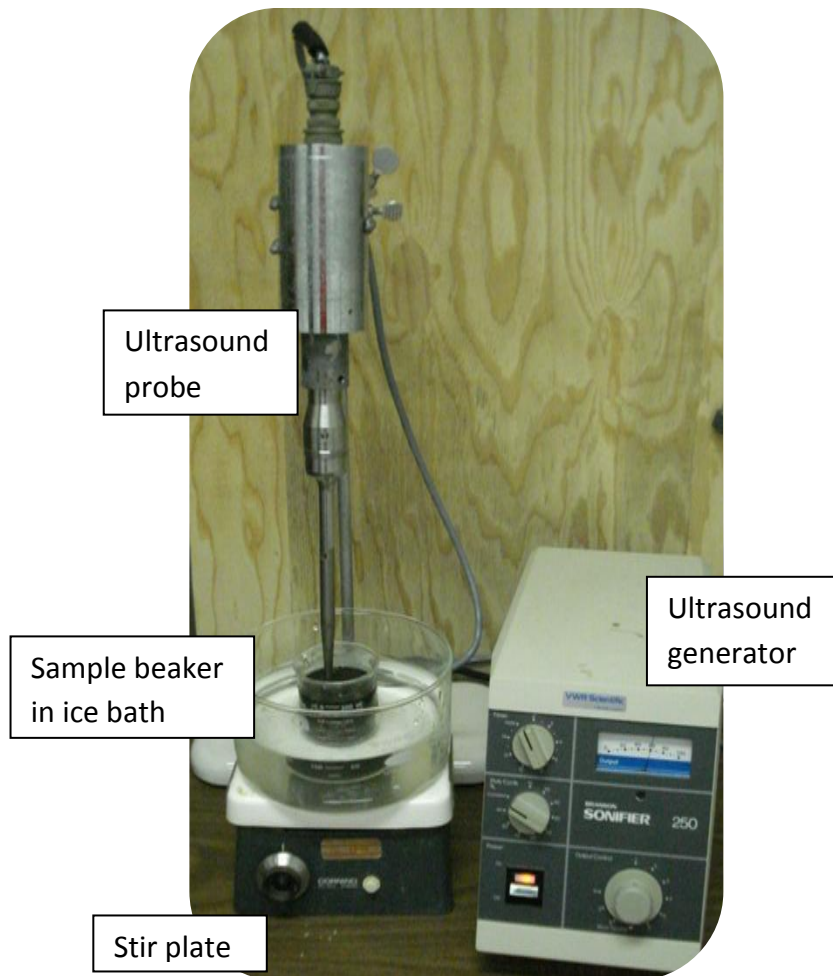


Figure 3.2. Ultrasound apparatus

Average power input to the ultrasound generator was approximately 68 W, as measured at the input to the ultrasound generator. Ultrasound pre-treatment was conducted on 200 mL samples at a target concentration of 1.5% solids. The resulting ultrasound density using this configuration was constant at approximately 340 W/mL, while doses tested ranged from 2 to 11 kJ/g TS.

The specific doses tested during each experiment were selected to provide a wide range of doses over the target range, with sufficient duplication to show repeatability. The actual solids concentration varied between 0.7 and 1.7%, but this value was only measured after the experiment was complete. This required a new evaluation of the doses which had been tested and those which remained to be tested after each pre-treatment dose had been calculated.

3.2.2. Ultrasound efficiency

Ultrasonic efficiency was estimated by conducting experiments using the same setup without the cooling jacket, and treating a sample of pure water. It was assumed that all of the energy consumed by the generator was available for degradation of solids except that which was converted to sensible heat in the bulk liquid. Under this assumption, Equation 3.1 was used to determine ultrasound efficiency.

$$n = \frac{E_{input} - \Delta T \times m_{H_2O} \times C_p}{E_{input}} \quad \text{Equation 3.1}$$

where n is the fraction of input power not converted to heat, or the efficiency (unitless), E_{input} is the energy input to the ultrasound generator (J), ΔT is the change in temperature observed at the reactor wall (K), m_{H_2O} is the mass of water present (g), and C_p is the heat capacity of water (J/g/K). Although heat capacity changes slightly over the range tested, for simplicity C_p was assumed to be constant at 4.2 J/g/K [Tchobanoglous and Schroeder, 1987]. Since most published research presents only the input power and does not take efficiency into account, input power is reported for the ultrasound results. Since all tests were conducted under the same condition, however, results could easily be scaled to account for the efficiency calculated as described.

3.2.3. Ozone reactor

Ozone pre-treatment was conducted using a 1 litre sample at a target concentration of 0.5% (w/w) solids. Ozone was generated at 4 to 5% (w/w) in pure oxygen by corona discharge using a Hankin Ozomat II generator (Hankin Ozone, Scarborough, ON). The ozone was

supplied to samples through a fine frit glass diffuser. The flow rate of ozone was maintained at 2 L/min and measured using a direct-reading rotameter (Aalborg tube model 014-02-N, Orangeburg, NY).

The ozone reactor consisted of custom-fabricated glassware with an integrated foam break. The wetted parts were made of glass, stainless steel, and silicone. The liquid column had a diameter of 6 cm and a depth of 35 cm, and the gas diffuser was located within one centimetre of the bottom. The integrated foam break was conical in shape, matching the diameter of the liquid column at the bottom and expanding to a diameter of 16 cm at the top. The apparatus was sealed using a silicone stopper of 60/70 mm diameter and 50 mm height, through which gas supply and return lines were inserted as well as lines for the foam suppression recirculation system. The apparatus is pictured in Figure 3.3.

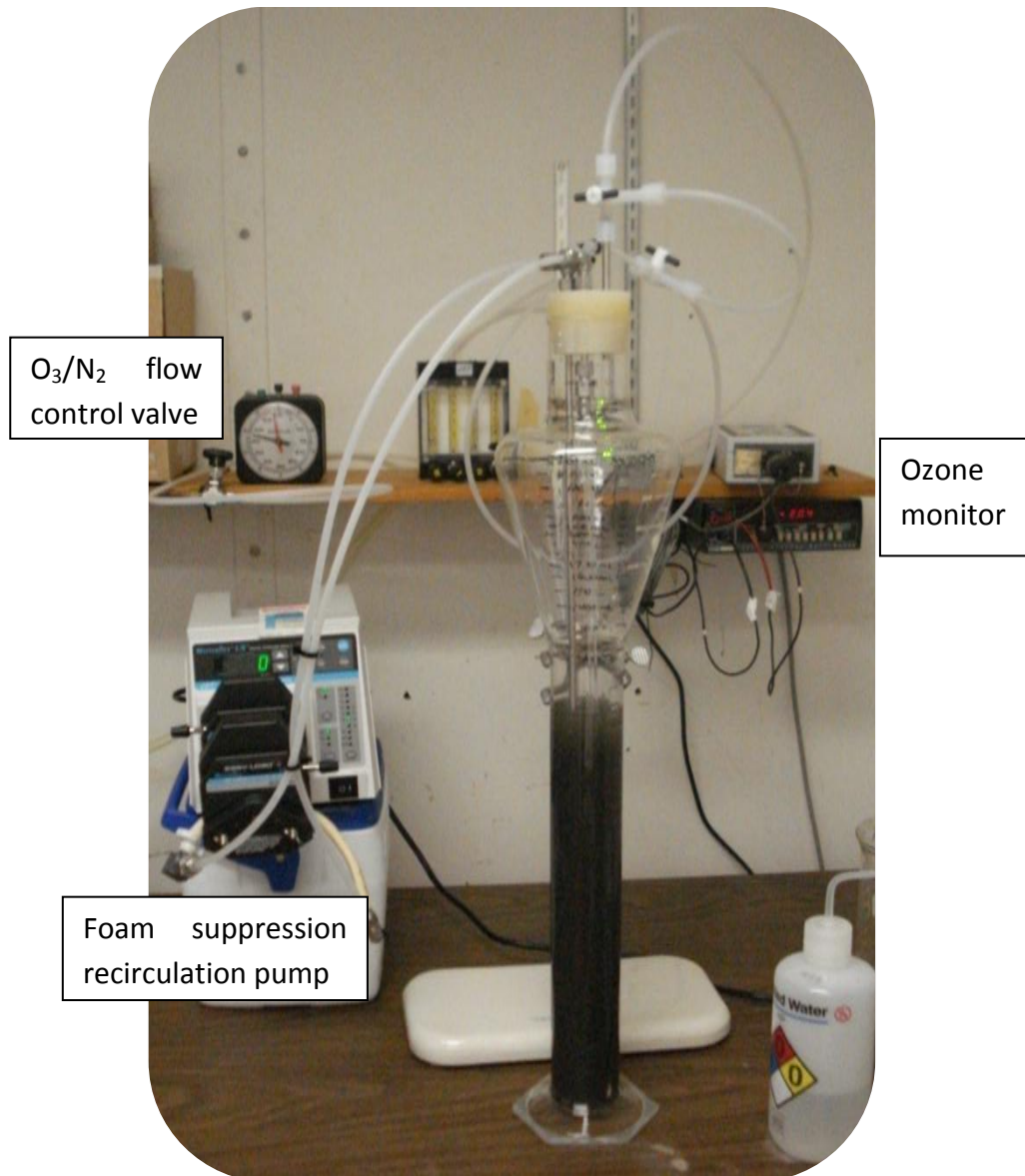


Figure 3.3. Ozone pre-treatment apparatus

The passive foam break was augmented with an active foam suppression system after early experiments showed that the foam break was not sufficient to allow ozone dosing in the desired range without foam exiting the reactor through the exhaust gas line. The recirculating spray system consisted of a stainless steel pickup tube for collecting sample, a spray nozzle (model 1S5.6, Bex Engineering, Mississauga, ON), and flexible tubing to connect the two. The sample was moved through this recirculating system using a peristaltic pump.

Samples were placed in the reactor and immediately ozonated. In order to vary the dosage applied, a constant concentration of ozone was applied for varying lengths of time. Higher doses required multiple treatments, since excessive foam was generated and had to be knocked down before further ozonation could take place. Following pre-treatment, samples were purged using nitrogen to ensure that unreacted ozone still in solution was removed and measured. This step allowed for precise estimation of the dose consumed.

Ozone concentration in the off-gas was measured continuously during tests using a Teledyne API 452 high concentration ozone monitor (Teledyne API, San Diego, CA). The measured concentration was recorded in one-second intervals. The feed ozone concentration was measured before and after the test by activating the reactor's bypass valves. During the test, feed gas concentration was not measured. The feed gas concentration during the test was estimated by linear interpolation between the initial and final concentrations. These concentrations were typically within 2% of one another, so the manner of interpolation was not important.

As with ultrasound, the specific doses tested during each experiment were selected to provide a wide range of doses over the target range as well as sufficient duplication to show repeatability. The COD concentration, required for calculation of dose, was only measured after the experiment was complete. For each trial the doses already tested were considered and doses which met the two broad goals of breadth and depth of experimentation were targeted.

3.3. Analytical Methods

Responses to pre-treatment were measured using conventional analyses as well as respirometry. The conventional analyses were chemical oxygen demand (COD), suspended and total solids analyses, soluble and total Kjeldahl nitrogen, ammonia, nitrite, and nitrate measurement. These analyses were all conducted according to the relevant sections of Standard Methods [Eaton *et al.*, 2005]. Standard operating procedures used for conducting these analyses are included in Appendix B. Total suspended solids (TSS) were measured as well as the ash, or inorganic, suspended solids (ISS) to allow for the determination of volatile suspended solids (VSS) by difference. Similarly, total solids and total inorganic solids measurements allowed for determination of total volatile solids. Dissolved solids could also be determined by the difference of these measurements. Nitrite (NO_2^-) and nitrate (NO_3^-) were both measured by ion chromatograph. Ammonia (NH_4^+) was measured using an automated alkaline phenate method.

COD was measured using flocculated and filtered sample as well as using the entire sample, to allow for the separation of COD into soluble and particulate fractions. The flocculated and filtered COD (ffCOD) sample used alum precipitation to sequester colloidal matter and then a 0.45 μm pore size filter to remove it from the sample. First, 1.25 mg of alum was added to 50 mL of sample as 0.1 mL of 12.5 g/L alum solution. The sample was mixed vigorously for 30 seconds to begin flocculation, allowed to stand for 10 minutes, then centrifuged for 15 minutes. Finally, the sample was filtered using a 0.45 μm pore size filter and the cake discarded. Blank and standard samples were also subjected to this procedure to confirm that soluble COD concentration was not changed significantly by this procedure.

The common analyses all had good repeatability, were easily performed by any commercial laboratory, and were capable of showing some important changes to sludge characteristics such as increased COD solubility. Respirometry was employed to complement these techniques, providing information about the active biomass and biodegradability of substrates in the form of oxygen response curves. Since the collection of respirometric data is not standardized and novel analysis techniques were employed, a separate chapter is devoted to the collection and analysis of these data.

4. Collection and Analysis of Respirometric data

Since biodegradability is so important in the context of sludge pre-treatment, considerable effort was expended to analyze this characteristic of the sludges tested. Respirometry is a direct measurement of biological activity, and measurement of this activity over time allows for estimation of the bioavailability of COD.

4.1. Respirometer and test setups

Respirometric responses were measured using a Challenge Technology AER-208 respirometer (Springdale, AR) equipped with a water bath for temperature control. Using this unit, up to 8 samples could be tested simultaneously. In each 250 mL sample cell, a small vial containing 30% w/w potassium hydroxide solution was inserted, consuming and reacting with the CO₂ in the sample headspace. This created negative pressure which in turn pulled oxygen through the measurement cells and into the bottle. This flow of oxygen was monitored continuously through Challenge's proprietary software, and the total oxygen consumed by each sample was recorded every few minutes. Each test was continued until a distinct decay curve was observed, indicating that most of the biodegradable material had been consumed. Upon conclusion of the test, the change in total oxygen data were calculated for each time step, providing an estimate of the oxygen uptake rate (OUR) in mg/l/hr. To each cell was added 267 mg of Hach 2533 Nitrification Inhibitor (Hach Co., Loveland, CO), and so heterotrophic processes dominated all responses. The respirometer is pictured in Figure 4.1.

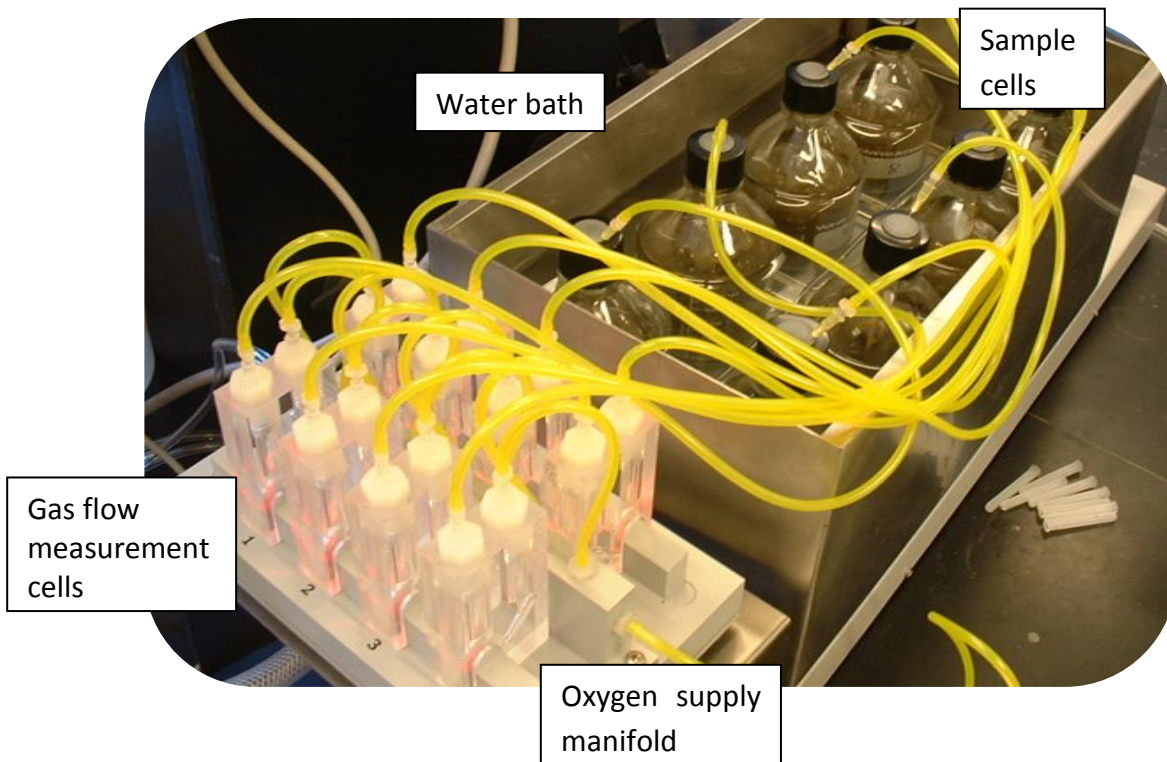


Figure 4.1. Challenge Technology respirometer

The 8 cells were prepared with raw or pre-treated sludges, or a combination of the two. The combinations of raw and pre-treated sludge were tested because it was unclear whether or not the pre-treated sludges would have sufficient active biomass remaining to result in a measurable OUR. Table 4.1 summarizes the contents of the cells for the respirometric tests.

Table 4.1. Cell contents for respirometric tests

Cell numbers	Raw sludge	Pre-treated sludge	
		Dose 1	Dose 2
Randomly assigned to evenly distribute any cell-specific errors	200 mL		
		200 mL	
			200 mL
	100 mL	100 mL	
	100 mL		100 mL
	<i>other 3 cells randomly assigned to replicates</i>		

In Table 4.1, Doses 1 & 2 refer to the two doses being tested during any given pre-treatment trial. The rationale for selecting the specific doses was explained in Section 3.2. In the

following results sections all data were calculated using the single-sludge cells since the results of the combined sludges (raw plus pre-treated) were not amenable to analysis by the methods employed. Specifically, the synthetic OUR curves described in the next section were not able to match the OUR responses of these combined sludges as well as the OUR responses of the individual sludges. Several other analysis techniques were attempted but only the most successful one is discussed in detail in the following sections.

4.2. Respirometric model

The OUR measurements recorded over time were used to estimate the starting values of three parameters: active heterotrophic organisms, the readily degradable substrate which they use for growth, and the slowly degradable substrate which may be enzymatically hydrolyzed into readily degradable substrate. For some simple situations, analytical solutions are available that describe OUR as a function of these initial conditions and time. The most commonly used are “pure” decay and growth curves, wherein the respective process dominates the response. For decay curves, the food to microorganism (F/M) ratio must be quite low so that after a short time, decay is the limiting process. Any F/M ratio below about 0.1 is adequately low, and in this case, oxygen uptake rate decays exponentially with time. Growth curves, conversely, require a high F/M ratio (ie. >10) so that the dominant response measured is due to growth of the microorganisms. In between these two are several orders of magnitude of intermediate F/M ratios, where one process is not dominant throughout the test. Samples in this middle range require a more nuanced approach. Since sludge pre-treatment converts microorganisms to food, changes in a pretreatment dose can result in changes to the F/M ratio and development of a new analysis procedure was helpful.

Since consumption of oxygen is included in ASM1, this model can be used to generate oxygen uptake rate curves by assuming starting conditions. To determine the oxygen uptake rate at a given time, the quantities of each contributing component must also be found at that time. Respirometric results were interpreted by fitting a simple response curve based on the ASM model described in Section 2.4 with the three most essential processes: heterotrophic growth, heterotrophic decay, and hydrolysis of particulate matter into soluble. Since the Challenge respirometer was designed such that only oxygen can enter sample cells, the starting concentrations determine the respirometric response for the duration of the test. Table 4.2 lists the general and specific kinetic and stoichiometric parameters used in the model for interpretation of respirometric data.

In order to provide consistency between analyses, typical values for kinetic and stoichiometric parameters were used. This avoids the potential for over-fitting, or obtaining an interpretation which appears excellent but violates essential assumptions of the model.

The values shown in Table 4.2 were the standard or default parameters used in BioWin as of March 2009 [Envirosim Associates, 2009].

Table 4.2. Model employed for interpretation of respirometric data: stoichiometry and kinetics

Process	S_{bs} (mg COD L ⁻¹)	X_s (mg COD L ⁻¹)	Z_{bh} (mg COD L ⁻¹)	rate (mg COD L ⁻¹ d ⁻¹)
Heterotroph growth	$\frac{-1}{Y_h} = \frac{-1}{0.66}$		1	$\mu_h \left(\frac{S_{bs}}{K_s + S_{bs}} \right) Z_{bh}$ $= 3.2 \left(\frac{S_{bs}}{5 + S_{bs}} \right) Z_{bh}$
Heterotroph decay		$1 - f_p = 1 - 0.08$	-1	$b_h \times Z_{bh} = 0.62 \times Z_{bh}$
Hydrolysis	1	-1		$\frac{X_s/Z_{bh}}{K_x + X_s/Z_{bh}} Z_{bh}$ $= 2.1 \frac{X_s/Z_{bh}}{0.06 + X_s/Z_{bh}} Z_{bh}$

For those unfamiliar with the type of model representation common in ASM/ADM-type models, an example is provided to illustrate the type of results which could be obtained with the model described in Table 4.2. For the example, the response of a fictitious sample is modeled. The sample contains 250 mg/L of active heterotrophic biomass, and the same concentration of readily degradable substrate. Finally, 500 mg/L of slowly degradable substrate is present, which requires hydrolysis before it can be metabolized by the biomass. Figure 4.2 shows the fate of the three COD fractions over time as predicted by this model.

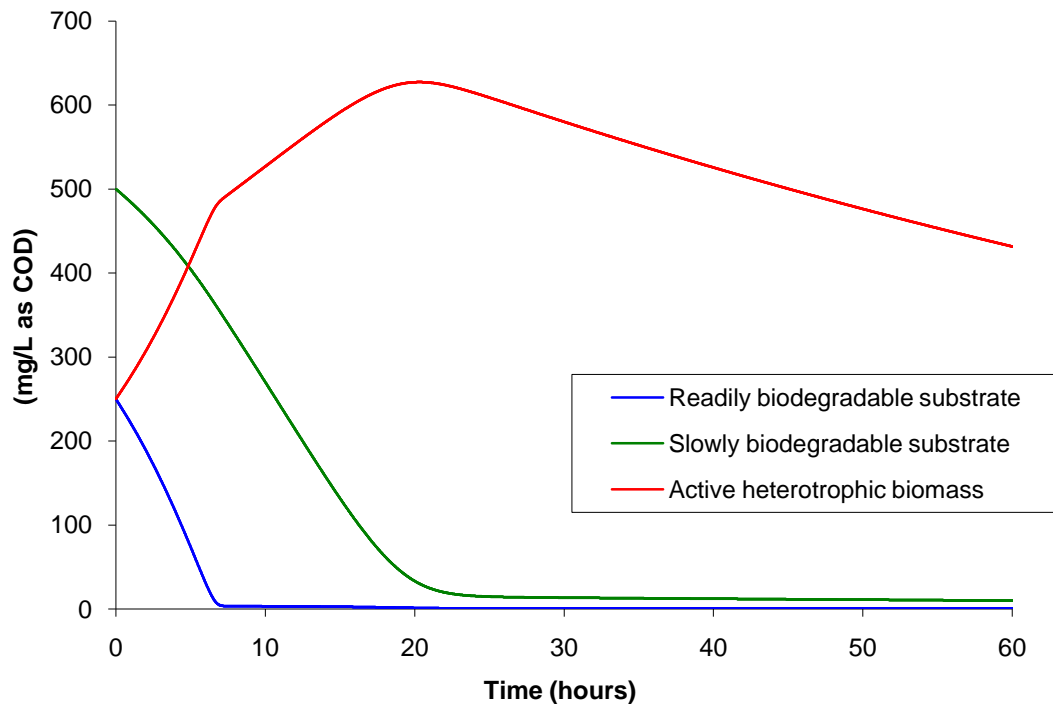


Figure 4.2. COD fractions predicted by simplified ASM over time

In Figure 4.2 three phases can be identified. First, the readily degradable substrate is exhausted in the first few hours of the test. Next, the concentration of active heterotrophs increases until nearly all of the readily and slowly degradable substrate is exhausted. Finally, after about 20 hours in the example, all biodegradable substrate has been consumed. In this third and final phase, decaying heterotrophs produce slowly biodegradable substrate which is then consumed due to growth. The net result is a declining heterotroph concentration and fairly stable concentration of slowly degradable substrate. This phase is commonly referred to as regrowth.

The only process in this simplified model which consumes oxygen is heterotroph growth, and the oxygen uptake rate is equal to the heterotroph growth rate multiplied by $\frac{1-Y_h}{Y_h} = \frac{1-0.66}{0.66}$ [after Henze *et al.*, 1987]. OUR curves generated using this simplified version of ASM1 show the same three distinct phases as can be seen in Figure 4.2; growth on readily degradable substrate, growth on slowly degradable substrate, and regrowth (decay). In each phase, one of the three processes is limiting – the growth process initially, followed by the hydrolysis process, and finally the decay process. Figure 4.3 shows the OUR curve generated using this

simplified ASM1 and corresponding to the concentrations in Figure 4.2. The three phases are again easily visible.

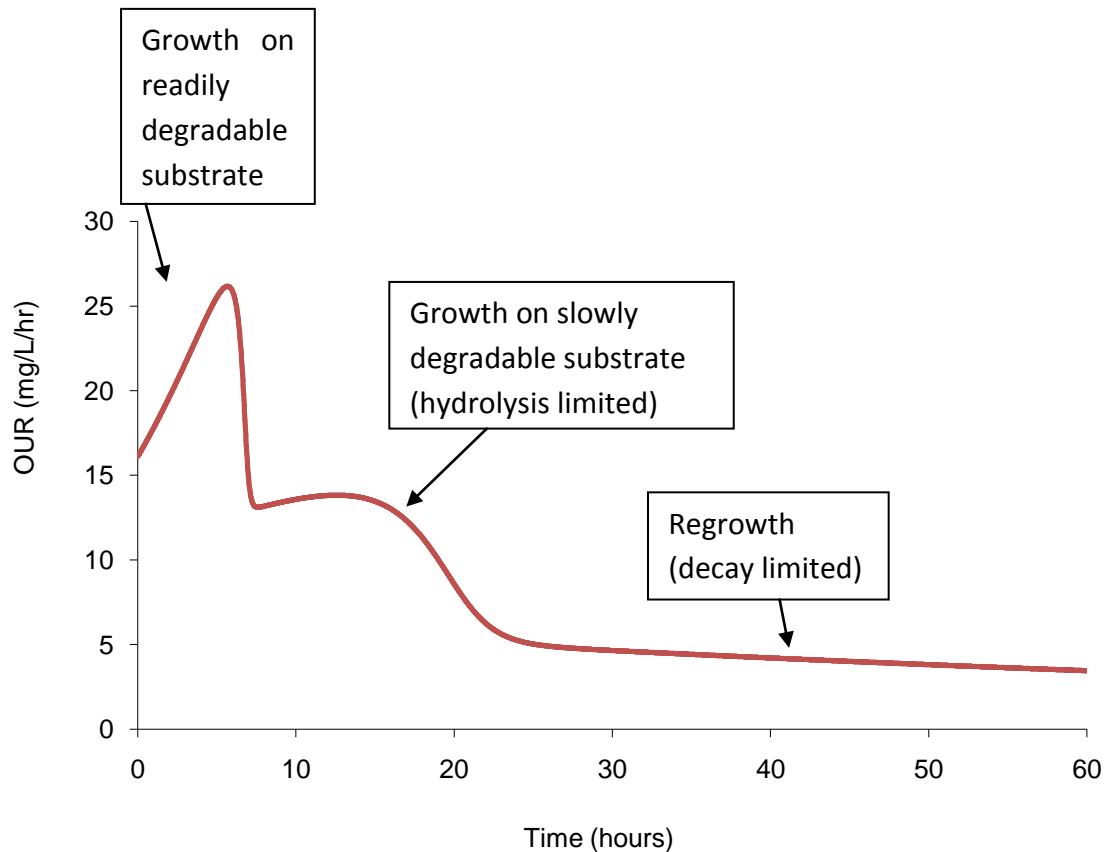


Figure 4.3. Sample OUR curve using simplified ASM1

Since all of the kinetic and stoichiometric parameters were assumed, the initial concentrations of heterotrophs, readily degradable substrate, and slowly degradable substrate defined the entire respirometry response for these synthetic curves. In order to find the synthetic curve which best represented measured data, a computer program was developed using Visual Basic which implemented a dynamically dimensioned search algorithm [Tolson and Shoemaker, 2007]. This program found the best model fit to the respirometric data by minimizing the sum of squared error between the synthetic and measured OUR curves with random perturbations of starting conditions. The algorithm is summarized in Figure 4.4. Complete source code for this computer program is provided in Appendix C.

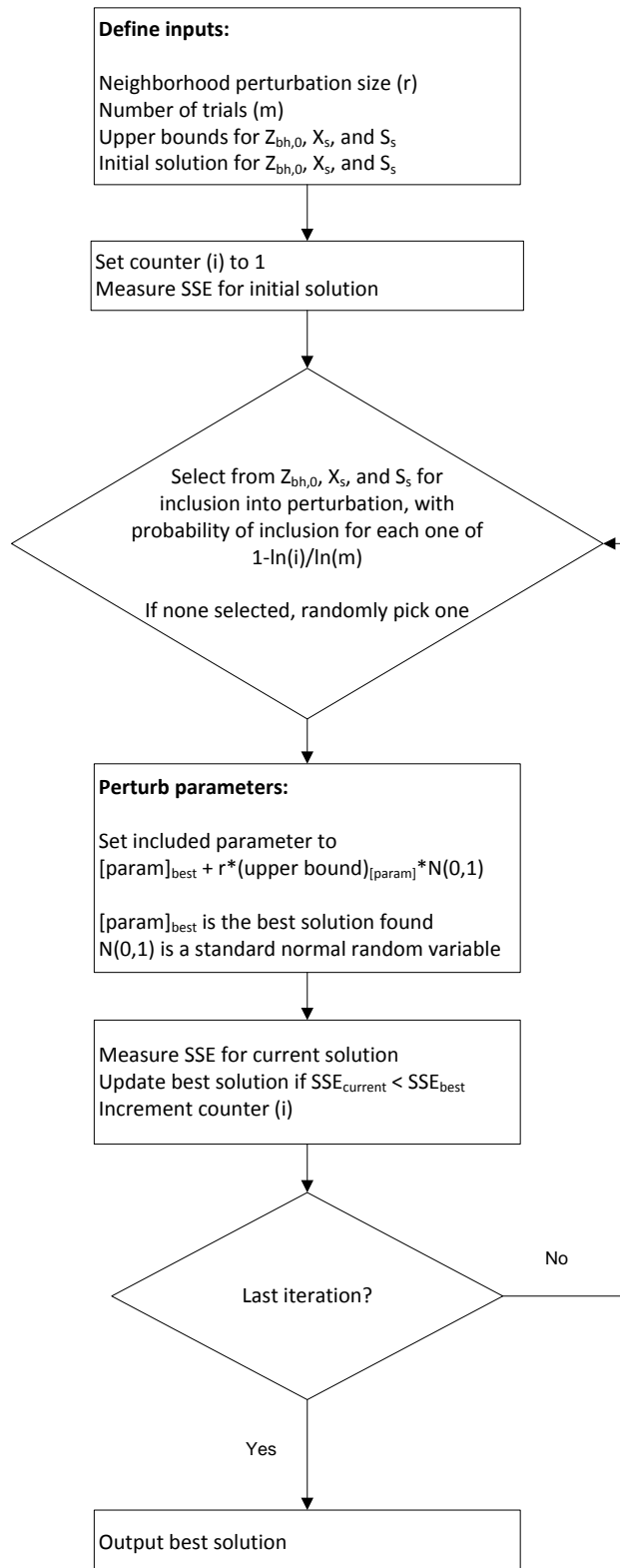


Figure 4.4. Dynamically dimensioned search algorithm [after Tolson and Shoemaker, 2007]

For each measured OUR curve the algorithm was run for one million iterations. In most cases the measured OUR curves were well-represented by the simple model and in these cases the algorithm found the best solution in the first thousand or so iterations. At other times, the best fit was less obvious and the existence of several alternate solutions of local minimum error meant that more iteration was required to find the global optimum solution.

4.3.Examples

Some results of the respirometric interpretation described in the previous section are provided here. The model was capable of describing the response well in most cases, especially considering the model simplicity and the biochemical complexity. Some changes to the model which might improve the fit to measured data are discussed.

In this section, figures show sample output from the software developed for respirometric interpretation. Figure 4.5 through Figure 4.8 show measured data in black and the corresponding modeled fit in red. All of the reported concentrations are in terms of COD, consistent with the usual model formulation. The scale of these plots was determined automatically by the analysis program, and so both vertical and horizontal scales vary slightly between the four figures.

The typical response for the untreated sludge was dominated by a decay curve. As shown in Table 4.2 (Page 24), the typical biomass decay rate assumed for this type of model is 0.62 d^{-1} . After the subsequent hydrolysis, the oxygen uptake rate related to regrowth, is expected to decay at a rate of 0.24 d^{-1} . Figure 4.5 shows a decay-dominated respirometric response.

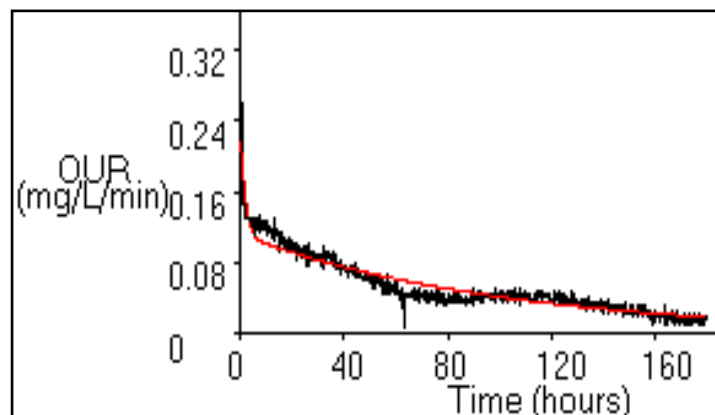


Figure 4.5. Example of decay-dominated respirometric response

In Figure 4.5 the model fit (red line) had a starting biomass concentration of 807 mg/L of heterotrophic biomass and a starting slowly biodegradable substrate concentration of 65 mg/L. The model matched the measured response well. Biodegradable substrate was consumed in the first 10 hours, after which OUR decayed at approximately the model rate of 0.24 d^{-1} .

Following pre-treatment it was expected that some biomass would have been converted to biodegradable substrate. In this case, the OUR would initially increase as biomass growth took place using the substrate. Figure 4.6 shows such a response, which culminated with a decay curve as in Figure 4.5, but not until almost 40 hours had elapsed.

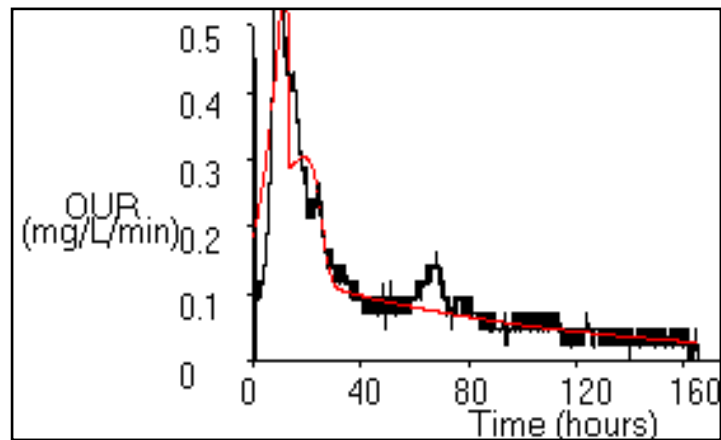


Figure 4.6. Example of complex respirometric response (good fit)

In Figure 4.6 the model fit used a starting biomass concentration of 168 mg/L, with 748 and 503 mg/L of slowly and readily degradable substrate, respectively. Again the model seems to adequately reproduce the measured response, however the region of peak OUR shows a few differences.

As the OUR increased, the model predicted an exponential increase at 3.2 d^{-1} which corresponds to the growth rate in Table 4.2. The measured data increased at a faster rate in every test which contained the initial growth phase, suggesting that a higher rate might be more appropriate. Since growth rate and heterotroph concentration are correlated in this model, the typical value of 3.2 d^{-1} was kept throughout in order that initial heterotroph concentrations could be compared directly. The model could easily have been modified to fit the growth rate as well, but separation of the error of initial heterotroph concentration and growth rate would not be possible.

In addition to raw and pre-treated samples, combinations of these two were tested. The proposed model was not capable of describing the results of these tests, though the reason for this is unknown. Figure 4.7 shows one such respirometric response.

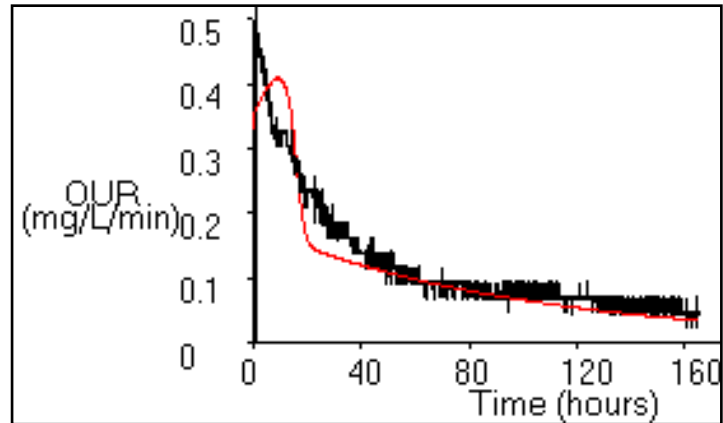


Figure 4.7. Example of complex respirometric response (poor fit)

In this case, the best model fit had an initial biomass concentration of 784 mg/L with 799 mg/L of slowly degradable substrate. The model shows that OUR should have increased over the first 10 hours but in fact it declined over this period. Because of the lack of fit, these data were discarded and the better-fitting separate data were used instead.

Following ozonation at high doses, near complete inactivation of heterotrophic biomass was observed. This resulted in respirometric responses in the same family as the one shown in Figure 4.6, but more extreme. Figure 4.8 shows one such response.

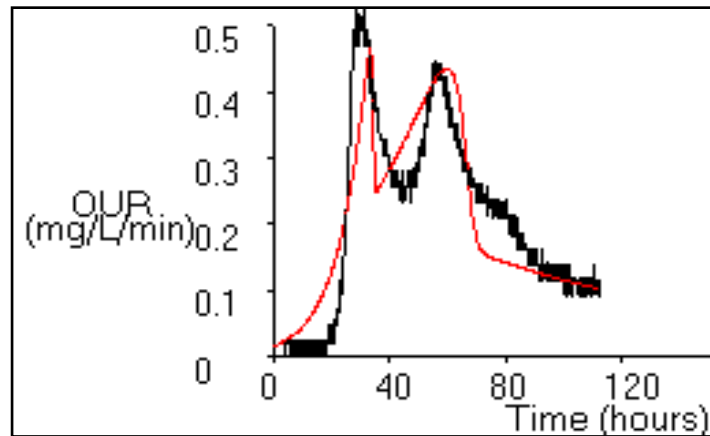


Figure 4.8. Typical oxygen uptake curve following high ozone dose

The model fit (red) in this case was just 15 mg/L of heterotrophic biomass, with 1791 and 522 mg/L of slowly and readily biodegradable biomass, respectively. The model over-predicted OUR for the entire first day, and although the modeled data has generally the same shape as the measured data, there were certainly some important differences.

5. Sonication results

When treating samples using ultrasound, two changes were readily apparent: an increase in temperature and an increase in colouration of the liquid phase that was particularly apparent following some settling. The change in settling characteristics observed during sonication is illustrated by the two samples pictured in Figure 5.1.

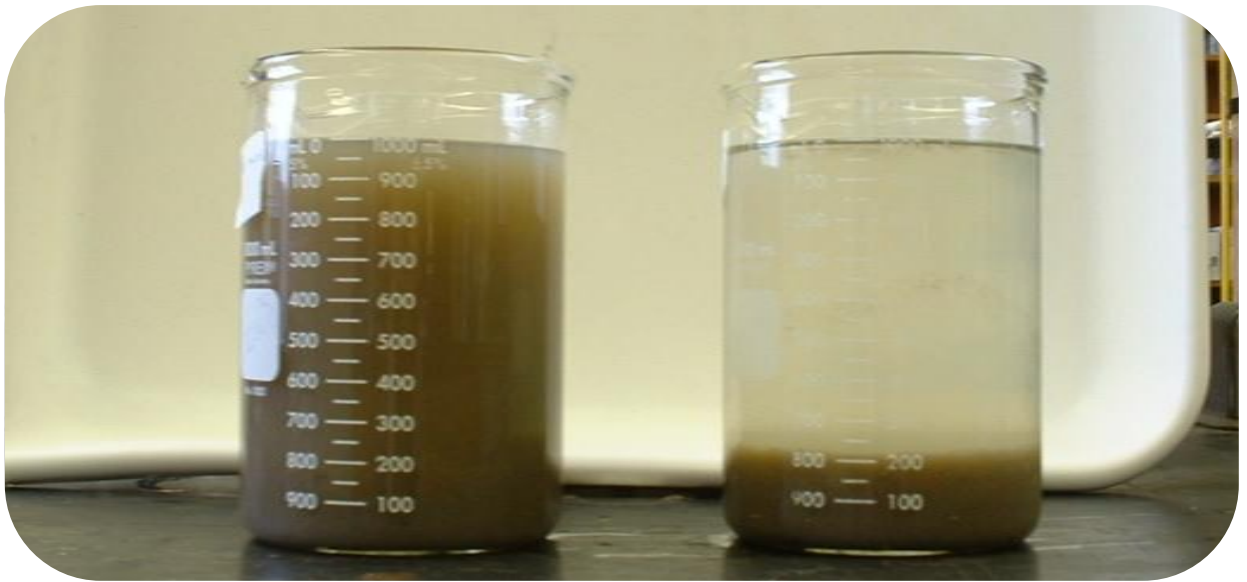


Figure 5.1. Appearance of sample following sonication

The two samples pictured above were collected on the same day and differ only in the pre-treatment performed. The two samples both contained approximately 0.3% total solids, but the sample on the left was sonicated at a dose of 2.2 kJ, while the sample on the right was not pre-treated at all. Following approximately 30 minutes of settling, it is clearly visible in Figure 5.1 that the suspended solids in the control sample had condensed into the bottom 200 mL. The pre-treated sample also had solids concentrated at the bottom of the sample, but a large amount of material was also present above this sludge blanket, obscuring the interface and not settling. Since the quiescent beakers performed in much the same way as a full-scale settler, some increase in colour following secondary settling would be likely, and effluent quality could be degraded. This effect would only occur when the pre-treatment process was upstream of a physical separation process: for pre-treatment before sludge digestion this effect would not be important.

The increase in temperature of samples was controlled for most experiments as described in Section 3.2 but also measured during separate experiments, and the increase in sensible heat was considered as wasted energy. The proportions of energy converted to heat and used to disrupt biomass depend on the particular reactor used.

5.1. Sonication efficiency

To obtain a preliminary estimate of the efficiency of the ultrasound apparatus, two tests were conducted using tap water without the cooling jacket. In these tests, the temperature increase was monitored during sonication to estimate the amount of energy being converted to sensible heat. Following sonication, the temperature decrease was monitored to estimate the cooling effect due to heat transfer into the surrounding air as well as into the metal base of the stir plate upon which the bench-scale reactor sat. Figure 5.2 shows the curves obtained during these experiments.

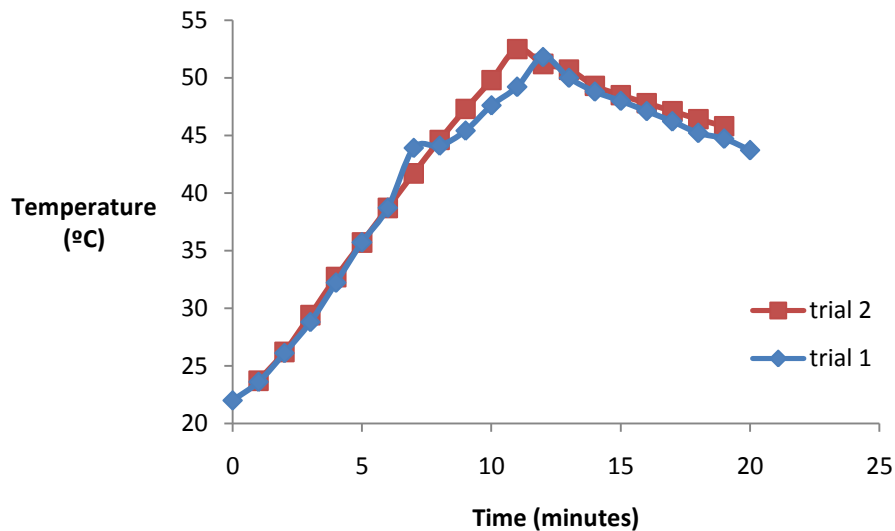


Figure 5.2. Un-moderated temperature curves due to sonication

During the sonication phase of the experiment, both heating and cooling were present, and after sonication only cooling took place. Heating was assumed to be linearly related to the power input, while the cooling was assumed to be linearly related to the difference in temperature between the reactor and the surrounding air. The assumed model for temperature change is summarized in Equation 5.1.

$$\Delta T = (1 - E) \frac{P_{in}}{c_p \times m} - (T - T_{air})k \quad \text{Equation 5.1}$$

Where

ΔT is the change in temperature of the sample ($^{\circ}\text{C s}^{-1}$),

E is the efficiency of ultrasound to solids transfer of the reactor,

P_{in} is the input power to the reactor (W),

c_p is the specific heat capacity of water ($\text{J g}^{-1} \text{ } ^{\circ}\text{C}^{-1}$),

m is the mass of water (g)

T and T_{air} are the temperatures of the sample and the surrounding air ($^{\circ}\text{C}$) and

k is a cooling rate coefficient (s^{-1}).

During the cooling phase P_{in} is equal to zero and Equation 5.1 simplifies so that the cooling rate can be estimated according to $\Delta T = -(T - T_{air})k$. For the two tests k was estimated at 6.5×10^{-4} and $5.2 \times 10^{-4} \text{ s}^{-1}$. The average of these two values was used, $5.8 \times 10^{-4} \text{ s}^{-1}$.

Once the cooling rate is known, the only other unknown was the efficiency E . By substituting all of the known values into Equation 5.1 and fitting the heating curves by minimizing the sum of squared error for both trials at the same time, the efficiency was estimated to be 26%. Figure 5.3 compares the model results to the experimental results.

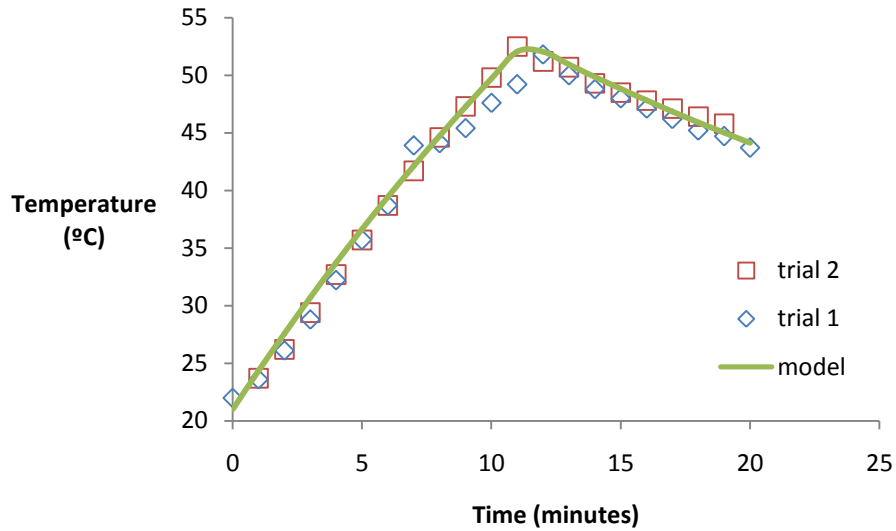


Figure 5.3. Sonication efficiency model results

It can be seen in Figure 5.3 that the dimensionally homogeneous model proposed in Equation 5.1 is capable of representing the heating well. The 26% efficiency means that the majority of the energy applied using the bench-scale apparatus was actually converted to heat, and since cooling was applied throughout the experiments, only one quarter of the energy applied was actually used for ultrasonic degradation of biomass.

5.2.COD and BOD responses

Since the ASM-based models all consider wastewater fractions in terms of COD fractions, the most basic consideration for modeling is directly measured COD. Also critical are the accompanying changes in biodegradability of these fractions. Biodegradability was assessed using respirometry, which also allows for estimation of biochemical oxygen demand (BOD) since a BOD measurement is a respirometric test of fixed interval.

In addition to total COD, soluble COD was measured in two ways. Flocculated and filtered COD provided a measure of the truly soluble COD, since during flocculation and filtration colloidal COD is captured by flocs and removed from the sample. On the other hand, conventional filtered COD, filtered using glass fibre filters without any flocculant, includes some of the colloidal material as well. Increases of both the soluble and the colloidal fractions were expected following ultrasound pre-treatment.

5.2.1. Total COD

Total and soluble COD were measured on the pre-treated and control samples and, despite significant variability in the samples, an increase in COD solubility without any change in overall COD was observed. Figure 5.4 shows the change in total COD that was observed through pretreatment, illustrating the variability of measurements. The change in total COD was calculated by difference between final and initial total COD measurements.

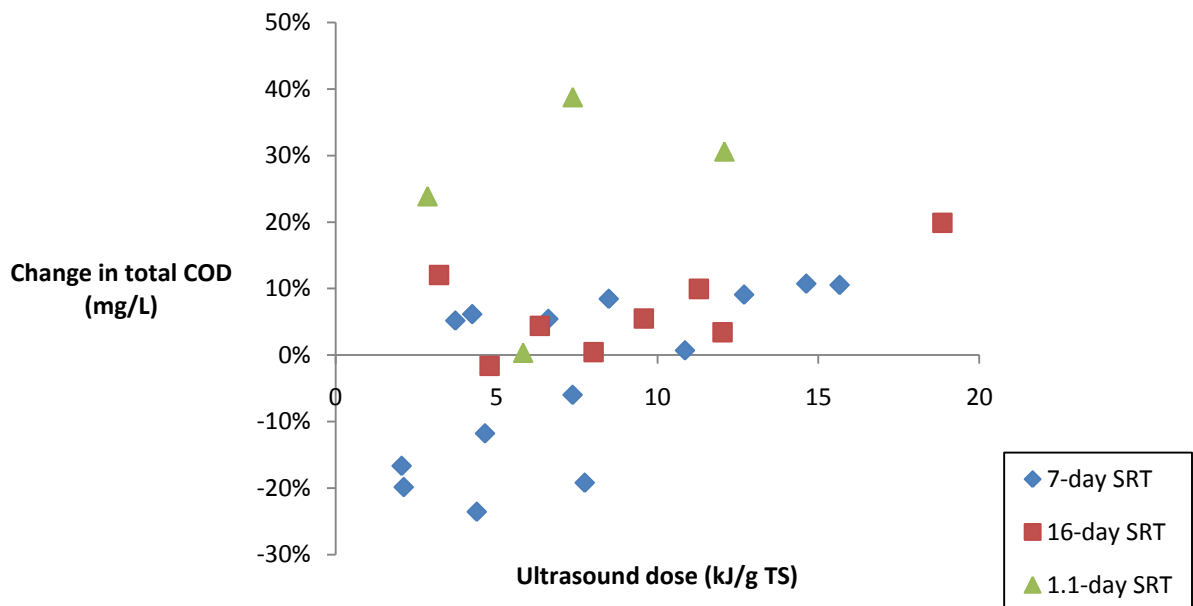


Figure 5.4. Change in total COD during sonication

Some of the change in total COD measured was likely due to the changing partitions of the total COD. It is possible that the COD digestion used did not completely break down all biomass, and digestion was aided by pre-treatment using ultrasound which increased the

soluble and colloidal (and therefore easily digested) COD. Allowing the sample to stand before sampling, or inadequate mixing in general, can allow samples to become stratified as was illustrated in Figure 5.1. It was assumed that the data scatter in Figure 5.4 was due to this sort of error. Considering increases in total COD as positive and decreases as negative, the average change in total COD was 4% with a standard deviation of 15%. It was not possible to reject a null hypothesis that the mean change of total COD was zero at a 90% confidence interval.

5.2.2. Soluble COD

Soluble COD, measured following flocculation and filtration with a 0.45 μm filter, increased for all ultrasound doses tested. The changes in soluble COD plateaued or leveled off for the higher doses. Figure 5.5 shows the changes in soluble COD fraction that were observed as a function of ultrasound dose, for the different sludge SRTs tested. The data collected using the 7-day SRT sludge show the most consistent trend, but trends for all three SRTs were consistent with one another. The model proposed for COD increase is plotted as a dashed line.

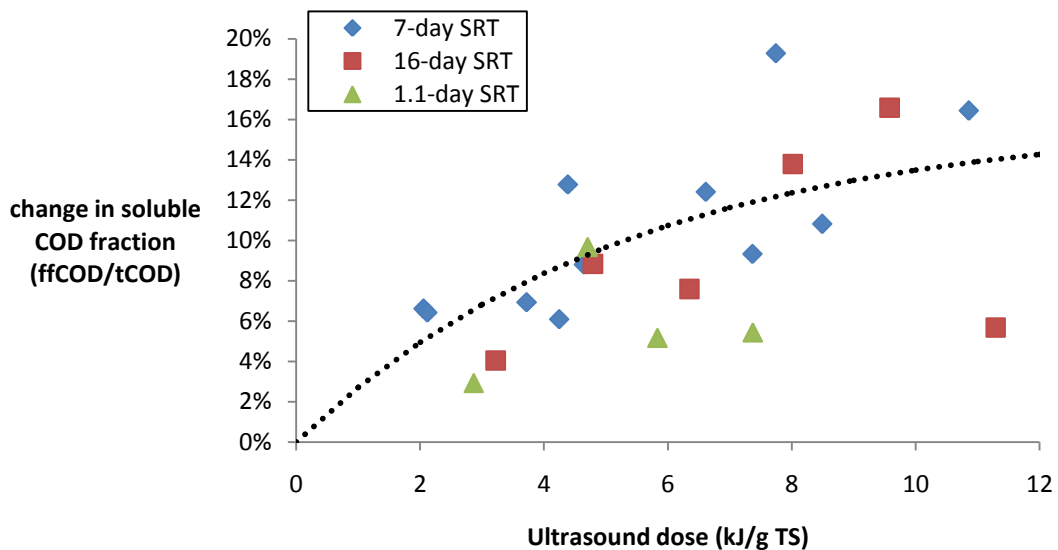


Figure 5.5. ffCOD fraction following pretreatment

The model for soluble COD increase as a function of ultrasound dose plotted as a dashed line in Figure 5.5 is

$$\frac{\Delta fCOD}{tCOD} = S_{max} \times e^{-\omega/k} \quad \text{Equation 5.2}$$

Where

$\Delta fCOD$ is the increase in truly soluble COD concentration (mg/L)

$tCOD$ is the total COD concentration (mg/L)

S_{max} is the maximum soluble fraction

ω is the ultrasound dose (kJ/g TS)

k is the dose constant (kJ/g TS)

To find the curve which best represented these data from the family of curves described by Equation 5.2, the sum of squared error was minimized. The long- and short-SRT data did not appear to fit this model well. Using the 7-day SRT data, S_{max} was determined to be 19% and the dose constant, k , was found to be 6.4 kJ/g TS. The average error between the values estimated by this equation and the measured data was 2.9%.

Since the overall trend for all SRTs seemed similar to that of the 7-day SRT data, the same procedure was used to fit the equation including all of the data: In this case, the fitted value for S_{max} was determined to be 16% and the dose constant, k , was found to be 5.3 kJ/g TS. The average estimate error increased slightly, to 4.2%, but the number of data points considered was doubled from 14 to 28. The second fit which included more data is the one shown on Figure 5.5.

5.2.3. Colloidal COD

The soluble plus some colloidal COD was measured by filtering samples with standard glass fibre filters before COD measurement. The amount of COD measured in this way also increased as the ultrasound dose applied increased. Figure 5.6 shows the COD values measured.

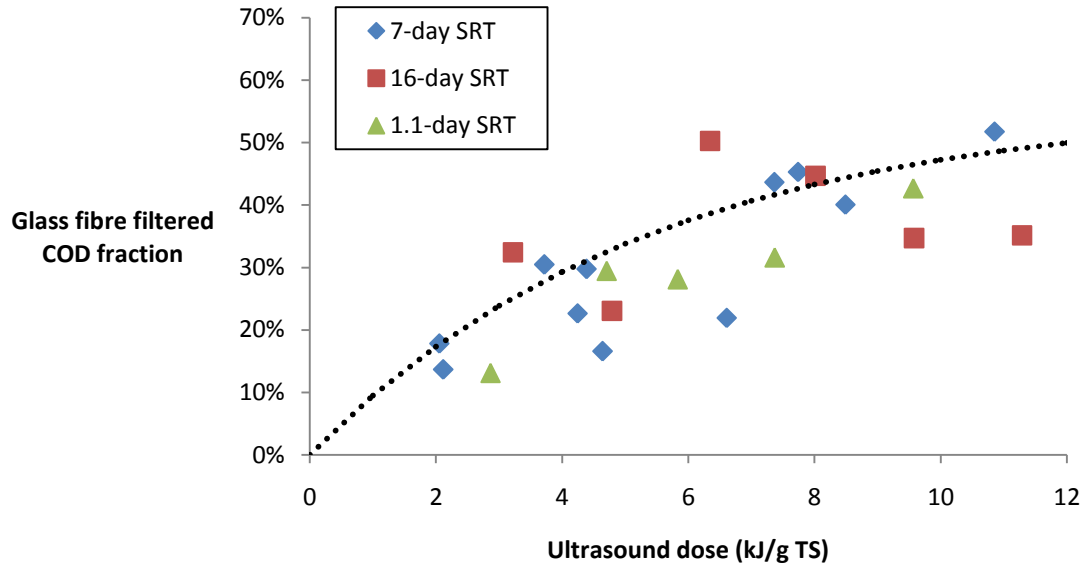


Figure 5.6. Glass filtered fraction following pretreatment

The curve fit to the glass fibre filtered (GFF) COD data, plotted as a dashed line in Figure 5.6, is described by:

$$\frac{\Delta sCOD}{tCOD} = S_{max,GFF} \times e^{-\omega/k} \quad \text{Equation 5.3}$$

Where

$\Delta sCOD$ is the change in soluble plus colloidal COD concentration (mg/L)

$tCOD$ is the total COD concentration (mg/L)

$S_{max,GFF}$ is the maximum glass fibre filtered fraction

ω is the ultrasound dose (kJ/g TS)

k is the dose constant (kJ/g TS)

Following the same procedure as used with the flocculated and filtered COD, Equation 5.3 was fit first to the 7-day SRT data and then to all of the data together. For the 7-day SRT data, the fitted value of $S_{max,GFF}$ was found to be 67%, and the dose constant was 9.0 kJ/g TS. The average estimate error was 6.4%. When all of the data were used, $S_{max,GFF}$ and k were both lower, at 62% and 7.9 kJ/g TS, respectively. The average estimate error was similar, at 7.3%. The model shown is for the second solution, using the data for all SRTs.

5.2.4. Particulate COD

Since total COD did not change significantly through ultrasonic pretreatment, the change in particulate COD was assumed to be equal but opposite to the combined change in soluble and colloidal COD. Equation 5.4 describes the change in particulate COD, and uses the same fitted constants as described in Section 5.2.3 above.

$$\frac{\Delta pCOD}{tCOD} = -S_{max,GFF} \times e^{-\omega/k} \quad \text{Equation 5.4}$$

Where

$\Delta pCOD$ is the change in particulate COD concentration (mg/L), always negative, to represent a decreasing value

$tCOD$ is the total COD concentration (mg/L)

$S_{max,GFF}$ is the maximum glass fibre filtered fraction

ω is the ultrasound dose (kJ/g TS)

k is the dose constant (kJ/g TS)

5.2.5. Heterotrophic organisms

In the secondary sludge of each reactor, the largest COD fraction was heterotrophic organisms, and it was expected that these organisms would be inactivated by ultrasonic pretreatment. The respirometry conducted in this study showed that under typical operation of the 7-day pilot SBR, these organisms comprised about 60% of the total COD. In the shorter SRT reactor, the proportion of COD made up of active heterotrophs was higher, due to washout of endogenous decay products and particulate inert matter. Figure 5.7 shows the observed response to ultrasound pretreatment, in terms of percent reductions of active heterotrophic biomass.

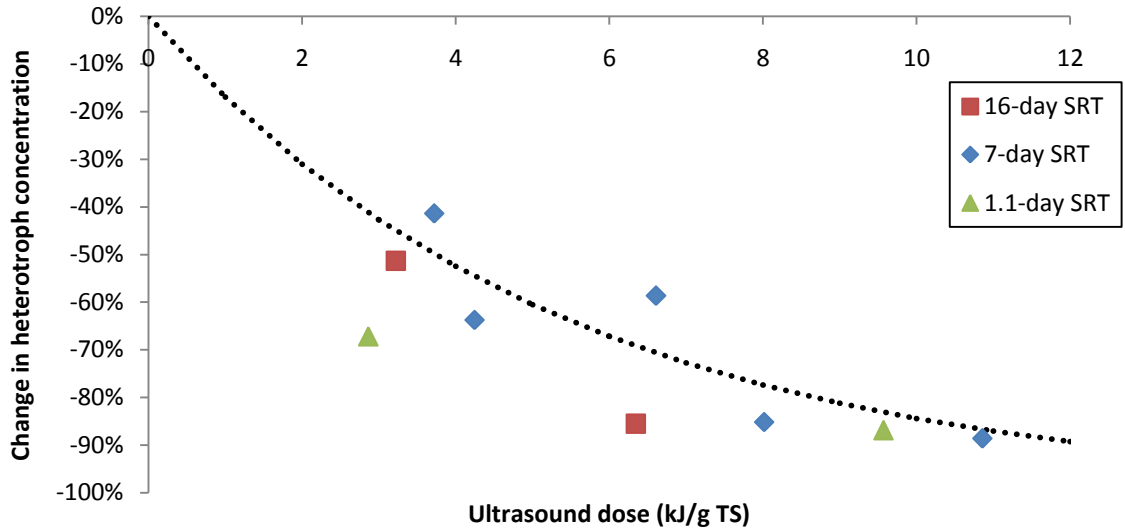


Figure 5.7. Inactivation of heterotrophic organisms

Active heterotrophs were observed to decrease exponentially with respect to ultrasound dose. The curve shown on Figure 5.7 is described by

$$\frac{Z_{bh} - Z_{bh,0}}{Z_{bh,0}} = e^{-\omega/k} - 1 \quad \text{Equation 5.5}$$

Where

Z_{bh} is the active heterotroph concentration (mg COD/L)

$Z_{bh,0}$ is the initial active heterotroph concentration (mg COD/L)

ω is the ultrasound dose (kJ/g TS)

k is the dose constant (kJ/g TS)

For these data, the different SRTs were not considered separately because of the smaller number of data. Unlike the earlier model fits, in this case a maximum conversion term was not used. The model was fit with minimum squared error for a dose constant of 4.8 kJ/g TS and an average error of 3% between the measured data and the proposed model. When a maximum conversion term was added to the model, the maximum conversion fit was over 91% and the average error remained at 3%. Since a very large pre-treatment dose would likely inactivate all the biomass, the model in Equation 5.5 seems more reasonable from a mechanistic perspective than one with a maximum conversion term.

5.2.6. Slowly biodegradable COD

Two other important responses to pretreatment are those of the biodegradable components, readily and slowly degradable substrates. The yield of degradable substrate due to sonication can be described by Equation 5.6.

$$Y_s = \frac{\Delta X_s + \Delta S_{bs}}{\Delta Z_{bh}} \quad \text{Equation 5.6}$$

Where

Y_s is the degradable substrate yield

ΔX_s is the change in slowly degradable substrate (mg COD/L)

ΔS_{bs} is the change in readily degradable substrate (mg COD/L)

ΔZ_{bh} is the change in heterotrophic biomass (mg COD/L)

Figure 5.8 shows the substrate yield described by Equation 5.6 as a function of ultrasound dose.

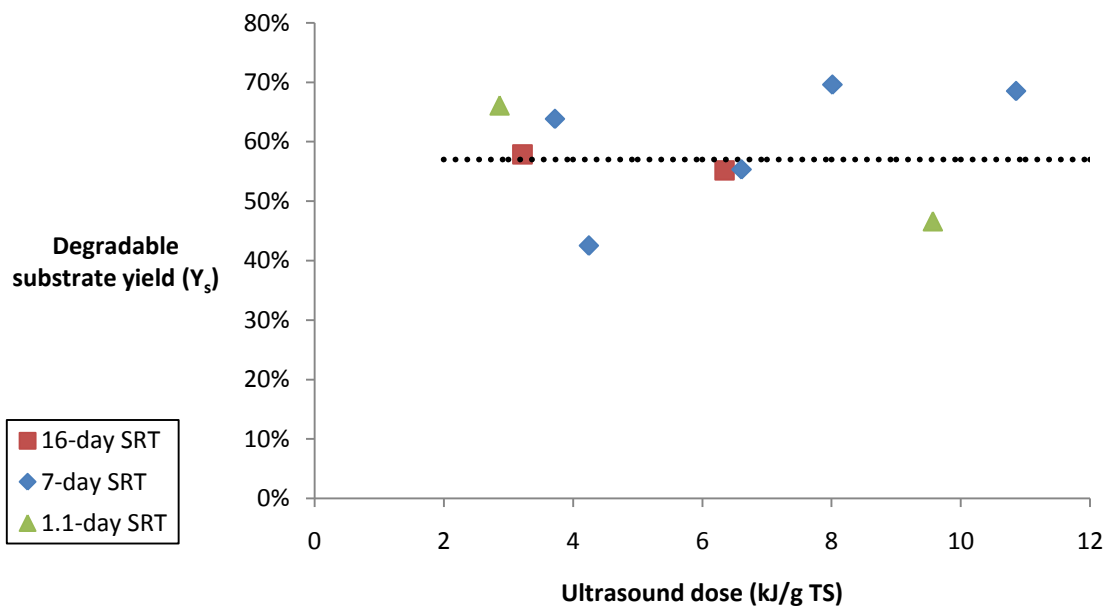


Figure 5.8. Conversion of heterotrophs to degradable substrate

The ratio of degradable substrate produced compared to the heterotrophs inactivated was found to be fairly constant over the range of ultrasound doses tested. On average, the value of Y_s was found to be 58% with a standard deviation of 10%. This value did not appear to depend on the SRT of the reactor which produced the sludge, however since only two data were measured for each of the long- and short-SRT reactors the confidence intervals for them were very large. When biomass is inactivated by endogenous decay, the simplified ASM model used predicted that 92% of the COD was bioavailable. This means that the methods used to measure biodegradable COD are missing 34% of the biomass COD which was expected to be biodegradable. To simplify the model, and to utilize similar bioavailable fractions, it was assumed that this 'missing' COD was biodegradable, but at a rate too slow for the analytical methods used.

5.2.7. Readily biodegradable COD

Although a constant fraction of biomass was converted to biodegradable substrate, the amount of readily degradable substrate produced was related not only to the heterotroph population inactivated. In addition to biomass conversion, slowly degradable substrate was converted to readily degradable substrate by sonication. The yield of readily degradable substrate is described by Equation 5.7.

$$Y_{sbs} = \frac{\Delta S_{bs}}{Y_s \times Z_{bh,0} + X_{s,0}} \quad \text{Equation 5.7}$$

Where

Y_{sbs} is the readily degradable substrate yield

ΔS_{bs} is the change in readily degradable substrate (mg COD/L)

Y_s is the degradable substrate yield defined in Equation 5.6

$Z_{bh,0}$ is the initial concentration of heterotrophic biomass (mg COD/L)

$X_{s,0}$ is the initial concentration of slowly degradable substrate (mg COD/L)

The initial particulate biodegradable COD which is available for conversion to readily degradable substrate was assumed to consist of the slowly degradable COD plus 57% (Y_s) of the initial heterotroph COD. Figure 5.9 illustrates the readily degradable substrate yield defined above as a function of the ultrasound dose applied.

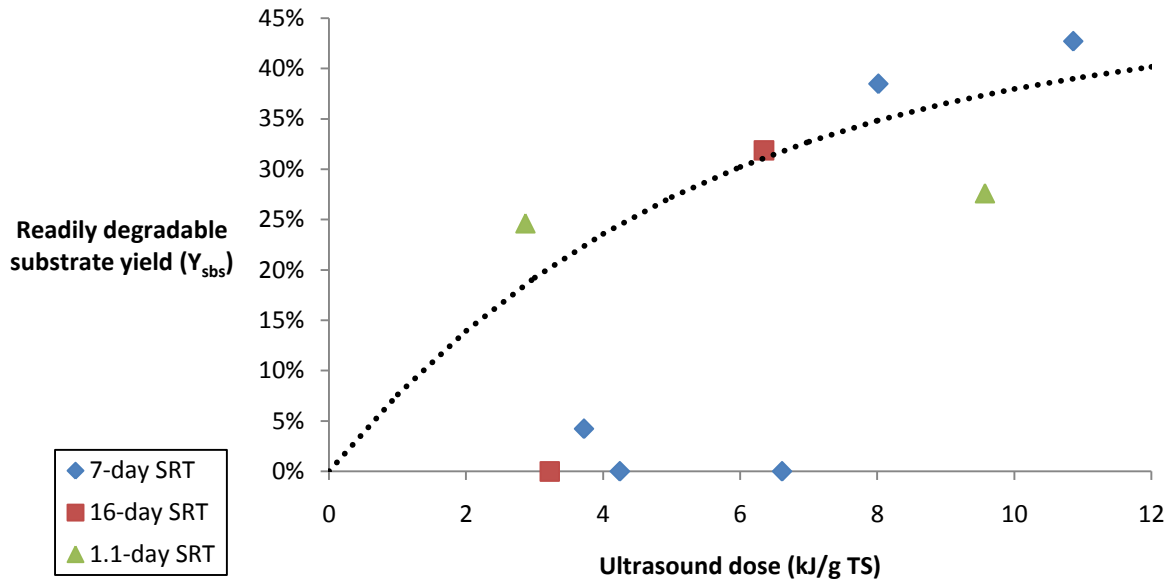


Figure 5.9. Formation of readily degradable substrate from heterotrophs and slowly degradable substrate

The data for readily degradable substrate were the least consistent of the respirometric data. Since the respirometric response to this fraction was very fast, it is possible that the readily degradable substrate was consumed between the time that pretreatment was performed and testing of the sample initiated. Nearly half of the tests conducted had no readily degradable substrate measured, however, those samples where readily degradable COD was found show a trend very similar to that of the other responses. The line in Figure 5.9 is described by

$$Y_{sbs} = 45\% \times (1 - e^{-\omega/k}) \quad \text{Equation 5.8}$$

Where

Y_{sbs} is the readily degradable yield defined in Equation 3

ω is the ultrasound dose (kJ/g TS)

k is the dose constant (kJ/g TS)

In this case the average value of k that had been obtained from fitting of the other responses shown in Section 5.2 provided a good fit of the non-zero data. The soluble COD produced

during sonication was less than the readily degradable COD measured by respirometry, as seen by comparing Figure 5.5 with Figure 5.9.

5.3. Nitrogen responses

Conversion between nitrogen species was not observed during ultrasound pre-treatment, however a decrease in total nitrogen occurred in most tests. Figure 5.10 shows the measured change in total nitrogen as a function of the ultrasound dose applied. Unfortunately the clear trends seen in the COD responses were not visible here.

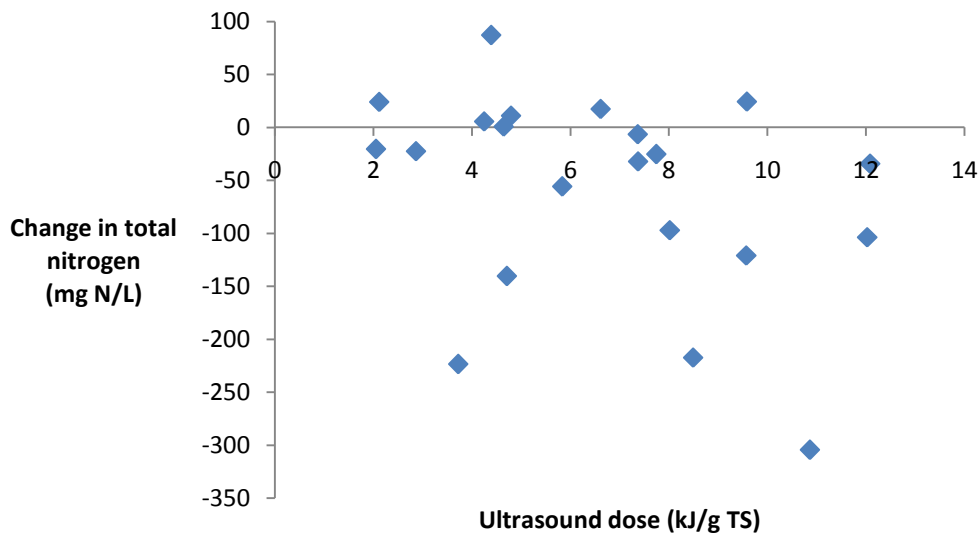


Figure 5.10. Change in total nitrogen during sonication

The majority of the change observed in total nitrogen can be attributed to the decrease in organic nitrogen, which was measured as the difference between total Kjeldahl nitrogen and ammonia. Figure 5.11 illustrates the changes in organic nitrogen measured. Although these are not identical to the changes in total nitrogen measured, the overall direction and magnitude of change for organic nitrogen are similar to those for total nitrogen.

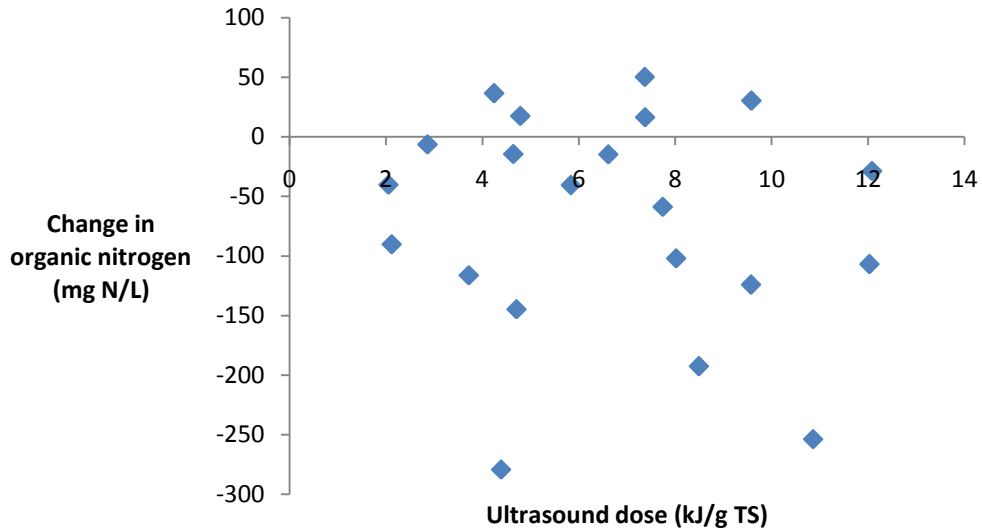


Figure 5.11. Change in organic nitrogen during ultrasound pre-treatment

The large variability observed in organic nitrogen was most likely caused by error in the measurement of TKN. The inorganic nitrogen species, measured by alkaline phenate (ammonia) and ion chromatograph (nitrite and nitrate) were all relatively unchanged through ultrasound pre-treatment. Figure 5.12 illustrates the measured changes in these species.

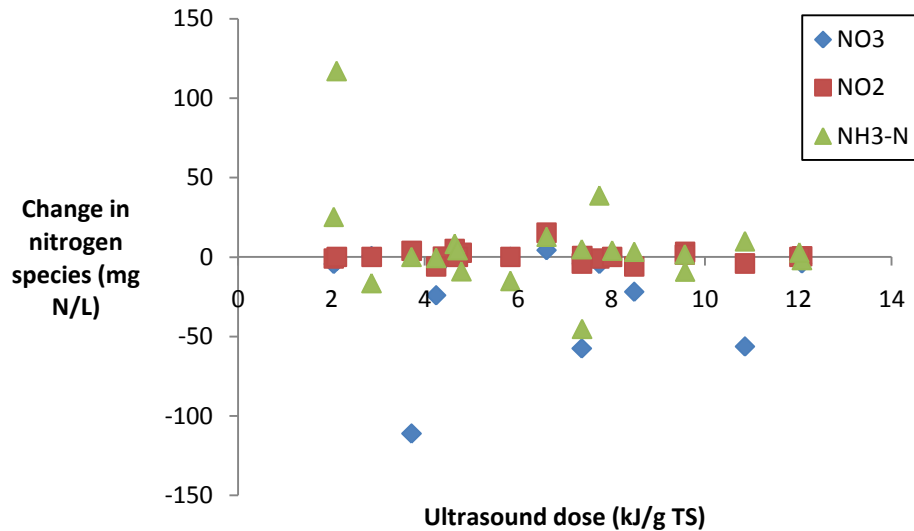


Figure 5.12. Change in inorganic nitrogen species during ultrasound pre-treatment

While there was one measured change around 100 mg N/L for each of ammonia and nitrate, the clear pattern is of very small changes about the axis. Based on Figure 5.12, no change in inorganic nitrogen was expected across ultrasound pre-treatment. Since the changes which were observed were only for organic nitrogen, and since these changes were not consistent and the majority of the values obtained were scattered around zero, no model was constructed for the conversion of nitrogen species.

5.4.pH response

In addition to COD and nitrogen fractions, the pH of samples was measured before and after pre-treatment. The maximum observed change in pH during pre-treatment was 0.4 pH units. In some cases, pH increased, while in other cases pH decreased. The change in pH resulting from sonication is shown in Figure 5.13.

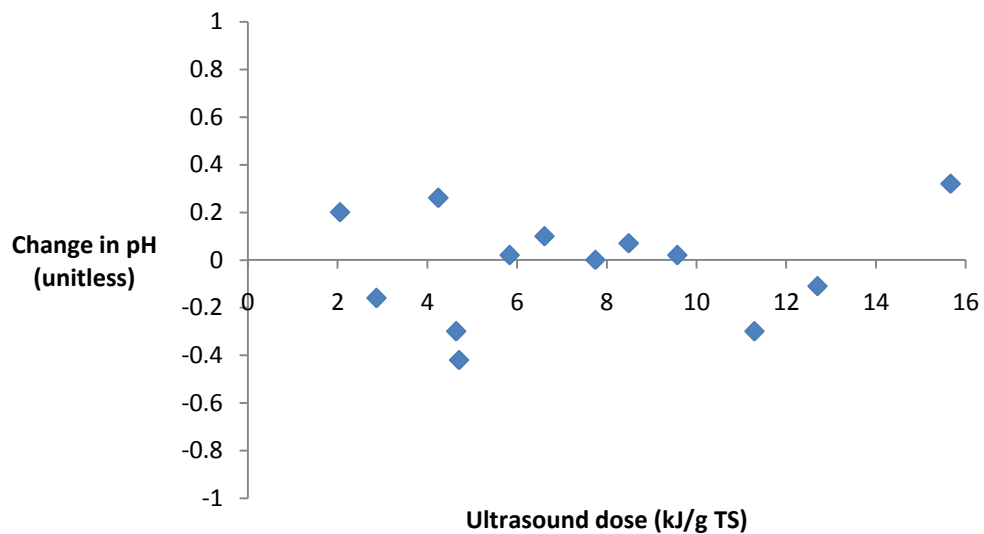


Figure 5.13. pH effects of ultrasound pre-treatment

The small observed changes in pH during sonication were not significant and did not show any clear trends.

6. Ozonation results

The overall goals of sludge ozonation are similar to sonication and other pre-treatments, but the mechanisms at work are different. Increased biodegradability is again the goal, but with ozonation there is potential for mineralization of biodegradable components, which is directly counter to the desired effect.

Most published research presents ozone dose in terms of suspended solids ($\text{mg O}_3/\text{mg SS}$). In these experiments the response was found to be more closely related to the COD content of sludge treated, and so the units used throughout this section are in these terms ($\text{mg O}_3/\text{mg COD}$). Since most systems have a stable ratio of suspended solids to COD, converting between these units is relatively straightforward in practice.

Due to time constraints, only the 7-day SRT sludge was tested using ozone. This resulted in slightly more useful data for the 7-day sludge compared to the ultrasound pre-treatment trials, but the effect of different sludge ages could not be estimated.

During pre-treatment, two changes to the sludge were observed visually. Both of the changes are illustrated by the photo shown in Figure 6.1. Both of the pictured samples contained the same amount of solids, approximately 0.7%, but different amounts of ozone had been consumed. The sample shown on the left consumed 70 mg of ozone, while the sample on the right consumed 364 mg. At the higher ozone dose, the apparent colour of the sample decreased. The smaller ozone dose showed only a slight change compared to the control sample (not shown here). From this change it was seen that ozone is able to oxidize colour-causing components of sludge, however this effect is not important for sludge pre-treatment.



Figure 6.1. Illustration of the decrease in colour following ozonation

At the same time as the decrease in colour, and also visible in Figure 6.1, a significant portion of the suspended solids floated to the top of the liquid phase during ozonation. This solids behaviour was in stark contrast to the control sample, where all of the suspended solids would settle to the bottom. The solids which floated to the top also produced large amounts of foam during pre-treatment. The change from settleable solids to floatable solids could mean that downstream gravity settling processes would be less effective, and at the same time flotation processes more effective.

6.1.Ozone transfer efficiency

The efficiency of ozone transfer for the reactor used was estimated by comparing the ozone supplied to the ozone consumed. This estimate provides a lower bound for the true transfer efficiency since dissolved ozone was purged after testing; some ozone may have been transferred and then stripped back out of the liquid. The measurement technique used to obtain these values is described in Section 3.2.3. At low doses, the efficiency was typically in

the range of 30 - 40% while at higher doses 40 - 70% of the supplied ozone was consumed. Figure 6.2 compares the ozone supplied to the ozone consumed when concentrated sludge was pre-treated. The data show that overall approximately half of the ozone supplied was consumed – the slope of the linear trendline is the average ozone transfer efficiency.

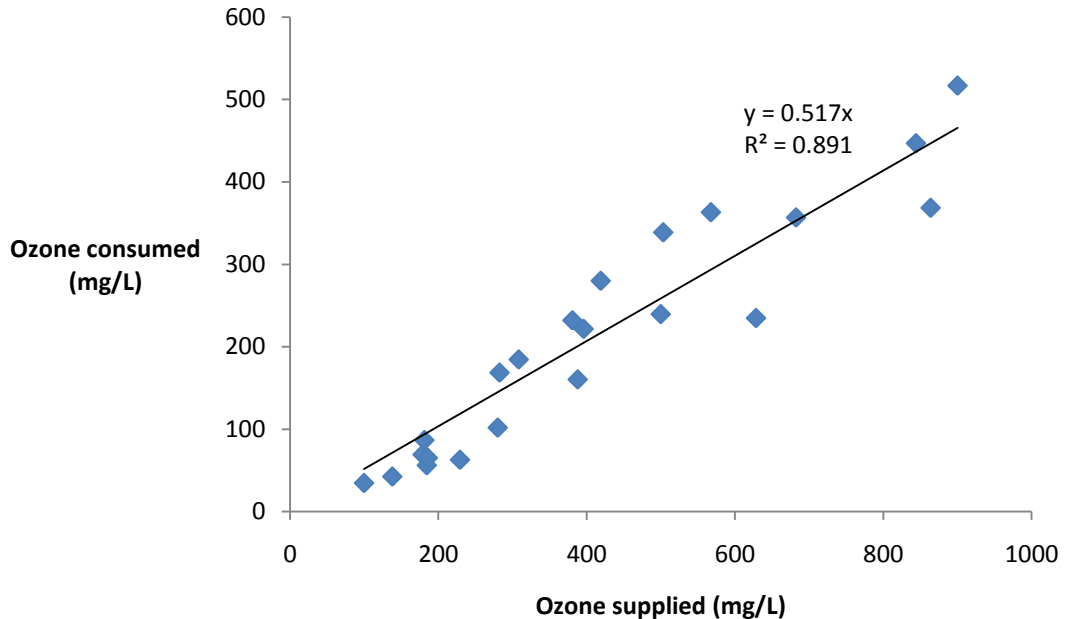


Figure 6.2. Ozone transfer efficiencies

The increased ozone transfer efficiency observed at higher doses may be attributed in part to the flotation and foaming of solids noted in the previous section. The foam which formed above the liquid column had extremely high surface area compared to the liquid column, and this could have enhanced gas transfer rates for the ozone.

As mentioned in Section 2.3.3, previous research has indicated that low ozone doses may be the most cost-effective for pre-treatment of sludge, but in this study these low doses were found to have the lowest transfer efficiency. Since the generation of ozone has a high energy cost, improvements to ozone transfer at low dose would be of great benefit for sludge pre-treatment.

6.2. COD and BOD responses

Total COD, glass fibre filtered COD, and flocculated filtered COD were measured in the same way as described for ultrasound pre-treatment. Respirometry was again used to obtain biochemical oxygen demand information. The measured responses are presented and discussed in the following section.

6.2.1. Total COD

The total COD of the pre-treated samples was measured for each pre-treatment trial, and compared to the total COD of the un-treated sludge. By taking the difference of these two measurements, the change in total COD during pre-treatment was calculated. Theoretically, this number should be less than or equal to zero, since adding an oxidant cannot increase the oxidant demand. In practice, however, a number of positive changes in total COD were measured. Figure 6.3 shows the measured changes in total COD.

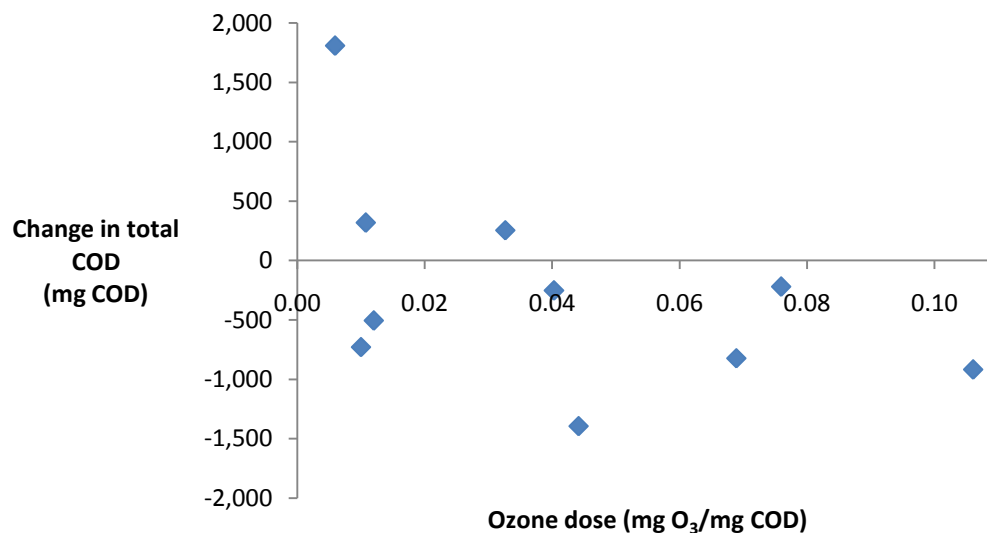


Figure 6.3. Change in total COD following ozonation

The data in Figure 6.3 show a generally decreasing trend in total COD with increasing ozone dose, but the overall trend was not specific enough to be useful for prediction. The average decrease was 247 mg/L with a standard deviation of 894 mg/L however if the large increase found in one test is excluded the average decrease in total COD was much larger, at 475 mg COD/L, while the standard deviation was lower at 559 mg/L.

While overall no trend could be fit to the measured data, two phases were expected for the total COD response. During the first and more desirable phase, slowly- or non-degradable matter would be converted to more degradable forms and little or no change in total COD would be observed. Following this desirable conversion, an undesirable oxidation of biodegradable matter would occur, resulting in a high energy cost for the removal of COD compared to more conventional wastewater treatment processes.

The rapid flotation of solids noted in the introduction to this chapter made the measurement of total COD following ozonation somewhat more challenging, since the samples were more difficult to mix.

6.2.2. Soluble and colloidal COD

Following ozonation the COD present in the filtrate increased for both glass fibre filtered and flocculated and filtered samples. Figure 6.4 illustrates the COD solubilization that was measured, the increase of which was described well by a linear model. For either of the filtration methods used, the solubility of COD as a function of the ozone dose could be fit linearly with R^2 values of about 0.94.

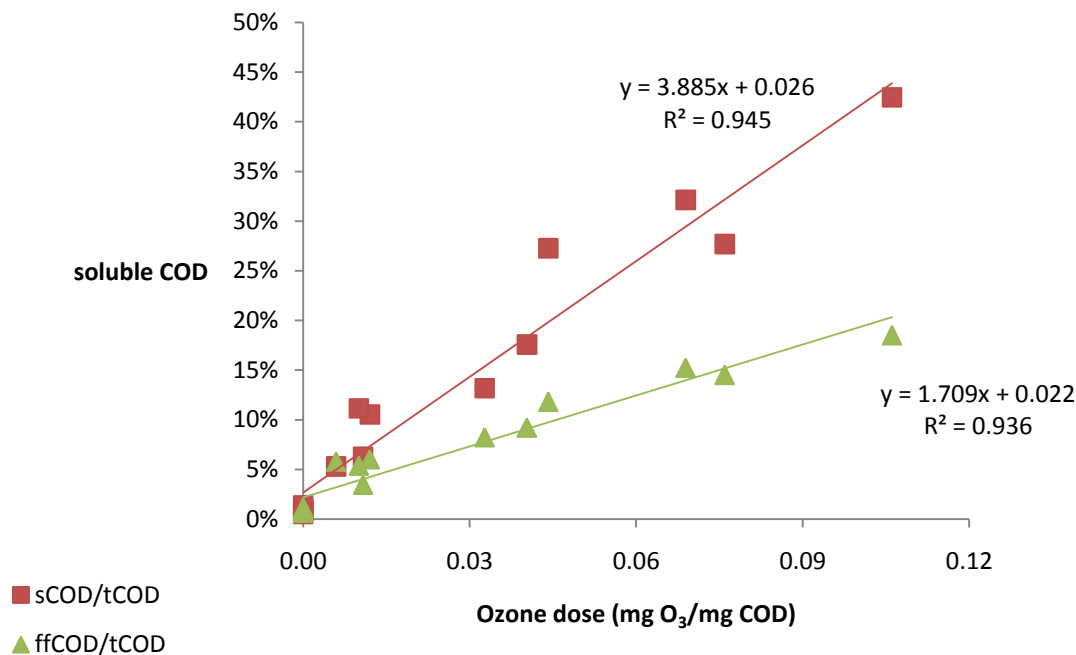


Figure 6.4. Change in filtered COD following ozonation

The rate of solubilization for truly soluble COD was $1.7\%/mg\ O_3/mg\ COD$, based on the flocculated and filtered COD data. Since the glass fibre filtered COD measured soluble plus some of the colloidal COD, the difference between the two lines in Figure 6.4 provides a lower bound estimate of the amount of colloidal COD produced: $3.9 - 1.7 = 2.2\%/mg\ O_3/mg\ COD$

The increase in soluble COD fits well with the conceptual model of increased biodegradability, since soluble COD is often correlated with biodegradable COD. At high doses it was expected that the soluble COD would be readily oxidized by the ozone and the soluble COD concentration would decline. One possible reason why a reduction in soluble COD was not observed is that the doses tested were not high enough for the mineralization effect to be important.

6.2.3. Heterotrophic biomass

As discussed in Section 4.3, the model used for analysis of respirometric data showed significant lack of fit, in particular for the higher ozone doses. Changing the model used to interpret these data could change the results presented in the next two sections significantly. In particular, further investigation into the mechanisms behind the high rate exponential curves observed could assist in improving this interpretation.

Figure 6.5 illustrates the change in active heterotroph concentration (plotted logarithmically) as a function of the ozone dose consumed. The inactivation of heterotrophs appeared to follow the typical inactivation which is assumed for pathogenic organisms when using ozone as a disinfectant [see for instance, Tchobanoglous and Schroeder, 1987]

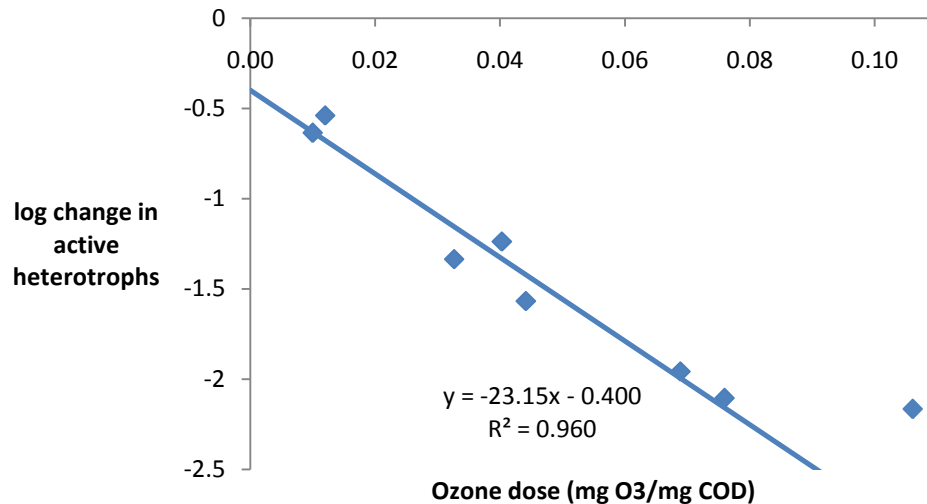


Figure 6.5. Change in heterotroph concentrations as a function of ozone dose

The linear fit shown in Figure 6.5 was determined excluding the value measured for the highest ozone dose. For the highest dose, the large amount of inactivation (>99%) could have resulted in a heterotroph concentration which was too low to be estimated well by the analysis technique used. The slope of the fitted dose-log inactivation curve could not be compared directly with disinfection curves, which do not have ozone dose relative to COD or solids since these are typically both very low during disinfection. Instead, for disinfection ozone dose is measured in terms of c-t (concentration times time).

6.2.4. Biodegradable COD

In most of the experiments the biodegradable substrate concentration, measured by respirometry, increased. Figure 6.6 illustrates the overall biodegradable COD produced relative to the initial heterotroph concentration.

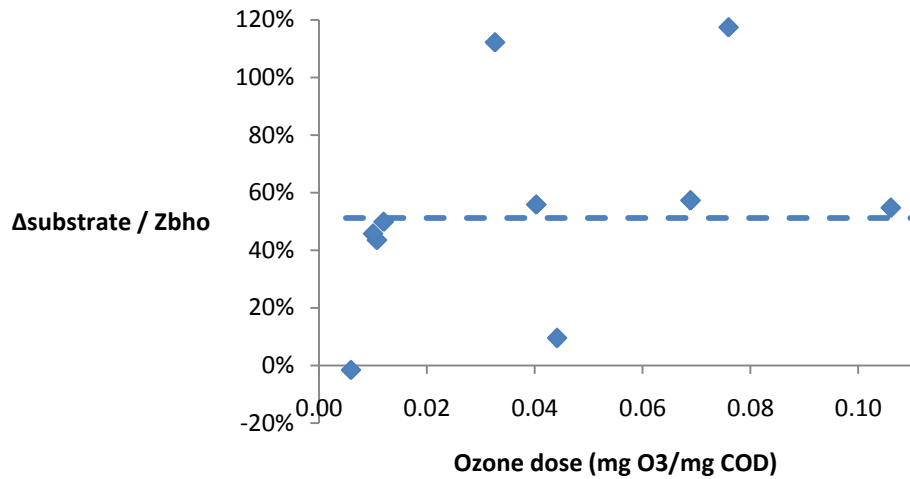
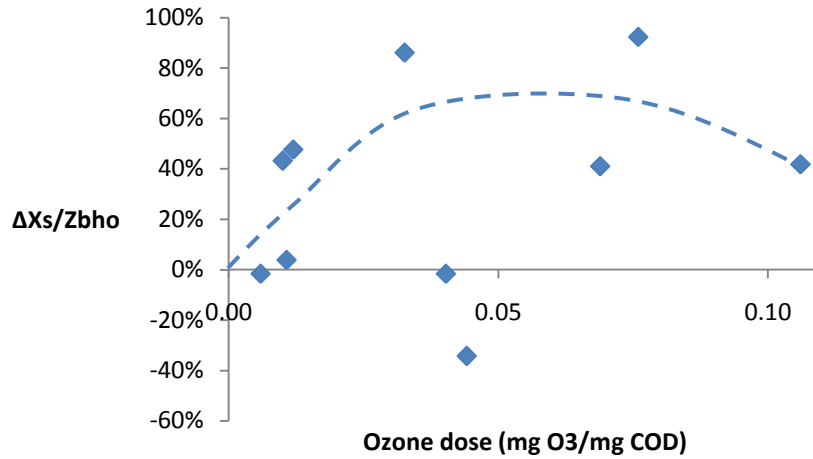


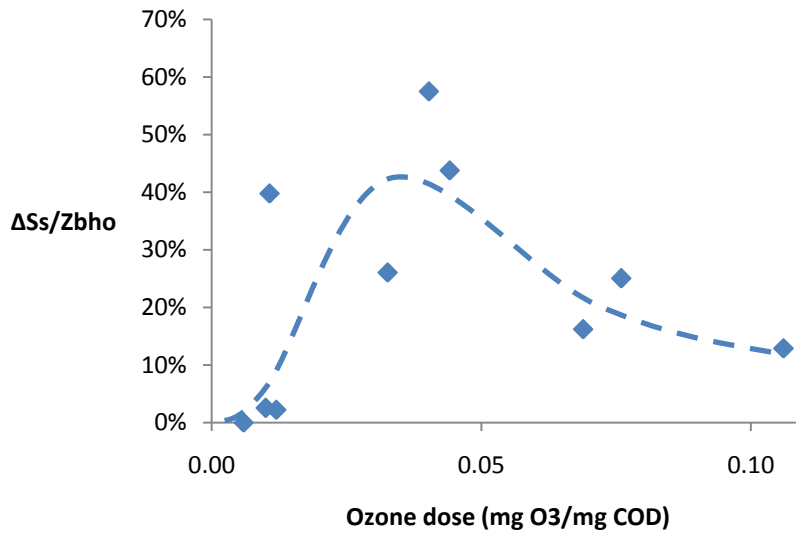
Figure 6.6. Biodegradable substrate produced on inactivation of heterotrophs

From Figure 6.6 it can be seen that the amount of degradable COD produced varied from none to more than the amount of heterotroph COD initially present. The ozone dose did not appear to be an important factor in the production of biodegradable substrate. Six of the tests, distributed over the whole range of doses tested, found the heterotroph COD was converted to biodegradable COD, with a mean conversion of 51% and standard deviation of just 6%. This mean conversion of 51% is indicated by the dashed line in Figure 6.6. The other data consisted of two tests with nearly zero yield and two with greater than 100% yield. When all 10 tests were considered, the mean yield changed only slightly, to 54%, but the standard deviation increased more than six-fold, to 38%.

Figure 6.7 shows the slowly and readily biodegradable fractions separately. These data did not show any clear relationship between the two biodegradable fractions and the ozone dose consumed.



a) Slowly biodegradable



b) Readily biodegradable

Figure 6.7. Slowly and readily biodegradable COD released by ozonation with speculative trendlines

Overall, the changes in biodegradable fractions did not follow consistent trends. The curves shown in the preceding figures are highly speculative and not clearly supported by the data.

The curves are, rather, intended to show one way in which the data could be interpreted. To describe the curves shown, the important conversions would be of heterotrophs to biodegradable material and biodegradable material to fully oxidized material. The conceptual curves show how the data could be loosely interpreted to show an increase in biodegradable COD up to a maximum which occurred around 0.04 mg O₃/mg COD. Following this dose, the readily degradable COD decreased rapidly and slowly degradable COD plateaued until the dose reached about 0.08 mg O₃/ mg COD. After this dose, readily degradable COD was present only in small quantities and slowly degradable COD started to decrease. Further study is needed to determine whether or not these trends were actually taking place under the experimental conditions used.

6.3.Nitrogen responses

Several conversions of nitrogen are possible, including oxidation, solubilization, and stripping. Oxidation would result in a conversion from lower to higher oxidation state, solubilization a conversion from particulate to soluble species, and stripping in an overall loss of nitrogen. Overall, the total amount of nitrogen present should only decrease by the last of these three processes. The total nitrogen should not increase by any of these processes since no nitrogen was introduced into the sample during the pre-treatment. Figure 6.8 shows the measured change in total nitrogen, calculated by summing the measured TKN, nitrate, and nitrite values.

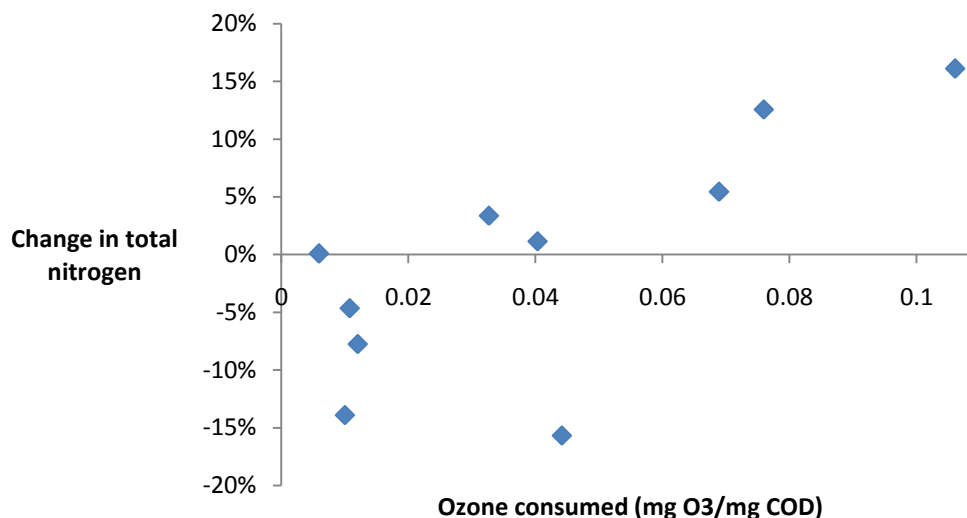


Figure 6.8. Change in total nitrogen during ozonation

The total amount of nitrogen present in the samples appeared to increase slightly with increasing ozone dosage. This measured change could be due to incomplete TKN digestion for the un-treated samples, with the treated TKN values being higher and more accurate. Overall, the changes in total nitrogen measured were mostly within the measurement errors on the order of 10% which were expected for high levels of TKN.

Since the various nitrogen fractions were measured separately, the response of each form of nitrogen was also considered separately. During ozonation, the oxidation state of nitrogen was expected to increase, and the following discussion considers nitrogen species in order of ascending oxidation state. The most reduced oxidation state for nitrogen occurs in ammonia and also most organic nitrogen (-III) and the highest in nitrate (+V).

Dissolved gaseous nitrogen (N₂) was not measured for these experiments, but would likely have been stripped from the samples by the ozone in pure oxygen used. Stripping of ammonia was not expected to be significant, since the sample pH was always below 7.5, at which point ammonium ion concentration predominates over ammonia by more than 50:1.

6.3.1. N^{III}: Ammonia and organic nitrogen

Ammonia and organic nitrogen were the most reduced forms of nitrogen present, and together make up the Total Kjeldahl Nitrogen. TKN was measured as well as soluble TKN, and

the changes in TKN and soluble TKN across pre-treatment (calculated by difference) are given in Figure 6.9 below.

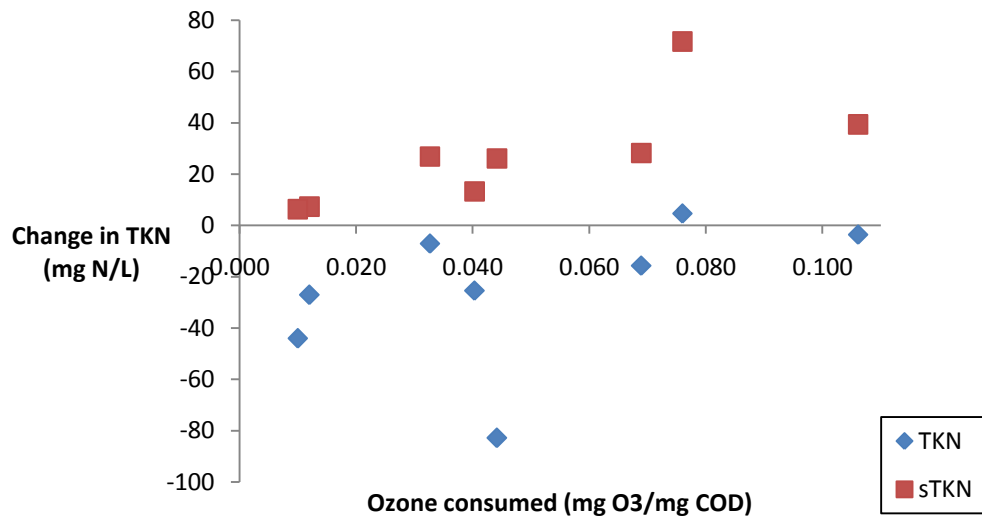


Figure 6.9. Change in TKN and sTKN due to ozonation

TKN values for the raw sludge were typically 200 – 400 mg/L, and most of the measured changes illustrated in Figure 6.9 were less than 10% of this range. Untreated sTKN values were between 30 - 60 mg/L, and this value increased for every ozone dose tested.

Ammonia was relatively unchanged by ozone pre-treatment, with small increases between 0 and 2 mgN/L measured. This suggests that the observed increases in sTKN observed represent increases in soluble organic nitrogen, and that the dominant response observed was solubilization of organic nitrogen, with very little oxidation or stripping.

6.3.2. N^{III+}: Nitrite

Nitrite levels were very low both before and after pre-treatment, with the exception of one untreated sample. Typical values were below 5 mg/L as nitrogen, with one sample at 17 mg/L. Figure 6.10 shows the change in nitrite due to ozonation, calculated by difference between treated and untreated samples.

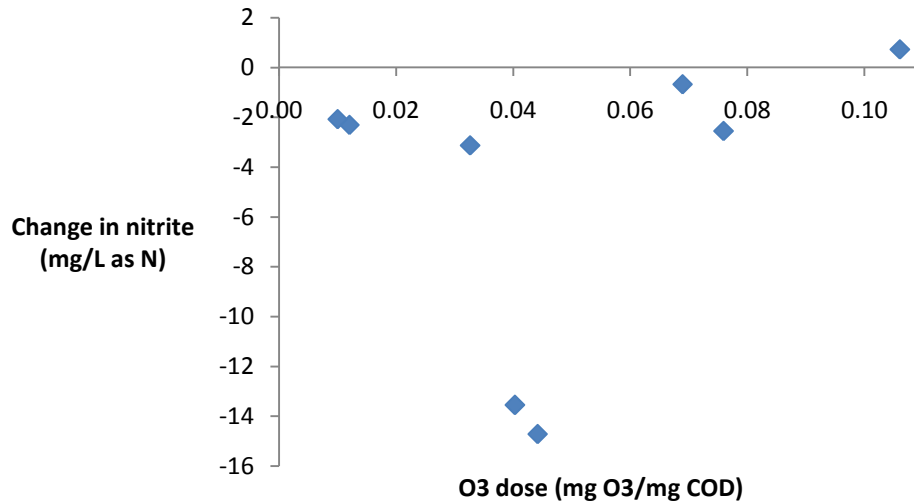


Figure 6.10. Change in nitrite during ozonation

The sample which contained significant nitrite seemed to have this oxidized to nitrate during ozonation, as shown in the next section.

6.3.3. N^{V+} : Nitrate

The most oxidized form of nitrogen is nitrate, and the concentration of this species was observed to increase for all the ozone doses tested. The production of nitrate increased with increasing dose for most samples. The exception was that much higher nitrate production was observed for the samples which contained elevated nitrite before pre-treatment. This oxidation of nitrite to nitrate by ozone is not considered further here.

The overall production of nitrate plus nitrite was considered instead of the two species separately. The production of these two species together appeared more predictable as a function of ozone dose than either one alone, as illustrated in Figure 6.11.

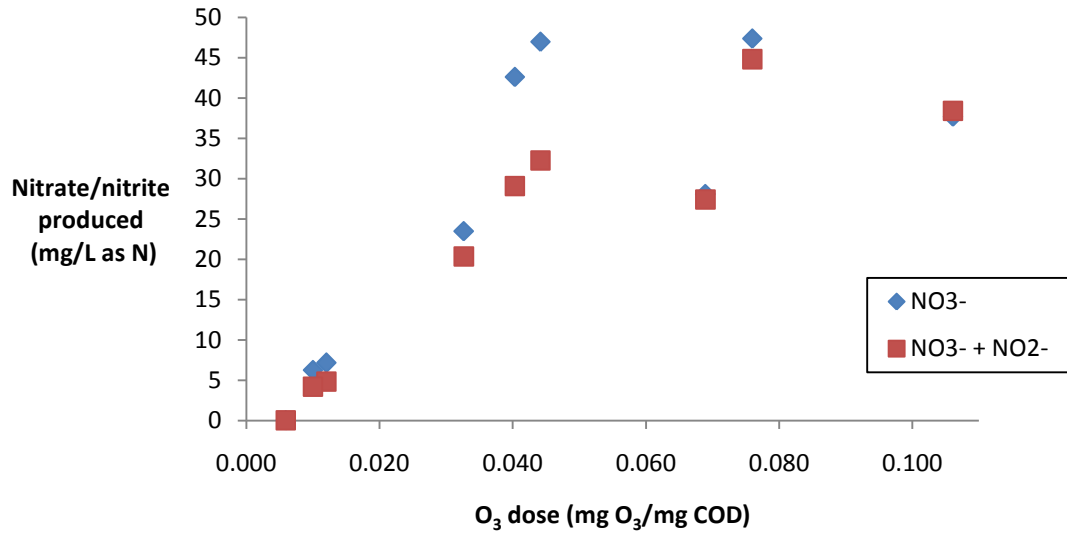


Figure 6.11. Nitrate & nitrite produced by ozonation

The production of nitrate and nitrite appeared to be related to the ozone dose applied, and an exponential model was fit to the conversion, as shown in Figure 6.12.

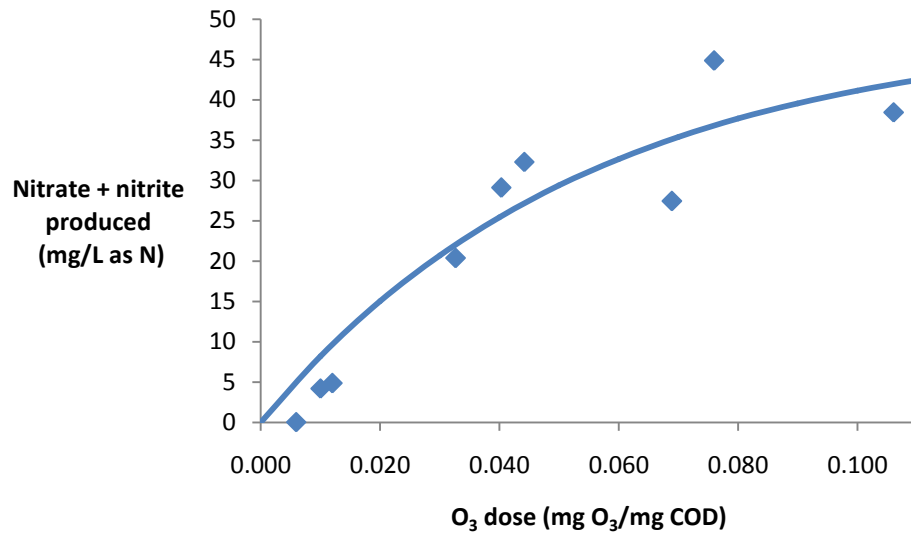


Figure 6.12. Ozone conversion model for nitrite and nitrate

The curved line which models nitrite and nitrate production is described by Equation 6.1:

$$\Delta NO_{2,3} - N = 49 \text{ mg/L} (1 - e^{-18.3 \times \text{dose}}) \quad \text{Equation 6.1}$$

Nitrite and nitrate should have been formed only due to the oxidation of the components of TKN. To see if this was true, the change in NO_3^- and NO_2^- was plotted as a function of the change in TKN in Figure 6.13.

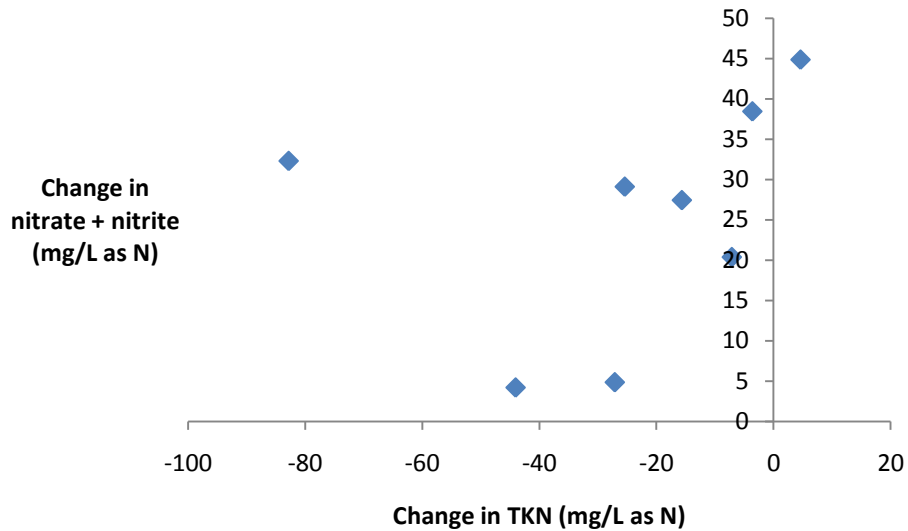


Figure 6.13. Change in nitrate & nitrite relative to change in TKN

Since all the nitrogen species were expressed in terms of nitrogen, the expected result in Figure 6.13 was a straight line with slope -1, passing through the origin. The data did not show this trend at all, possibly because the change in TKN measurements was small compared to the values being measured. The nitrate and nitrite measurements were more sensitive and the initial concentration was typically close to zero.

6.4.pH response

The pH of the raw sludge was neutral, with values between 7.3 and 7.5 measured. Following ozonation, the pH remained in the neutral range but tended to be slightly lower than before pre-treatment. Figure 6.14 illustrates the pH measured before and after pre-treatment.

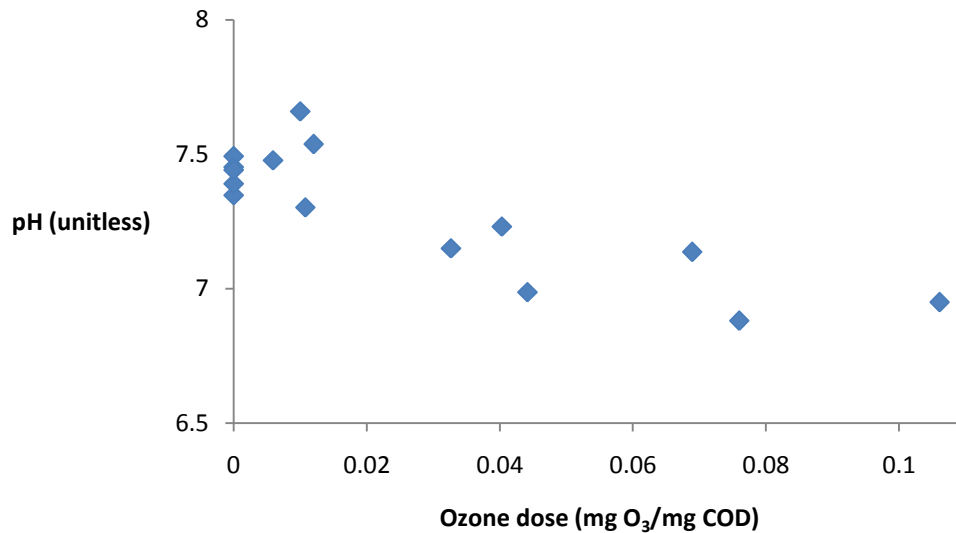
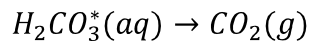


Figure 6.14. pH before and after ozonation

Since pure oxygen was the source gas for the ozone used, the slight depression in pH observed during ozonation was probably caused by stripping of carbonate species according to Henry's law, by the pathway described in Equation 6.2.



Equation 6.2

If air were used for ozone generation rather than oxygen the pH change would not follow this pattern, and less pH change would probably occur. Regardless of the gas used, the amount of pH depression observed would likely be insignificant in practice, though poorly buffered systems could experience a more significant pH change.

7. Whole-plant modeling approaches

The long-term goal of this research was to provide designers with the capability of modeling the behaviour of plants when pre-treatment is added to process streams. With this goal in mind, the experimental results presented in the last two chapters were used to construct pre-treatment models in appropriate terms for a whole-plant model, and the changes due to pre-treatment for one simple plant were observed and compared qualitatively to the changes reported in earlier published literature.

For the modeling portion of this work, the BioWin whole-plant model was employed. BioWin was the whole-plant model software produced by the project partner, EnviroSim. At the time of writing, the current version (Version 3.0) of BioWin was equipped with several ASM- and ADM-based models. The default and most complex of these models was simply called the BioWin model. In all of the models available in BioWin, the majority of processes were modeled as reactions, while some physical separation processes were modeled as point processes instead. The choice of BioWin for this portion of the work was somewhat arbitrary and a similar process could easily have been carried out using another of the commercially available software packages.

The conversions of heterotrophs and slowly degradable components of activated sludge were modeled using two conversions. Figure 7.1 illustrates conceptually the expected conversions between the biodegradable (green) and unbiodegradable (red) fractions. The blue arrows indicate the desirable reactions – those that improve the rate and overall amount of biodegradability. The black arrows show the less desirable reactions – a decrease in particle size for unbiodegradable COD and the production of inerts upon inactivation of organisms.

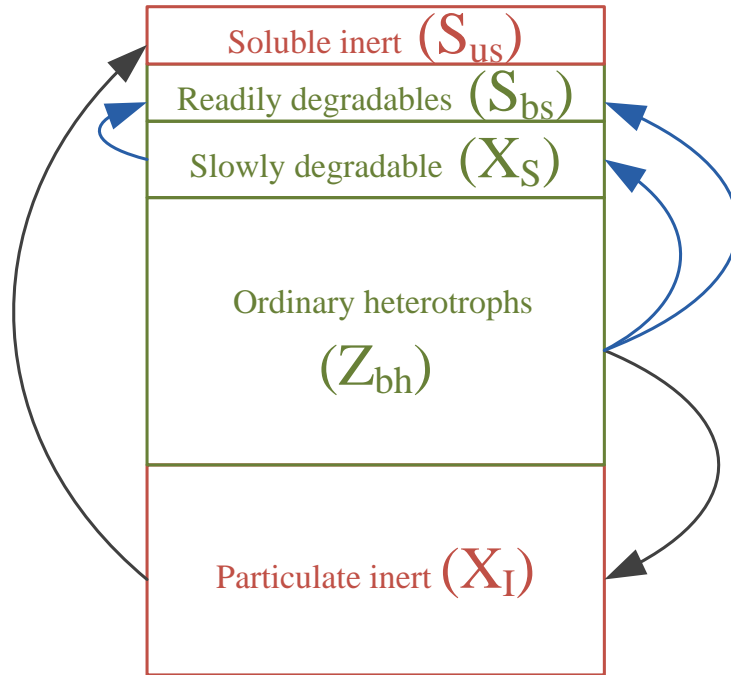


Figure 7.1. Wastewater fraction conversions for pre-treatment

In addition to the reactions shown in Figure 7.1, some loss of COD due to oxidation was expected to be possible during ozonation. This mineralization pathway is not shown but is also undesirable due to the high energy cost of the ozone required to convert material in this way.

Since a pre-treatment can be implemented either on a return sludge line or prior to anaerobic digestion, BioWin was utilized to model each of these scenarios. In order to model the effects of return sludge pre-treatment, a conventional activated sludge plant was modeled both with and without each pretreatment. The model plant is shown in Figure 7.2 before the addition of pre-treatment to the process stream. The plant shown was considered only in a steady-state configuration. This simplification was made largely because most published results only provide enough detail for qualitative comparison, even at steady state. In addition, the technique used to integrate pre-treatment into BioWin, discussed in Section 7.1, did not readily lend itself to dynamic simulation.

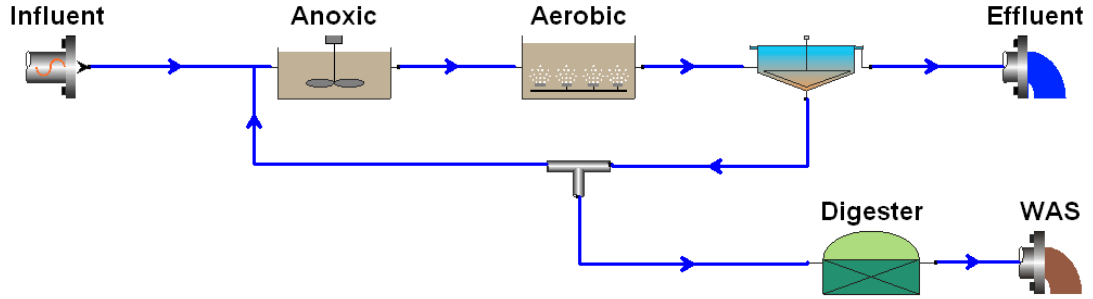


Figure 7.2. Model plant for consideration of pre-treatment responses

The plant consisted of a simple single-sludge activated sludge system with an anoxic zone preceding the aerobic zone. As well, an anaerobic digester was simulated to treat the waste activated sludge. The same model plant was used to check effects of pre-treatments in terms of reduced sludge production as well as enhanced biogas production during anaerobic digestion. Each pre-treatment option was tested using the return and waste activated sludge lines. The operational and influent parameters for the model plant are listed in Table 7.1.

Table 7.1. Model plant parameters

Parameter	Value
Anoxic HRT	3 Hours
Aerobic HRT	8.5 Hours
Recycle Ratio	1:1
Activated sludge solids residence time	7 Days
Digester residence time	15 Days
Digester temperature	35 °C
Total COD	500 mg/L
Total Kjeldahl Nitrogen	40 mg/L
Total Phosphorus	6.5 mg/L

When pre-treatment is implemented at full scale, the volume of sludge produced typically decreases. Since many plants are operated at a constant suspended solids concentration, this can result in an increasing solids residence time. As mentioned previously, this increase in SRT can confound the effects of pre-treatment and so in this study SRT was maintained at a constant value by decreasing the WAS rate as pre-treatment dose increased. At the same

time, the size of the anaerobic digester was reduced so that the anaerobic digester residence time also remained the same.

7.1. BioWin Integration

The pre-treatments were conducted in batch for this project, allowing for the development of a point conversion model, with no associated volume. This type of model works like a black box, converting inputs and doses to outputs. Unfortunately aside from physical separation, all of the other processes in the model are reactive, and modeled in terms of rates. Because of this, the addition of such a point conversion module proved somewhat difficult. Prior to presentation of results, the methodology used to model the point conversions determined from the data in Chapters 5 and 6 is given.

The BioWin model builder module simulated a fully mixed reactor, and in this type of reactor first-order conversion takes place according to

$$\frac{M}{M_0} = \frac{1}{1 + HRT} \quad \text{Equation 7.1}$$

Where M_0 and M are the item being converted, at initial and final concentrations respectively, and HRT is the hydraulic residence time. Since BioWin rates have units of inverse days, the HRT for Equation 7.1 should also be expressed in days. The model proposed in this section, on the other hand, utilizes a first order decay model instead (the same form as Equation 5.5 on page 41 for instance). To adapt the BioWin model to this, the HRT of the model builder module can be set to specify a dose. Combining Equation 5.5 with Equation 7.1 and setting the conversion rate equal to the concentration of the item being converted results in Equation 7.2, which defines the HRT required for the model builder module.

$$HRT = e^{\omega/k} - 1 \quad \text{Equation 7.2}$$

This approach to modeling the pre-treatment had one significant drawback, namely the high residence time required for significant pre-treatment doses. Dynamic modeling results will not be useful when high doses are applied, since the large reactor volume will serve to dampen responses – a dampening effect that would not be caused by actual pre-treatment modules since the size of both ultrasonic and ozone reactors is small, with residence times in the range of minutes. As well, since high pre-treatment doses can result in very high HRTs for the model builder module, it was important that other reactions were not simulated in the pre-treatment reactor.

Since the BioWin model includes 9 biomass fractions, if only conversion of heterotrophs is modeled then another biomass fraction takes over and begins to dominate the microbial population. This result is not very helpful, since ultrasound indiscriminately works on all of the particulate matter present, including all the various types of organisms. For simplicity, it was assumed that the other 8 biomass fractions are converted in the same way as the ordinary heterotrophs. In some other ways the BioWin general model uses this same assumption, for instance with the same endogenous, nitrogen, and phosphorus fractions which are the same for all 9 biomass fractions.

7.2. Sonication modeling approach

The observed conversions between sludge fractions due to ultrasound pre-treatment were all described reasonably well by a model of the form $C_1 \times e^{-\omega/c_2}$, where C_1 is a maximum conversion constant, ω is the ultrasound dose (kJ/g TS), and C_2 is a dose constant with the same units as ω (see Chapter 5). When each individual conversion was modeled, dose constants between 4.8 and 9.0 kJ/g TS were found. If the conversions in fact occur at different rates, then some intermediate products must be formed. A simpler model would use one dose constant for all of the processes and thereby provide closure of COD for any dose. Since the fitted dose constants were all fairly similar, the simpler closed-COD type of model was investigated by fitting the curves simultaneously to all of the data. The procedure was the same with the exception of a normalization step to give equal weight to the different conversions. When the normalized sums of squares for all of the conversions were minimized simultaneously, a model with one dose constant of 5.9 kJ/g TS was found. This model provided COD closure for all ultrasound doses and the fit to measured data was nearly indistinguishable from the models shown earlier.

During sonication, heterotrophic biomass was observed to be inactivated according to Equation 5.5. The data in Section 5.2 show that 45% of the biomass was converted to readily degradable substrate and 12% to slowly degradable substrate. In BioWin, as well as other whole-plant models, readily degradable substrate is soluble, though the truly soluble fraction increased more slowly than the readily degradable fraction. In practice, the distinction is likely unimportant for this 45% of converted biomass, since this material is consumed quickly in any downstream biological process. The 12% of slowly biodegradable substrate was assumed to be colloidal. A typical value of 8% is assumed for cell residue, and the remainder (35%) was assumed to be biomass which was inactivated but not broken up. This fraction was assigned to particulate slowly biodegradable COD. This assignment is based on the

assumption that aside from the cell residue, all of the components of biomass are biodegradable. These conversions are summarized in Figure 7.3.

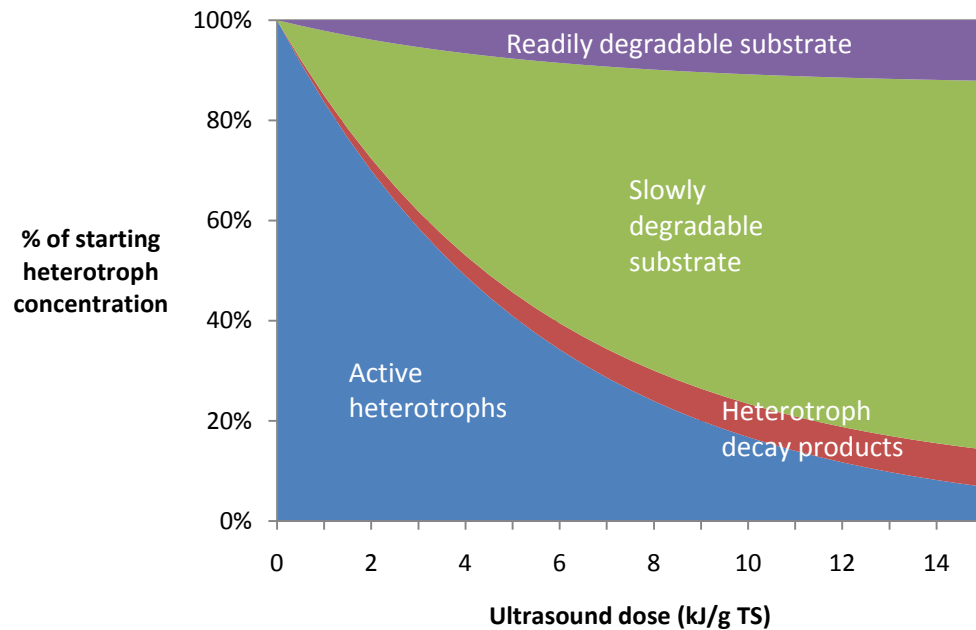


Figure 7.3. Modeled fate of heterotrophs following sonication

Figure 7.3 shows that according to the model, the majority of biomass which is inactivated is converted to slowly degradable substrate. Since the increase of biodegradable matter was the most desirable conversion, the model shows that pre-treatment with ultrasound is effective. With this model the more difficult question of whether or not it is also *cost-effective* can also be explored. In addition to the conversion of heterotrophic biomass, the model accounted for the conversion of 57% of slowly degradable substrate to readily degradable.

As described in Section 7.1, each conversion proceeded according to the rate of the product undergoing conversion. Table 7.2 shows the conversion products in terms of the BioWin model parameters.

Table 7.2. Ultrasound conversion processes

	Biomass (Z_{bh})	Decay products (Z_e)	Particulate biodegradable (X_{sp})	Colloidal biodegradable (X_{sc})	Soluble biodegradable (S_{bsa})
Conversion of Z_{bh}	-1	f_{Ze}	$1 - f_{Ze} - Y_s$	$Y_s - Y_{sbs}$	Y_{sbs}
Conversion of X_{sp}			-1	$\frac{Y_s - Y_{sbs}}{Y_s}$	$\frac{Y_{sbs}}{Y_s}$

In addition to the conversions listed in Table 7.2, the conversion of heterotrophs results in the release of organic nitrogen and phosphorus. These nutrients are released according to the BioWin default parameters of 0.07 grams N and 0.022 grams P per gram of COD.

7.3.Ozone modeling approach

In Chapter 6 three responses which could be well-described by simple mathematical models were found to occur during ozonation. These three were solubilization of COD, inactivation of heterotrophic organisms, and the sum of production of nitrite & nitrate. The other responses which were measured could not be described as neatly, and so the conversions due to ozonation were modeled using these three responses.

Inactivation and destruction of heterotrophic biomass was expected to be the most significant single process, and Figure 6.5 illustrates that the logarithm of the heterotroph inactivation was found to be directly proportional to the ozone dose applied. The slope of the log inactivation - dose line found was -23 mg COD/mg O₃, and so the inactivation can be modeled by either of the two equivalent forms of Equation 7.3:

$$Z_{bh} = Z_{bh,0}10^{-23\epsilon} = Z_{bh,0}e^{-53\epsilon} \qquad \text{Equation 7.3}$$

where Z_{bh} and Z_{bh,0} are the final and initial heterotroph concentrations respectively, and ε is the ozone dose in mg O₃/mg COD.

The increase in nitrate could not be directly matched to a decrease in TKN (For simplicity, since nitrite is readily oxidized by ozone to nitrate, the former is omitted from this discussion). Rather, it is proposed that the measured increase was a result of the solubilization and subsequent oxidation of organic nitrogen which resulted from the breakdown of cellular structure. Assuming that the nitrate produced all originated as organic nitrogen, that all the organic nitrogen was oxidized to nitrate, and that typical nitrogen and decay fractions apply, the release of biodegradable material can be calculated according to Equation 7.4.

$$bCOD\ released = \frac{\Delta NO_3^-}{(1-f_d) \times f_{ON}} = \frac{\Delta NO_3^-}{(1-0.08) \times 0.07} = 15.5 \times NO_3^- \text{ released}$$

Equation 7.4

Combining Equation 7.4 with Equation 6.1 results in Equation 7.5. Dividing this by the average heterotroph concentration of 1736 mg/L produces Equation 7.6 which describes the release of readily biodegradable COD in terms of starting heterotroph concentration:

$$bCOD\ released = 760\text{mg/L}(1 - e^{-18.3\epsilon}) \quad \text{Equation 7.5}$$

$$bCOD\ released = Z_{bh,0} \times 43.8\%(1 - e^{-18.3\epsilon}) \quad \text{Equation 7.6}$$

Using Equation 7.3 and Equation 7.6 together, assuming again the typical cell residue fraction of 8%, and considering the remainder as slowly degradable, the fate of heterotrophs can be estimated following ozonation. Figure 7.4 illustrates the resulting model's predicted fate of heterotrophs after ozonation.

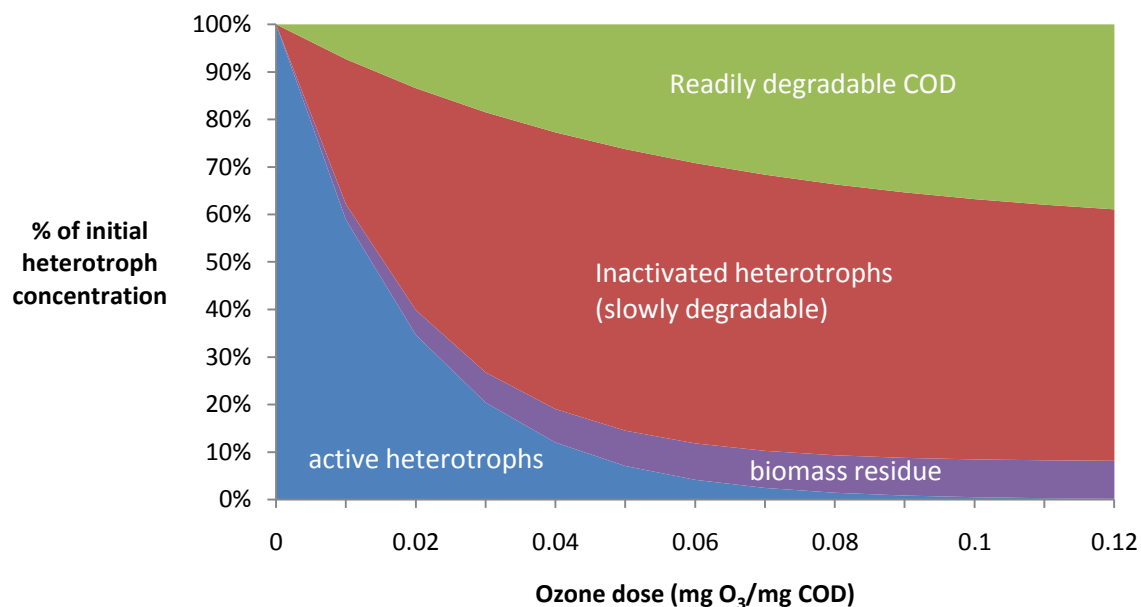


Figure 7.4. Modeled fate of heterotrophs after ozonation

In addition to the conversion of heterotrophs, the ozone pre-treatment model assumes that all nitrite present is oxidized to nitrate. No other conversions were included in this model, since the data were inconclusive.

7.4. Modeling approach comparison: physical vs. chemical pre-treatments

Both of the pre-treatments considered were described with a 2-variable exponential decay model, where the two constants describe the maximum conversion and the conversion rate. The ultrasound pre-treatment was modeled with a single conversion rate, which simplifies the modeling by allowing direct conversion from heterotrophs to biodegradable fractions for any dose. The ozone pre-treatment data, on the other hand, showed rapid inactivation of heterotrophs but a much slower rate of production of readily degradable COD. In order to model this, a more complex two-stage conversion process is required, whereby heterotrophs are inactivated (or equivalently converted to slowly degradable COD) and then in a second stage converted to readily degradable substrate.

The simpler model which was proposed for the ultrasound pre-treatment was based largely on the respirometric data collected. In contrast, the ozone pre-treatment model was based on a combination of respirometric and nitrogen fraction data. Both approaches showed the same exponential decay with increasing doses, with just the rate and maximum conversion varying.

8. Whole-plant modeling results

The whole-plant model introduced in the previous chapter and pictured in Figure 7.2 was modified by adding in turn each of the pre-treatment modules developed. Since pre-treatment can in practice be added either to a return sludge line or a waste sludge line, each of these options was also considered. In this section, the results of this modeling exercise are presented and discussed in order to demonstrate the qualitative similarities between results presented in the literature and those obtained with the models developed.

8.1. Sonication results

The first configuration tested was the addition of ultrasound to the return activated sludge line of the model plant. A screen capture of this configuration is shown in Figure 8.1.

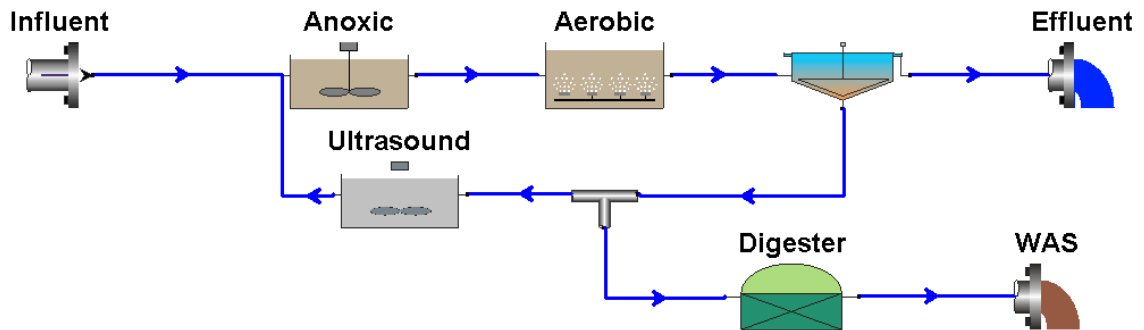


Figure 8.1. Model plant with ultrasound on return sludge line

Using the plant configuration illustrated in Figure 8.1, the effects of adding ultrasound on the return sludge line could be investigated. These changes were first investigated using a stable-SRT system where the activated sludge system was operated on an SRT of 7 days. Under these conditions, the model predicts lower sludge production, with lower solids concentrations throughout the plant. Figure 8.2 shows the decrease in waste activated sludge production for this system under the fixed-SRT operational strategy.

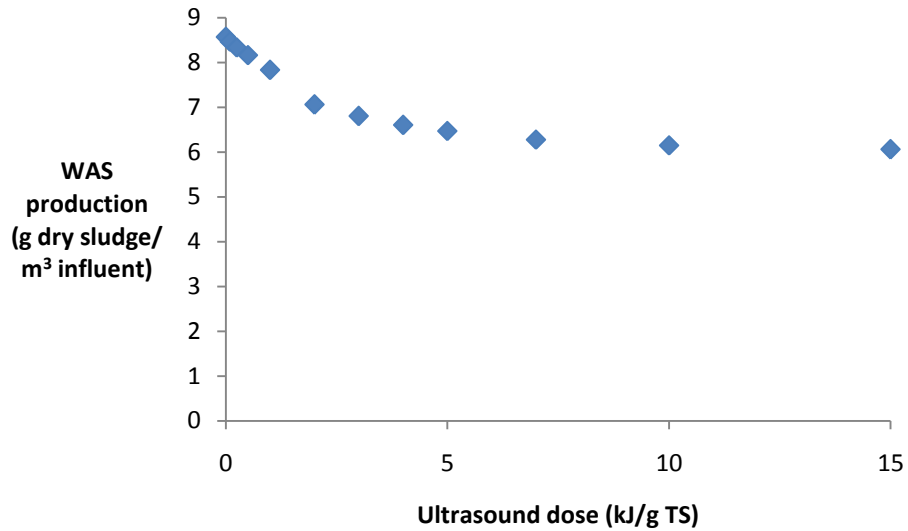


Figure 8.2. Sludge production for various ultrasound doses with fixed SRT

In addition to the lower amount of dry sludge produced, the solids concentrations throughout the plant decreased. Figure 8.3 shows how the mixed liquor volatile suspended solids (MLVSS) concentrations in both of the basins decreased with increasing ultrasound dose, leveling off near two-thirds of their original value.

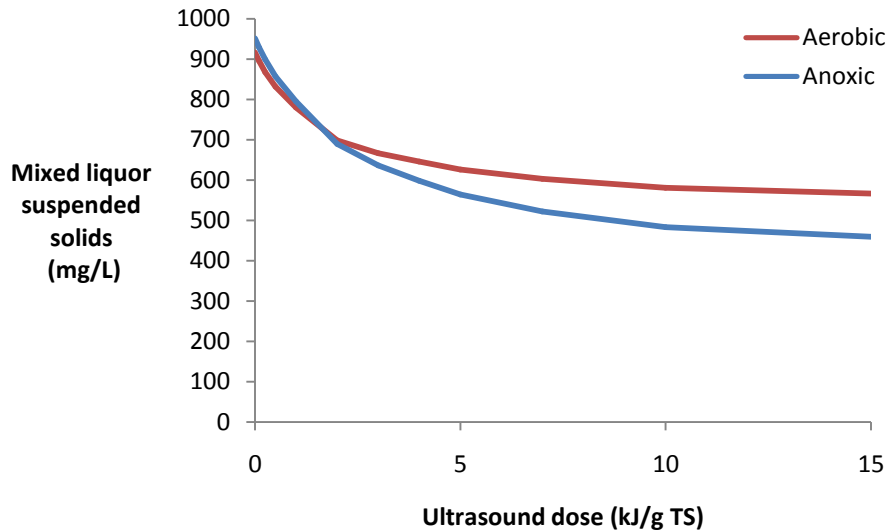


Figure 8.3. Changes to MLVSS concentrations due to sonication of RAS

At the same time as the mixed liquor solids concentrations were decreasing, corresponding decreases in waste and return sludge concentrations occurred. Digester gas production declined even faster, with more of the substrate being readily degradable and treated in the activated sludge process. The decreases in digester gas production modeled are shown in Figure 8.4. While the overall quantity of biogas produced decreased, the methane content increased slightly between 0 and 15 kJ/g TS of ultrasound, from 77% methane to 80%.

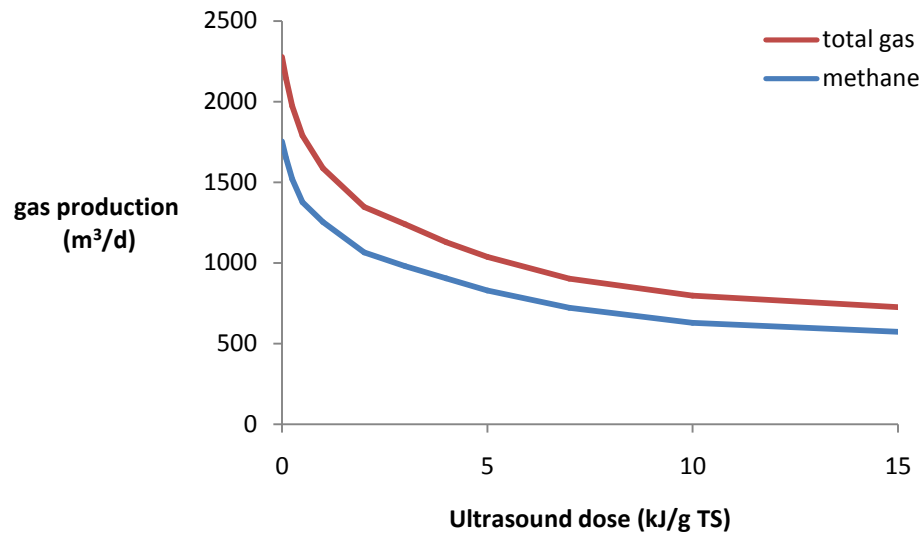


Figure 8.4. Digester gas production as a function of ultrasound dose

The decrease in biogas production due to pre-treatment of RAS had not been reported in the literature. This was likely due to the fact that the situation tested would be unlikely to occur in practice; only plants which do not have anaerobic digestion normally consider pre-treatment for return activated sludge.

In practice, measurement and control of solids residence time itself is a task beyond the instrumentation capability of most plants. The most common proxy for this ideal type of control is to maintain a fixed MLVSS concentration. Ultrasound pre-treatment decreased MLVSS, and so in order to keep this value constant the sludge wasting rate (and thereby SRT) was varied to maintain a fixed MLVSS concentration. This alternate strategy was also tested using the plant pictured in Figure 8.1.

When the MLVSS is fixed, the sludge output of the plant decreased with increasing ultrasound dose, following very similar trends to the ones shown when the SRT was fixed. Overall both the methane and sludge production rates were lower for the fixed MLVSS

strategy since the activated sludge SRT was higher. Figure 8.5 illustrates the decrease in sludge production under this operational strategy, which is even greater than with a fixed SRT.

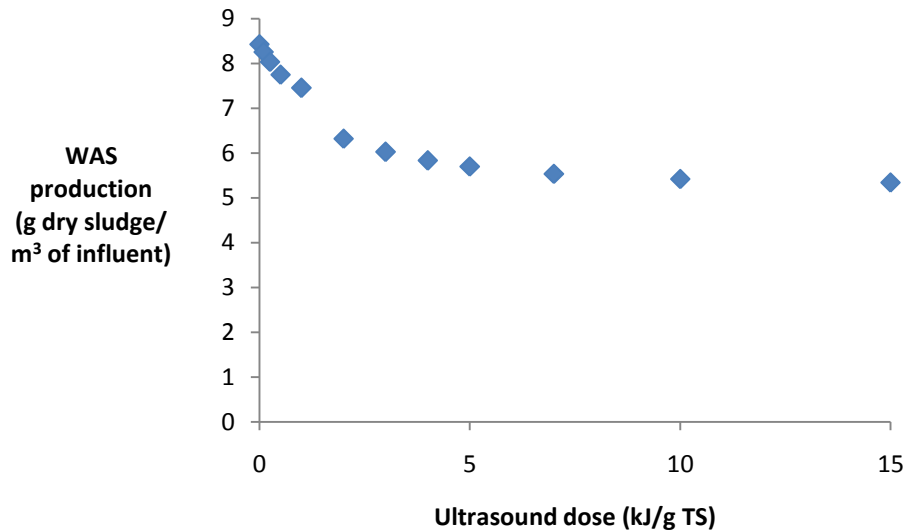


Figure 8.5. Sludge production for various ultrasound doses with fixed MLVSS

The additional reduction in sludge production observed was due to the synergistic effect of increasing SRT. This increase in activated sludge SRT was also responsible for the decreased biogas production, since more biodegradation occurs in the activated sludge process and less in the anaerobic digester. Overall, the results of modeling ultrasound pre-treatment of return activated sludge suggest that this may be an effective way to reduce sludge production and also a way to increase the SRT of a plant with limited solids handling capacity.

In addition to the configuration shown in Figure 8.1, pretreatment of waste activated sludge prior to anaerobic digestion was also modeled. The BioWin configuration for this part of the testing is illustrated in Figure 8.6.

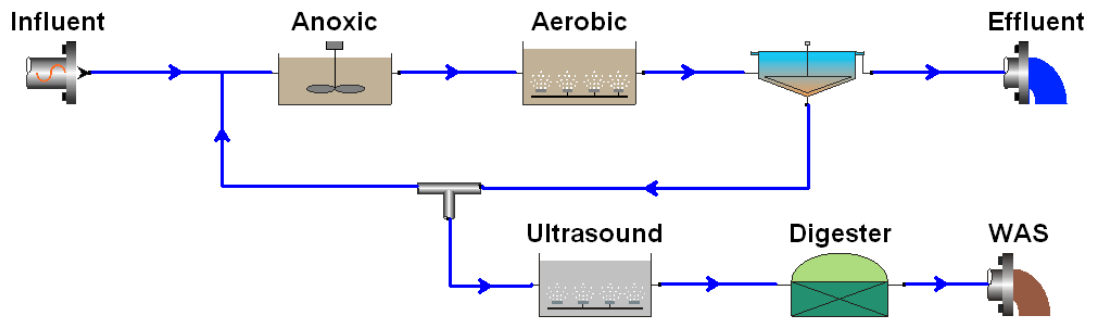


Figure 8.6. BioWin model for WAS pre-treatment with ultrasound

In the case of pre-treatment prior to anaerobic digestion, the model predicts both sludge reduction and enhancements in methane production. These two changes are shown in Figure 8.7 and Figure 8.8 respectively.

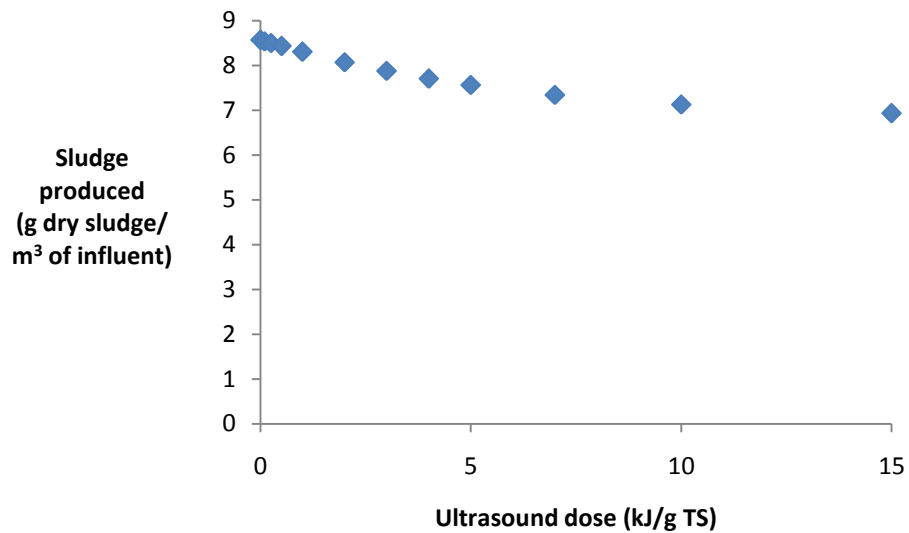


Figure 8.7. Sludge production for various WAS pre-treatment ultrasound doses

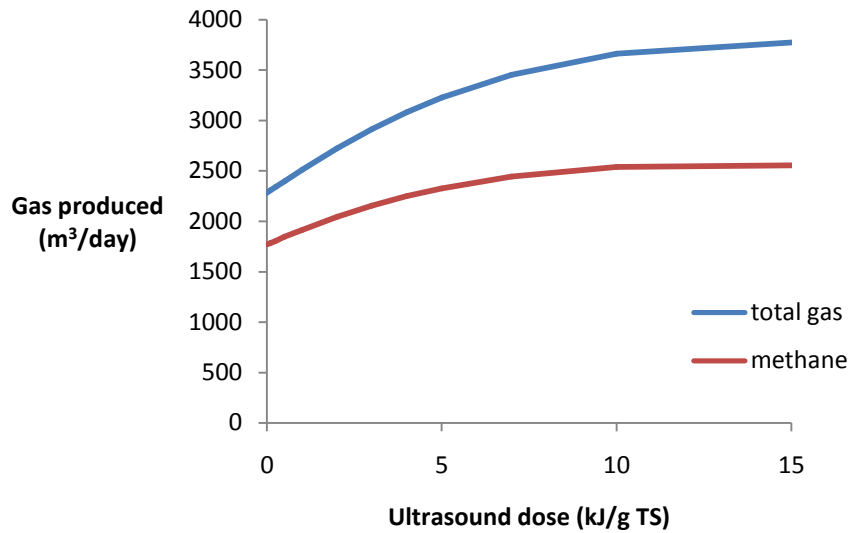


Figure 8.8. Gas production for various WAS pre-treatment ultrasound doses

The decreased sludge production shown in Figure 8.7 is similar to, but somewhat smaller in quantity than, the decrease in sludge production found when pre-treatment of the return sludge line was modeled instead. To the contrary, the increase in gas production shown in Figure 8.8 shows the opposite trend as that seen when RAS pre-treatment was modeled. The methane production for the two pre-treatment configurations is compared in Figure 8.9.

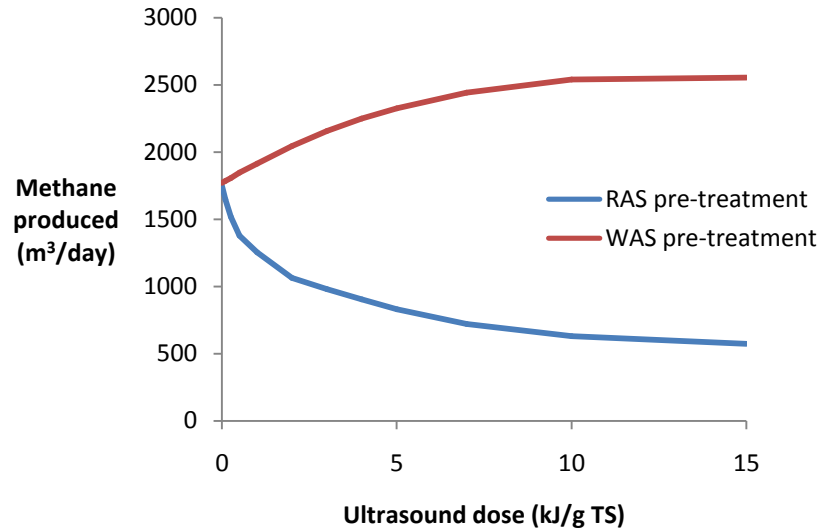


Figure 8.9. Comparison of gas production for RAS vs. WAS pre-treatment

This clear benefit in terms of methane production would in most cases make pre-treatment of WAS clearly superior to pre-treatment of RAS. In addition, and not considered here, addition of pre-treatment to a return sludge line would in many cases increase oxygen demand. This results in a double energy return benefit for pre-treatment of WAS compared to pre-treatment of RAS for the plant considered.

8.2. Ozone results

As with sonication, a conventional activated sludge plant was modeled in BioWin including ozone pre-treatment. Only pre-treatment of waste activated sludge was modeled, since the effects of ozone are similar to those of ultrasound according to the models, and pre-treatment of waste sludge was shown to be far superior to pre-treatment of return sludge in the previous section.

The model of ozone pre-treatment of waste activated sludge predicts enhanced biogas production and reduced sludge production. The amount of sludge produced as a function of the ozone dose applied is illustrated in Figure 8.10. The applied ozone dose is described in terms of the COD of the sludge being treated, for comparison with the results shown in Chapter 6. In addition, the ozone dose is shown in relation to the plant influent in order to show the amount of ozone which the model shows as an input.

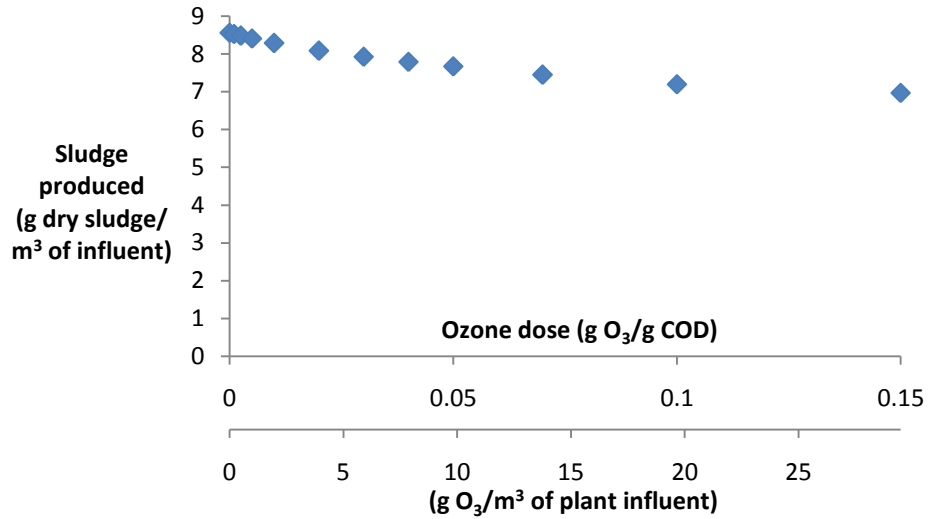


Figure 8.10. Sludge production for various WAS pre-treatment ozone doses

Figure 8.10 shows that for the model plant considered, total solid production could be decreased by as much as 20%. At the same time as the dry solids produced decreased, the amount of biogas produced increased. The amount of biogas as well as the methane content of the biogas is shown in Figure 8.11.

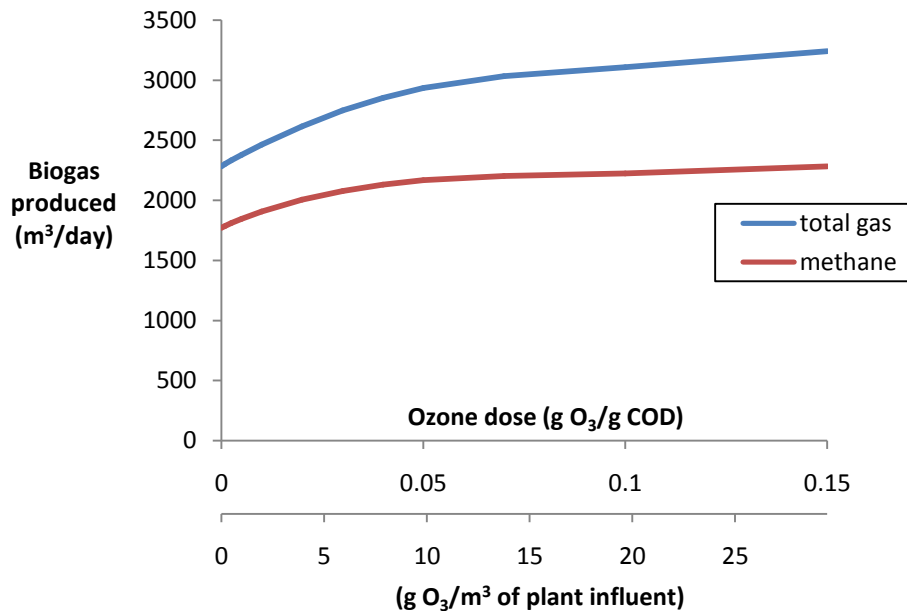


Figure 8.11. Gas production for various WAS pre-treatment ozone doses

Figure 8.11 shows that the model predicted an initial phase at low ozone doses where both total gas and methane production increased rapidly. When ozone doses increased beyond

about 0.05 g O₃/g COD, the amount of total gas produced continued to increase, however methane content decreased resulting in only small increases in the methane produced.

8.3. Comparison of modeling results

Both the ultrasound and ozone pre-treatment modeling exercises showed a reduction in sludge production and increases in biogas and methane production. Direct and equal comparison of the two pre-treatments was not possible since ultrasound reactor design and efficiency was not considered in this study. In lieu of such comparison, the two may be compared qualitatively, since both were considered over the range of typical doses utilized in earlier research.

Since the two models were similar in form, it was expected that the results would largely be the same between the two pre-treatments, and this was in fact the case. The main difference between the models was in conversion of biodegradable fractions, with ozone inactivating biomass at low doses but not converting it to readily degradable forms until higher doses. Ultrasound, conversely, was modeled as a direct conversion of biomass into biodegradable fractions.

For WAS pre-treatment the sludge was reduced by approximately 20% by either 15 kJ/g TS of ultrasound or 0.15 g O₃/g COD. The shape of the pre-treatment dose-sludge production curve was also the same for both treatments. This suggests that the conversion of the heterotrophs to some form of biodegradable COD, rather than the rate of biodegradability, governs the sludge reduction attainable by waste activated sludge pre-treatment.

The increase in biogas production potential also increased with both pre-treatments, though with ultrasound the benefit was greater over the tested range. For ultrasound, overall biogas production increased by over 60% and methane production by more than 40%. Ozone, on the other hand, increased biogas production by 40% and methane production by less than 30%. This shows that the particular biodegradable fraction created is important for prediction of biogas improvements, even though it is not very important for sludge reduction prediction.

Overall, both of the pretreatment models showed the same trends described in earlier research, namely that sludge production can be reduced and biogas production enhanced. In addition, the results of the modeling exercise support the recent suggestion that low pre-treatment doses may provide the most benefit per unit of pre-treatment dose.

9. Recommendations

The experimental and theoretical works described in this thesis have helped to open a previously unexplored branch of wastewater treatment modeling. Pre-treatment models were proposed which demonstrated the expected outcomes qualitatively. Further research can provide these models with the precision required for predictive use. This section outlines several possibilities for building on the results of this research and achieving pre-treatment models with good predictive capabilities.

For any research into pre-treatment of wastewater sludges:

- Particular attention to accurate measurement of pre-treatment dose is recommended. These measurements are difficult but necessary for any meaningful comparison both within a single study and with other published results.
- The use of low pre-treatment doses has been described elsewhere as being the most cost-effective and this research has confirmed this finding. Future research should focus in particular on the doses near the lower end of those considered.
- For tests which need to occur over a protracted period of time (for example due to the constraints of laboratory equipment) the stability of the sludge being tested is critical. The variable wastewater feed source and pilot-scale reactors used for this work likely contributed a large fraction of the variability in the data, and use of stable full-scale sludge source could provide more statistically significant results.

Particular to ozone pre-treatment:

- Further research into the oxidation of sludge by ozone is needed. The model presented here included closure of COD through ozone pre-treatment, but in theory the reaction of ozone with sludge should decrease the COD. A model which includes oxidation of the sludge will fare better under mechanistic scrutiny.
- Low doses should receive particular attention. This researcher recommends focusing on the reactions which occur in the range up to 0.01 g O₃/g COD as a starting point.
- Modeling of dissolved oxygen changes due to ozonation should be considered. Ozone feed gas typically includes more oxygen (O₂) than ozone, and so ozonation has the potential to significantly increase dissolved oxygen levels. Since most whole-plant models track dissolved oxygen, more accurate prediction of pre-treatment effects can be obtained if the changes in DO are modeled as well. Modeling of the ozone/oxygen gas transfer could also broaden the applicability of a model by making it more general.

Particular to ultrasound pre-treatment:

- A model for the temperature increase due to sonication would be useful. Some of the energy applied as ultrasound is dissipated as heat, and this heat may be useful when digestion at elevated temperatures follows. To evaluate the true costs of ultrasound pre-treatment, the savings in heating costs should be considered.
- Low doses should also be considered here. Those below 1 kJ/g TS are difficult to accurately apply but may provide the most benefit at full scale.

Particular to modeling:

- Whole-plant models require modification to allow the point conversions such as pre-treatments. This will allow for dynamic modeling of pre-treatments and allow them to be fully integrated into design considerations.

References

- Akin, B. (2008), Waste activated sludge disintegration in an ultrasonic batch reactor, *Clean-Soil Air Water*, 36, 360-365.
- Andreottola, G. and P. Foladori (2006), A review and assessment of emerging technologies for the minimization of excess sludge production in wastewater treatment plants, *Journal of Environmental Science and Health Part A-Toxic/hazardous Substances & Environmental Engineering*, 41, 1853-1872.
- Braguglia, C. M., G. Mininni, and A. Gianico (2008), Is sonication effective to improve biogas production and solids reduction in excess sludge digestion?, *Water Science and Technology*, 57, 479-483.
- Cao, X. Q., J. Chen, Y. L. Cao, J. Y. Zhu, and X. D. Hao (2006), Experimental study on sludge reduction by ultrasound, *Water Science and Technology*, 54, 87-93.
- Chiavola, A., M. Naso, E. Rolle, and D. Trombetta (2007), Effect of ozonation on sludge reduction in a SBR plant, *Water Science and Technology*, 56, 157-165.
- Chu, C. P., B. Chang, G. S. Liao, D. S. Jean, and D. J. Lee (2001), Observations on changes in ultrasonically treated waste-activated sludge, *Water Res.*, 35, 1038-1046.
- Çokgör, E. U., S. Sözen, D. Orhon, and M. Henze (1998), Respirometric analysis of activated sludge behaviour - I. Assessment of the readily biodegradable substrate, *Water Res.*, 32, 461-475.
- Dytczak, M. A., K. Londry, H. Siegrist, and J. A. Oleszkiewicz (2006), Extracellular polymers in partly ozonated return activated sludge: Impact on flocculation and dewaterability, *Water Science and Technology*, 54, 155-164.
- Dytczak, M. A., K. L. Londry, H. Siegrist, and J. A. Oleszkiewicz (2007), Ozonation reduces sludge production and improves denitrification, *Water Research*, 41, 543-550.
- Eaton, A. D., M. A. H. Franson, American Public Health Association, American Water Works Association, and Water Environment Federation (2005), *Standard Methods for the Examination of Water & Wastewater*, 21st 2005, Centennial ed., American Public Health Association, Washington, DC.
- Elliott, A. and T. Mahmood (2007), Pretreatment technologies for advancing anaerobic digestion of pulp and paper biotreatment residues, *Water Res.*, 41, 4273-4286.

Envirosim Associates (2009), BioWin Process Model Formulation, accessed online at www.envirosim.com/downloads/modelsusedinbiowin.pdf 12 March 2009.

Fabiyi, M. E. and R. E. Novak (2007), System and method for eliminating sludge via ozonation, US Patent Number 7,309,432 B1.

Grönroos, A., H. Kyllönen, K. Korpijärvi, P. Pirkonen, T. Paavola, J. Jokela, and J. Rintala (2005), Ultrasound assisted method to increase soluble chemical oxygen demand (SCOD) of sewage sludge for digestion, *Ultrason. Sonochem.*, 12, 115-120.

Henze, M. (1992), Characterization of wastewater for modelling of activated sludge processes, *Water Science and Technology*, 25, 1-15.

Henze, M., C. P. L. Grady, W. Gujer, G. V. R. Marais, and T. Matsuo (1987), Activated sludge model No1, IAWQ Scient, and Techn. Report.

Huysmans, A., M. Weemaes, P. A. Fonseca, and W. Verstraete (2001), Short communication ozonation of activated sludge in the recycle stream, *Journal of Chemical Technology and Biotechnology*, 76, 321-324.

Kappeler, J. and W. Gujer (1992), Estimation of Kinetic-Parameters of Heterotrophic Biomass Under Aerobic Conditions and Characterization of Waste-Water for Activated-Sludge Modeling, *Water Science and Technology*, 25, 125-139.

Müller, J., G. Lehne, J. Schwedes, S. Battenberg, R. Näveke, J. Kopp, N. Dichtl, A. Scheminski, R. Krull, and D. C. Hempel (1998), Disintegration of sewage sludges and influence on anaerobic digestion, *Water Science and Technology*, 38, 425-433.

Müller, J. A. (2000), Pretreatment processes for the recycling and reuse of sewage sludge, *Water Science and Technology*, 42, 167-174.

Nagare, H., H. Tsuno, W. Saktaywin, and T. Soyama (2008), Sludge ozonation and its application to a new advanced wastewater treatment process with sludge disintegration, *Ozone: Science and Engineering*, 30, 136-144.

Park, K. Y., K. H. Ahn, S. K. Maeng, J. H. Hwang, and J. H. Kwon (2003), Feasibility of sludge ozonation for stabilization and conditioning, *Ozone-Science & Engineering*, 25, 73-80.

Paul, E., P. Camacho, M. Sperandio, and P. Ginestet (2006), Technical and economical evaluation of a thermal, and two oxidative techniques for the reduction of excess sludge production, *Process Safety and Environmental Protection*, 84, 247-252.

Paul, E. and H. Debellefontaine (2007), Reduction of excess sludge produced by biological treatment processes: Effect of ozonation on biomass and on sludge, *Ozone-Science & Engineering*, 29, 415-427.

Rai, C. L., G. Struenkmann, J. Mueller, and P. G. Rao (2004), Influence of ultrasonic disintegration on sludge growth reduction and its estimation by respirometry, *Environ. Sci. Technol.*, 38, 5779-5785.

Sakai, Y., T. Fukase, H. Yasui, and M. Shibata (1997), An activated sludge process without excess sludge production, *Water Science and Technology*, 36, 163-170.

Saktaywin, W., H. Tsuno, H. Nagare, and T. Soyama (2006), Operation of a new sewage treatment process with technologies of excess sludge reduction and phosphorus recovery, *Water Science and Technology*, 53, 217-227.

Scheminski, A., R. Krull, and D. C. Hempel (1999), Oxidative treatment of digested sewage sludge with ozone, *IAQW-specialised Conference on Disposal and Utilisation of Sewage Sludge: Treatment Methods and Application Modalities*, 241-248.

Show, K. Y., T. H. Mao, and D. J. Lee (2007), Optimisation of sludge disruption by sonication, *Water Res.*, 41, 4741-4747.

Sievers, M., A. Ried, and R. Koll (2004), Sludge treatment by ozonation - Evaluation of full-scale results, *Water Science and Technology*, 49, 247-253.

Spanjers, H. and P. Vanrolleghem (1995), Respirometry as a Tool for Rapid Characterization of Waste-Water and Activated-Sludge, *Water Science and Technology*, 31, 105-114.

Spérandio, M. and P. Etienne (2000), Estimation of wastewater biodegradable COD fractions by combining respirometric experiments in various S_o/X_o ratios, *Water Res.*, 34, 1233-1246.

Stensel, H. D. and S. E. Strand (2004), *Evaluation of Feasibility of Methods to Minimize Biomass Production from Biotreatment*, Water Environment Research Foundation ; IWA Publishing, Washington; Colchester.

Strünkmann, G. W., J. A. Müller, F. Albert, and J. Schwedes (2006), Reduction of excess sludge production using mechanical disintegration devices, *Water Science and Technology*, 54, 69-76.

Suslick, K. S. (1990), Sonochemistry, *Science*, 247, 1439-1445.

Tchobanoglous, G. and E. D. Schroeder (1987), *Water Quality : Characteristics, Modeling, Modification, Water Quality Management* ; v, Addison-Wesley, Reading, Mass. ; Don Mills, Ont.

Tolson, B. and C. A. Shoemaker (2007), The Dynamically Dimensioned Search Algorithm for Computationally Efficient Automatic Calibration of Environmental Simulation Models, *Water Resources Research*, 43(1), W01413.

Wang, F., S. Lu, and M. Ji (2006), Components of released liquid from ultrasonic waste activated sludge disintegration, *Ultrasonics Sonochemistry*, 13, 334-338.

Wang, F., Y. Wang, and M. Ji (2005), Mechanisms and kinetics models for ultrasonic waste activated sludge disintegration, *Journal of Hazardous Materials*, 123, 145-150.

Weemaes, M., H. Grootaerd, F. Simoens, and W. Verstraete (2000), Anaerobic digestion of ozonized biosolids, *Water Research*, 34(8), 2330-2336.

Yasui, H. and M. Shibata (1994), An Innovative Approach to Reduce Excess Sludge Production in the Activated-Sludge Process, *Water Science and Technology*, 30, 11-20.

Yeom, I. T., K. R. Lee, Y. H. Lee, K. H. Ahn, and S. H. Lee (2002), Effects of ozone treatment on the biodegradability of sludge from municipal wastewater treatment plants, *Water Science and Technology*, 46, 421-425.

Zhao, Y. X., J. Yin, H. L. Yu, N. Han, and F. J. Tian (2008), Observations on ozone treatment of excess sludge (vol 56, pg 167, 2007), *Water Science and Technology*, 57, 637-637.

Appendix A – BioWin Model

BioWin software was produced by EnviroSim Associates Ltd. of Flamborough, Ontario. The information in this appendix, which describes BioWin version 3, was obtained from their website at www.envirosim.com. The reader is referred to this website for more information on the current version, or for more detail than is provided in this document. BioWin software is capable of modeling using a variety of different ASM- and ADM-based frameworks. According to EnviroSim Associates (2009),

The BioWin General Model has fifty state variables and sixty process expressions. These expressions are used to describe the biological processes occurring in activated sludge and anaerobic digestion systems, several chemical precipitation reactions, and the gas-liquid mass transfer behavior for six gases. The model formulation requires pH determination which is described in the pH chapter. This complete model approach frees the user from having to map one model's output to another model's input which significantly reduces the complexity of building full plant models, particularly those incorporating many different process units.

Although the work described in this thesis focused on the response of heterotrophic organisms in an aerobic environment, many other reactions were modeled by BioWin. The model used in BioWin included the following processes:

- Growth and decay of: ordinary heterotrophic organisms, methylotrophs, ammonia oxidizing biomass, nitrite oxidizing biomass, anaerobic ammonia oxidizers, phosphate accumulating organisms, propionic acetogens, methanogens
- Heterotrophic growth through fermentation
- Hydrolysis, adsorption, ammonification and assimilative denitrification
- Chemical phosphorus precipitation by alum or ferric
- Struvite and calcium phosphates precipitation

In addition, some non-ASM/ADM processes could be modeled in BioWin:

- Flux-based solid/liquid separation models
- pH modeling
- Gas transfer modeling for aeration

Appendix B – Standard Operating Procedures

B.1. Chemical Oxygen Demand	89
B.2. Solids Analysis.....	91
B.3. Ion Chromatograph	94

B.1. Chemical Oxygen Demand

This method describes the procedure for measurement of chemical oxygen demand (COD).

B.1.1. Apparatus

Sample homogenizer, Polytron, Luzern, Switzerland; COD reactor (block heater), Hach Company, Loveland, CO; DR/2010 spectrophotometer, Hach Company, Loveland, CO.

B.1.2. Principle

Measurement of chemical oxygen demand is made by quantifying the amount of dichromate ($\text{Cr}_2\text{O}_7^{2-}$) reduced to chromic ion (Cr^{3+}), a reduction from +VI to +III. These oxidation states have distinctive colours in solution; $\text{Cr}_2\text{O}_7^{2-}$ is deep yellow while Cr^{3+} is green in colour. This method measures the amount of Cr^{3+} produced as a function of sample absorbance at 600 nm. It is also possible to measure the amount of $\text{Cr}_2\text{O}_7^{2-}$ remaining in solution by spectrophotometry at 420 nm. The oxidation is conducted at lowered pH (using sulfuric acid) and elevated temperature (150°C) to ensure complete reaction in a short time.

B.1.3. Notes and Cautions

The mixture of chromic acid, sulfuric acid, and mercuric sulfate used in COD analysis is acutely poisonous and highly corrosive. COD reagents should be kept from all contact with skin, and breathing of vapour should be eliminated by working under a fume hood whenever COD vials are open. The MSDS for the mixture of chemicals involved includes the following warnings:

- May be fatal if swallowed
- Causes severe burns
- Harmful if inhaled or absorbed through skin
- Cancer hazard – contains material which may cause cancer
- Can cause kidney and central nervous system effects

The waste generated following COD analyses contains mercury.

Potential interferences include chloride, nitrite, and reduced inorganic species such as ferrous iron. This procedure complexes chloride using mercuric sulfate, neutralizing the interference of Cl^- concentrations up to 2000 mg/L. Nitrite may be neutralized using 10 mg of sulfamic acid per mg of nitrite as nitrogen. When reduced inorganic species are expected in large quantities, separate determination of their quantities followed by correction of measured COD is necessary.

B.1.4. Sample Preparation

Samples should be homogenized to allow for complete reaction with added reagents. Concentrated samples must be diluted to less than the method upper limit of 800 mg COD/L. For each set of samples prepared, a blank must also be prepared using organic-free water.

B.1.5. Reagents

Two reagents are required in the absence of interfering compounds; a digestion solution and a sulfuric acid solution.

i. Digestion solution (High strength COD digestion solution)

This solution consists of the indicating oxidant, potassium dichromate, with sulfuric acid and mercuric sulfate, which complexes with halides to remove their interference with this test. To prepare, work under the fume hood with appropriate personal protective equipment. Add to about 500 mL of distilled water 10.216 g $\text{K}_2\text{Cr}_2\text{O}_7$, 167 mL concentrated H_2SO_4 , and 33.3 g HgSO_4 . Dissolve, cool to room temperature, and dilute to 1000 mL.

ii. Sulfuric acid solution

This solution consists of concentration sulfuric acid with a small amount of silver sulfate, which catalyzes the oxidation of straight-chain aliphatic compounds. To prepare, work under the fume hood with appropriate personal protective equipment. Add 5.5 g Ag_2SO_4 per kg of concentrated H_2SO_4 , and let stand for 1 to 2 days to dissolve the Ag_2SO_4 .

B.1.6. Method Outline

i. Add 2.5 mL of sample (or diluted sample) to a COD vial.

The following steps must be performed under a fume hood to avoid breathing of toxic fumes. The sample will become very hot when the acid is mixed with it.

- i. Add 1.5 mL of digestion solution.
- ii. Add 3.5 mL of sulfuric acid solution.
- iii. Cap the sample vial and gently mix by inverting the vial several times. The sample may now be removed from the fume hood.

- ii. Place COD samples in reactor (block heater) for 3 hours at 150°C. Allow to cool for several hours until samples are at room temperature.
- iii. Turn on the Hach DR/2010 and wait for it to initialize. Set the DR/2010 to read absorbance directly by entering "0 [Enter]." If needed, turn the wavelength dial to 600 nm: The display will show "Zero Sample."
- iv. Clean the blank using ethanol and a soft wipe, insert it in the spectrophotometer, replace the vial cover, and press "Zero." The display will show "Zeroing..." and then "0.000"
- v. For each sample, clean the vial as in the previous step, insert the sample in the DR/2010 and press "Read" then wait for the measurement.
- vi. Compare sample readings to a standard curve to obtain COD values.

B.1.7. Quality Control

All samples should be analyzed in duplicate.

B.1.8. References:

HACH Company, DR/2010 Spectrophotometer Procedures Manual. Hach Company, 2000.

HACH Company, COD MSDS (available online through hach.com)

Standard Methods for the Examination of Water and Wastewater (18th edition), 1992.

B.2. Solids Analysis

This method describes the analysis of solids procured from wastewater. This method was described with the assistance of Marissa Bale, a co-op student.

B.2.1. Principle

- **Suspended Solids**

A well-mixed sample is filtered and the residue retained on the filter is dried to a constant weight in an oven at 105°C. The increase in weight of the filter represents the total suspended solids. The residue is then ignited to constant weight at 500 ± 50°C. The remaining solids represent the fixed suspended solids while the weight lost on ignition is the volatile suspended solids. The determination is useful because the volatile suspended solids offer a rough approximation of the amount of organic matter present in the solid fraction of wastewater.

- **Total Solids**

A well-mixed sample is evaporated in a weighed dish and dried to a constant weight at approximately 105°C. The increase in weight over that of the empty dish represents the total solids.

B.2.2. Apparatus

Vacuum filter, furnace, oven, electronic scale, dessicator.

B.2.3. Safety

The furnace operates at a very high temperature – about 500°C. Do not touch any part of the furnace other than the handles. Use long-handled tongs to handle samples going into and coming out of the furnace, and wear heat-resistant gloves. The oven (operating at 105°C) is also very hot. Avoid touching any surfaces in the oven. The samples will also be hot when they come out of the furnace or oven; handle these samples with tongs.

B.2.4. Method

- a) Set up the following table, adding one blank row for each sample to be processed:

		weights (g)			mL
Sample	Tray #	Tare	Dry	Ash	Volume

- b) Mark the bottom of the required number of metal filter trays. Obtain filters for suspended solids.
- c) Check that the furnace is operating at the appropriate temperature ($500 \pm 50^\circ$). Place the trays (and their filters for suspended solids) into the furnace for 15 minutes in order to evaporate any water present and combust any volatiles on the filters or trays.
- d) Place the trays in a desiccator for at least 5 minutes in order to allow the trays to cool to room temperature without absorbing any moisture as they cool.
- e) Weigh the filter trays - each with a filter in it for suspended solids. This is your “Tare” weight in the table.

- f) Measure out an appropriate volume of the sample – this value will depend on the solids concentration. In general, filtration of one sample should not take more than a few minutes, but sufficient volume should be filtered to ensure reproducible values. Record the sample volume, and:
- for suspended solids – using the vacuum filters, filter each sample. The samples do not have to be measured on consecutively numbered trays, but filters must be returned to the trays they came from. In the column titled “Sample”, note the sample source.
 - for total solids – pour the sample directly into the tray. Note the sample source.
- g) Set the sample trays into the drying oven (operating at 105°C) for a minimum of 1 hour to dry to a constant weight.
- h) Place the samples in a desiccator for 5 minutes to allow them to cool.
- i) Once the samples have dried, re-weigh each filter and tray. This is your “Dry” weight.
- j) Place the samples into a furnace at about 500°C ($\pm 50^\circ\text{C}$) for 15-20 minutes for 200 mg of residue. More residue may necessitate longer ignition times.
- k) Place the samples into a desiccator for 5 minutes.
- l) Re-weigh the samples. Take note of this weight. It may be your “ash” weight.
- m) Place the samples into the furnace for another 5 minutes.
- n) Place the samples into a desiccator for 5 minutes.
- o) Re-weigh the samples again. If this weight is less than 4% or 0.5 mg of the weight taken in step xii, then this is your “Ash” weight. If the weights are not equal, repeat steps xiii-xv until they are within the given parameters. This will be your ash weight.

B.2.5. Calculations

Calculations for total solids and suspended solids are similar, and each can be determined individually from the numbers collected using the following formulae. In addition, it is possible to determine total dissolved solids by the difference between total solids and total suspended solids.

$$VS \text{ or } VSS \text{ (mg/L)} = \frac{(\text{dry wt} - \text{ash wt (g)}) \times 10^6}{\text{Volume (mL)}}$$

$$IS \text{ or } ISS \text{ (mg/L)} = \frac{(\text{ash wt} - \text{tare wt (g)}) \times 10^6}{\text{Volume (mL)}}$$

$$VS \text{ or } VSS \text{ (mg/L)} = \frac{(\text{dry wt} - \text{tare wt (g)}) \times 10^6}{\text{Volume (mL)}}$$

B.2.6. References:

Greenberg, Arnold E.; Clesceri, Lenore S.; and Eaton, Andrew D. [ed], Standard Methods for the Examination of Water and Wastewater. American Public Health Association, American Water Works Association, and Water Environment Federation, 1992.

B.3. Ion Chromatograph

This method describes the procedure for measurement of anions or cations using ion chromatography. The method does not describe a procedure for simultaneous measurement of both anions and cations.

B.3.1. Apparatus

- Ion Chromatograph (Dionex Corporation)
- AS3500 Autosampler

For anions:

- AS9-HC separation column (Dionex)
- AG-9HC guard column (Dionex)

For cations:

- CS-16 separation column (Dionex)
- CG-16 guard column (Dionex)

B.3.2. Principle

Samples are eluted through a separatory column and ion concentrations are quantified based on the change in conductivity with respect to a baseline. Each ion passes through the column at a different rate, with the retardation being a function of the specific column used. For a given combination of operating conditions, each ion will have a characteristic time of retardation. When an ion leaves the column a spike in the ionic strength of the eluent occurs, and the corresponding spike in conductivity is measured using a sensitive conductivity

detector. By comparing the area of the conductivity spikes with samples of known concentration and ionic compositions, the values of the ions of interest may be calculated.

B.3.3. Notes and Cautions

Preparation of regenerant requires dilution of concentrated sulfuric acid. Use appropriate precautions

Samples must be filtered using 0.45µm filters before they are analyzed in the ion chromatograph to prevent clogging of the elution column.

B.3.4. Reagents

Eluant: 9mM Na₂CO₃. Dilute 20mL of 900 mM eluant concentrate to a total volume of 2L using ultrapure (18.2 MΩ-cm) water. Mix well.

Regenerant: 14mM H₂SO₄. Add 3mL concentrated sulfuric acid to 4L of ultrapure (18.2 MΩ-cm) water. Mix well

Autosampler rinse: 25% v/v IPS. Dilute 250mL isopropyl alcohol to 1L using ultrapure (18.2 MΩ-cm) water. Mix Well.

B.3.5. Method Outline

- A. Create or check the method file that you will use.
 - From the PeakNet main menu, select **Method**.
 - From the pull down menu select method, then load method
 - Set the standards you will use: Select **Detector -> Components -> Calibration Standards**
 - Check that the method sample size corresponds to the installed sample loop (25µL) by selecting **calibration** from the Method menu.
 - The Method file (.MET) always has two associated files: Gradient and Timed Events. Save these two files whenever the method is changed.
- B. Create the schedule for the current run.
 - From the PeakNet main menu, select **Schedule**
 - Select **File -> New -> AS3500 schedule**.
 - The recommended sequence for a schedule is:
 - Standards ranging from low to high, covering the expected range of results.
 - Blank
 - One standard
 - 10 samples
 - Repeat: Blank, standard, 10 samples until finished.

- For each line, the following information must be provided:
 - **Vial #:** Indicate the sample location as *XYZ* where *X* is the tray (A,B, or C) and *YY* is the 2-digit slot number in the selected tray.
 - **Injection Volume:** Indicate the volume of the sample loop you are using (25µL).
 - **Injections/Vial:** Indicate the number of injections you wish you perform from each vial. For most applications 2 or 3 is appropriate.
 - **Sample:** The sample name. This should be descriptive for your samples. For calibration standards, use the names AUTOCAL*n*R where *n* is the standard number (AUTOCAL1R, AUTOCAL2R, etc.). The sample name AUTOCAL*n* indicates to the PeakNet software that you are running a calibration standard, while appending an R to the sample names indicates that this should replace any previous standard that might have been present.
 - **Sample Type:** Select the appropriate sample type from the drop-down list, either Calibration Standard, Sample, or Blank.
 - **Level:** For calibration standards only, indicate the level of the calibration standard. This is the same as *n* from the sample name and corresponds to the level from the method.
 - **Method:** Select the standard method, AS9YYYY.MET, or another method that you prepared previously.
 - **Data File:** Select a file name to save under. The directory you choose must be located within /PeakNet/Data/.
 - **Dilution, etc.:** Do not adjust these parameters.
- Following the last sample, insert a line referring to a sample blank with one injection and use the method SHUTANS.MET. This stops the flow of helium to the ion chromatograph following the run.
- Save your schedule. The directory you choose must be located within /Peaknet/Schedules/YYYY where YYYY is the year.
- The figure below shows a sample schedule: 3 standards, a blank, and a sample.

Vial #	Inj. Vol.	Inj./Vial	Sample	Sample Type	Level	Method	Data File	Dilution
A01	25	2	AUTOCAL1R	Cal. Std.	1	AS92009.MET	/PeakNet/Data/Std1	1
A02	25	2	AUTOCAL2R	Cal. Std.	2	AS92009.MET	/PeakNet/Data/Std2	1
A03	25	2	AUTOCAL3R	Cal. Std.	3	AS92009.MET	/PeakNet/Data/Std3	1
A04	25	2	Sample	Blank		AS92009.MET	/PeakNet/Data/Blank	1
A05	25	2	Sample	Sample		AS92009.MET	/PeakNet/Data/Sample	1
A04	25	1	Sample	Blank		SHUTANS.MET	/PeakNet/Data/Blank	1

C. Check that the appropriate detector is selected.

- From the PeakNet main menu, select **Method**
- Select the IC by double clicking, and then **Configure**
- Set the detector channels to the correct configuration:

For anions:

- Channel 2: CDM-II conductivity detector
- Channel 4: None

For cations:

- Channel 2: None
- Channel 4: CDM-II conductivity detector

D. Operate ion chromatograph manually to obtain a stable baseline.

- Check that all reagents are present in sufficient quantities for the desired number of samples prior to starting the ion chromatograph: Na₂CO₃ eluant (number 3), H₂SO₄ regenerant, helium, and IPA autosampler rinse. Refresh according to section 5 as required.
- Check that the waste container has sufficient room for the amount of waste you will generate - typically about 5 litres per day or 100 millilitres per injection. This waste may safely be disposed of down the drain since it is typically more pure than tap water.
- Check that the desired column is connected to the regenerant lines (AS9-HC).
- Check that the desired sample loop size is installed (25µL).
- Check that gradient pump and conductivity detector modules are in remote mode.
- Load the PeakNet software. Select **Run** to initialize the autosampler
- Select **Load** then **Method** and choose the standard anion file or the method you will use. The standard anion method file is AS9yyyy.MET where yyyy is the current year. The helium valve will open and flow through the ion chromatograph will begin.
- Check that helium pressure is supplied at approximately 100 psi at the ion chromatograph.
- Check that regenerant pressure is between 5 and 7 psi.
- Wait 15 to 30 minutes for a stable baseline. The conductivity at the baseline will depend on the regenerant pressure, eluant used, and eluant flow rate. Read the operation log to obtain recent baseline values observed.

E. Start the run.

- Place samples in the autosampler in accordance with the schedule created in part C.

- From the PeakNet main menu, select **Run**.
 - Select **File -> Load AS3500** and select the appropriate schedule.
 - Press **Start**. The first injection should begin immediately.
- F. End the run.
- Ensure that the program has finished properly. Close the helium supply at the tank and remove your samples from the autosampler.
- G. Getting Data from the run
- Select batch from the peaknet main menu
- File->New
- Processing-> export-> browse-> C:/peaknet\data\... where ever file is
- Summary options-> fields-> in data fields select component amount, componat name, peak retention time, peak area
- Click okay, and then okay
- Processing-> input-> select appropriate file and click open
- Processing-> start
- Close batch, do not save changes.
- Search for file in C:\ peaknet\data\.....

B.3.6. Quality Control

Each sample should be injected at least twice.

A standard curve with at least 5 points should be run every time the ion chromatograph is operated.

Every 10 samples, a standard should be tested to ensure that the values obtained are stable over the run.

B.3.7. References

Standard Methods for the Examination of Water and Wastewater (18th Edition) 1992.

B.3.8. Attribution

This standard was developed by Jonathan Musser, M.A.Sc. candidate and last modified in May 2009

Appendix C – Visual basic source code for interpretation of respirometry

Option Explicit

```
' used to change the process priority during optimization

Private Declare Function SetPriorityClass Lib "kernel32" (ByVal hProcess As Long, _
    ByVal dwPriorityClass As Long) As Long
Private Declare Function GetCurrentProcess Lib "kernel32" () As Long
Private Const BelowNormal As Long = &H4000&
Private Const Normal As Long = &H20&
Dim CurrentProcessHandle As Long

' data arrays
Dim sngRawData() As Single
Dim sngOURData() As Double

' counter for the optimization trials
Dim sngCounter As Single

' maximum OUR found, used for scaling the plots
Dim sngMaxOUR As Single

' starting values filled from the text boxes to be used in the arrays
Dim sngOHO As Single
Dim sngSlowly As Single
Dim sngReadily As Single

' best values found so far:
Dim sngOHOBest As Single
Dim sngSlowlyBest As Single
Dim sngReadilyBest As Single

' a boolean used for the "stop" button
Dim bnInterrupt As Boolean

' biokinetic constants
Const sngBh As Single = 0.62 / 1440
Const sngMuh As Single = 3.2 / 1440
Const sngKh As Single = 2.1 / 1440
Const sngKs As Single = 5
Const sngKoh As Single = 0.05
Const sngKx As Single = 0.06
Const sngYh As Single = 0.666
Const sngFp As Single = 0.08

Private Sub btnInterrupt_Click()

' this subroutine is used to interrupt the optimization subroutine, which can be useful when a very
' long run is selected.

bnInterrupt = True

End Sub

Private Sub btnOptimize_Click()

' this procedure optimizes the parameters according to the Dynamically Dimensioned Search Algorithm
' described in Water Resources Research Volume 43 (Tolson & Shoemaker) 2007
' Step numbers indicated in notes refer to the algorithm as described in this paper.

Dim RetVal As Long

Dim sngR As Single
Dim sngNumTrials As Single
Dim i As Integer
Dim j As Integer
Dim k As Integer
Dim inI As Integer
Dim sngN As Single
Dim SSE As Double
Dim LowSSE As Double
Dim StartSSE As Single

Dim bnChange(3) As Boolean
Dim X As Double
Dim XprimeX(1 To 3, 1 To 3) As Double
Dim XprimeXinv(1 To 3, 1 To 3) As Double
Dim XprimeXdet As Double
```

```

Dim sngSeedtCOD As Single
Dim sngSeedsCOD As Single
Dim sngTreatedtCOD As Single
Dim sngTreatedsCOD As Single
Dim sngBhMin As Single
Dim sngBhMax As Single

Dim SeedAmount As Single
Dim TotalVolume As Single
Dim bnError As Boolean

' lower process priority so that the computer continues to function
' This part of the code is particularly helpful if you wish to run many copies of the program at
' once, since the operations of starting more programs will take precedence over the ones that are
' already running.
' The code for lowering priority was due to Richard L. Grier and found at
' http://www.hardandsoftware.net/
' accessed June 16, 2009 : "You may freely use this code in your applications."

RetVal = SetPriorityClass(CurrentProcessHandle, BelowNormal)

btnInterrupt.Visible = True
bnInterrupt = False

Call ValidateChkCell(SeedAmount, TotalVolume, bnError)
If bnError = True Then Exit Sub

sngSeedtCOD = txtSeedtCOD.Text
sngSeedsCOD = txtSeedsCOD.Text

sngNumTrials = txtNumTrials.Text
sngR = txtPerturbation.Text

'***** STEP 1 *****
'Start with the initial values in the text boxes:

sngOHO = txtBestSeedActive.Text
sngSlowly = txtBestSeedSlowly.Text
sngReadily = txtBestSeedReadily.Text

sngOH0Best = sngOHO
sngSlowlyBest = sngSlowly
sngReadilyBest = sngReadily

lblCurrentSeedActive.Caption = Format(sngOHO, "0.0") & " mg COD/L"
lblCurrentSeedSlowly.Caption = sngSlowly & " mg COD/L"
lblCurrentSeedReadily.Caption = sngReadily & " mg COD/L"
lblCV1.Visible = False
lblCV2.Visible = False
lblCV3.Caption = ""
lblCV4.Caption = ""
lblCV5.Caption = ""

'***** STEP 2 *****
' calculate squared error for base scenario for comparison

SSE = 0

For i = 1 To 8
    If chkCellOn(i) Then
        Call ASM(i)
        For inI = 0 To UBound(sngOURData, 2) - 10
            SSE = SSE + (sngOURData(i, inI) - sngOURData(8 + i, inI)) ^ 2
        Next inI
    End If
Next i

Call OURPlot
LowSSE = SSE
StartSSE = SSE
picProgressBar.Cls
picProgressBar.Scale (0, SSE)-(txtNumTrials.Text, 0)
Randomize

'*****
'***** main loop is here
'*****
For sngCounter = 1 To sngNumTrials

```

```

If bnInterrupt = True Then
  If MsgBox("Do you wish to stop the analysis?", vbOKCancel, "Abort Run") = vbOK Then
    For inI = 1 To 8
      chkCellOn(inI).Enabled = True
      txtSeed(inI).Enabled = True
      txtVolume(inI).Enabled = True
    Next inI
    btnInterrupt.Visible = False
    Exit Sub
  Else
    bnInterrupt = False
  End If
End If

'***** STEP 3 *****
' add parameters to change set with probability based on how many trials complete

bnChange(0) = False

For inI = 1 To 3
  bnChange(inI) = False
  If Rnd > Log(sngCounter) / Log(sngNumTrials) Then
    bnChange(inI) = True
    bnChange(0) = True
  End If
Next inI

' if no parameters added then randomly pick one from the list
If bnChange(0) = False Then inI = (CInt(Int(3 * Rnd()))) + 1

For i = 1 To 3
  If i = inI Then bnChange(i) = True
Next i

'***** STEP 4 *****
' for each parameter, approximate normal distribution and perturb parameter
' normal distribution approximation is based on the one found at
http://home.online.no/~pjacklam/notes/invnorm/
' end with check that we are not below min or above maximum

If bnChange(1) Then
  X = Sqr(-2 * Log(Rnd) / Log(Exp(1)))
  sngOHO = sngOHO + sngR * sngSeedtCOD * ((((-0.00784 * X - 0.322) * X - 2.4) * X - 2.55) * X + 4.37) * X + 2.94) / -
  (((0.0078 * X + 0.322) * X + 2.45) * X + 3.75) * X + 1)
  If sngOHO < 1 Then
    sngOHO = -1 * sngOHO
    If sngOHO > sngSeedtCOD Then sngOHO = 1
  ' since heterotroph population cannot be zero for ASM calculations
  End If
  If sngOHO > sngSeedtCOD Then
    sngOHO = 2 * sngSeedtCOD - sngOHO
    If sngOHO < 1 Then sngOHO = sngSeedtCOD
  End If
End If

If bnChange(2) Then
  X = Sqr(-2 * Log(Rnd) / Log(Exp(1)))
  sngSlowly = sngSlowly + sngR * sngSeedtCOD * ((((-0.00784 * X - 0.322) * X - 2.4) * X - 2.55) * X + 4.37) * X + 2.94) / -
  (((0.0078 * X + 0.322) * X + 2.45) * X + 3.75) * X + 1)
  If sngSlowly < 0 Then
    sngSlowly = -1 * sngSlowly
    If sngSlowly > sngSeedtCOD Then sngSlowly = 0
  End If
  If sngSlowly > sngSeedtCOD Then
    sngSlowly = 2 * sngSeedtCOD - sngSlowly
    If sngSlowly < 0 Then sngSlowly = sngSeedtCOD
  End If
End If

If bnChange(3) Then
  X = Sqr(-2 * Log(Rnd) / Log(Exp(1)))
  sngReadily = sngReadily + sngR * sngSeedsCOD * ((((-0.00784 * X - 0.322) * X - 2.4) * X - 2.55) * X + 4.37) * X + 2.94) / -
  (((0.0078 * X + 0.322) * X + 2.45) * X + 3.75) * X + 1)
  If sngReadily < 0 Then
    sngReadily = -1 * sngReadily
    If sngReadily > sngSeedsCOD Then sngReadily = 0
  End If
  If sngReadily > sngSeedsCOD Then

```

```

        sngReadily = 2 * sngSeedsCOD - sngReadily
    If sngReadily < 0 Then sngReadily = sngSeedsCOD
End If
End If
End If

lblCurrentSeedActive.Caption = Format(sngOHO, "0") & " mg COD/L"
lblCurrentSeedSlowly.Caption = Format(sngSlowly, "0") & " mg COD/L"
lblCurrentSeedReadily.Caption = Format(sngReadily, "0") & " mg COD/L"

'***** STEP 5 *****
' find error using perturbed estimates

SSE = 0

For i = 1 To 8
    If chkCellOn(i) Then
        Call ASM(i)
        For inI = 0 To UBound(sngOURData, 2) - 10
            SSE = SSE + (sngOURData(i, inI) - sngOURData(8 + i, inI)) ^ 2
        Next inI
    End If
Next i

If SSE < LowSSE Then
    LowSSE = SSE
    sngOHOBest = sngOHO
    sngSlowlyBest = sngSlowly
    sngReadilyBest = sngReadily
    Call OURPlot
    If Abs(sngOHO - sngSeedtCOD) < 1 Then txtBestSeedActive.ForeColor = vbRed Else
txtBestSeedActive.ForeColor = vbBlack
    txtBestSeedActive.Text = Format(sngOHO, "0")
    If Abs(sngSlowly - sngSeedtCOD) < 1 Then txtBestSeedSlowly.ForeColor = vbRed Else
txtBestSeedSlowly.ForeColor = vbBlack
    txtBestSeedSlowly.Text = Format(sngSlowly, "0")
    If Abs(sngReadily - sngSeedsCOD) < 1 Then txtBestSeedReadily.ForeColor = vbRed Else
txtBestSeedReadily.ForeColor = vbBlack
    txtBestSeedReadily.Text = Format(sngReadily, "0")
    ' estimate variances
    sngN = 0
    For j = 1 To 3
        For k = 1 To 3
            XprimeX(j, k) = 0
        Next k
    Next j

    For i = 1 To 8
        If chkCellOn(i) Then
            sngN = sngN + UBound(sngOURData, 2) - 2
            Call ASM(i)
            Call ASM(i + 8)
            Call ASM(i + 16)
            Call ASM(i + 24)
            ' calculate X'X matrix directly from these values:
            For j = 1 To 3
                For k = 1 To 3
                    For inI = 1 To UBound(sngOURData, 2)
                        XprimeX(j, k) = XprimeX(j, k) + 10000 * _
                            (sngOURData(8 + 8 * j + i, inI) - sngOURData(8 + i, inI)) * _
                            (sngOURData(8 + 8 * k + i, inI) - sngOURData(8 + i, inI))
                    Next inI
                Next k
            Next j
        End If
    Next i

    ' invert X'X matrix using A-1 = adj(A)/det(A)
    ' first calculate the adjoint matrix
    XprimeXinv(1, 1) = XprimeX(2, 2) * XprimeX(3, 3) - XprimeX(2, 3) ^ 2
    XprimeXinv(1, 2) = XprimeX(2, 3) * XprimeX(3, 1) - XprimeX(3, 3) * XprimeX(2, 1)
    XprimeXinv(1, 3) = XprimeX(2, 1) * XprimeX(3, 2) - XprimeX(2, 2) * XprimeX(3, 2)
    XprimeXinv(2, 1) = XprimeXinv(1, 2)
    XprimeXinv(2, 2) = XprimeX(1, 1) * XprimeX(3, 3) - XprimeX(1, 3) ^ 2
    XprimeXinv(2, 3) = XprimeX(1, 1) * XprimeX(3, 2) - XprimeX(1, 2) * XprimeX(3, 1)
    XprimeXinv(3, 1) = XprimeXinv(1, 3)
    XprimeXinv(3, 2) = XprimeXinv(2, 3)
    XprimeXinv(3, 3) = XprimeX(1, 1) * XprimeX(2, 2) - XprimeX(1, 2) ^ 2

```

```

' next calculate the determinant (cheating a little - actually calculating the 1,1 entry
' of X times adj(X) but this should be the same thing)
XprimeXdet = 0
For i = 1 To 3
    XprimeXdet = XprimeXdet + XprimeX(1, i) * XprimeXinv(1, i)
Next i

' next divide each entry of the inverse by the determinant
For i = 1 To 3
    For j = 1 To 3
        XprimeXinv(i, j) = XprimeXinv(i, j) / XprimeXdet
    Next j
Next i

' now multiply each entry in this matrix by RSS and divide by n-p to get the standard error
' n is UBound(sngOURData,2) - 2 and p is fixed at 3
' also in here, convert back to original concentrations

For i = 1 To 3
    For j = 1 To 3
        XprimeXinv(i, j) = XprimeXinv(i, j) * LowSSE / (sngN - 3)
        XprimeXinv(i, j) = XprimeXinv(i, j) * TotalVolume ^ 2 / SeedAmount ^ 2
    Next j
Next i

LblCV1.Visible = True
LblCV2.Visible = True

LblCV3.Caption = Format(XprimeXinv(1, 1), "0.0") & vbCr & Format(XprimeXinv(2, 1), "0.0") & vbCr & _
Format(XprimeXinv(3, 1), "0.0")
LblCV4.Caption = Format(XprimeXinv(1, 2), "0.0") & vbCr & Format(XprimeXinv(2, 2), "0.0") & vbCr & _
Format(XprimeXinv(3, 2), "0.0")
LblCV5.Caption = Format(XprimeXinv(1, 3), "0.0") & vbCr & Format(XprimeXinv(2, 3), "0.0") & vbCr & _
Format(XprimeXinv(3, 3), "0.0")

Else
    sngOHO = sngOHOBest
    sngSlowly = sngSlowlyBest
    sngReadily = sngReadilyBest
End If

'***** STEP 6 *****

Label23.Caption = Format(sngCounter, "#,##0") & " complete"

picProgressBar.Line (sngCounter, 0)-(sngCounter, LowSSE), vbBlue

DoEvents
Next sngCounter

' ***** End of main loop *****

' Fine tune parameters if option selected (reduces variances)

If chkFine = 1 Then
    If sngR > 0.1 Then
        txtPerturbation.Text = sngR / 100
        txtNumTrials.Text = sngNumTrials / 10
        Call btnOptimize_Click
    End If
End If

' estimate ending variances
sngN = 0
For j = 1 To 3
    For k = 1 To 3
        XprimeX(j, k) = 0
    Next k
Next j

For i = 1 To 8
    If chkCellOn(i) Then
        sngN = sngN + UBound(sngOURData, 2)
        Call ASM(i)
        Call ASM(i + 8)
    End If
Next i

```



```

    Call ASM(i + 16)
    Call ASM(i + 24)
    ' calculate X'X matrix directly from these values:
    For j = 1 To 3
        For k = 1 To 3
            For inI = 1 To UBound(sngOURData, 2)
                XprimeX(j, k) = XprimeX(j, k) + 10000 * _
                    (sngOURData(8 + 8 * j + i, inI) - sngOURData(8 + i, inI)) * _
                    (sngOURData(8 + 8 * k + i, inI) - sngOURData(8 + i, inI))
            Next inI
        Next k
    Next j
    End If
Next i

' invert X'X matrix using A-1 = adj(A)/det(A)
' first calculate the adjoint matrix
XprimeXinv(1, 1) = XprimeX(2, 2) * XprimeX(3, 3) - XprimeX(2, 3) ^ 2
XprimeXinv(1, 2) = XprimeX(2, 3) * XprimeX(3, 1) - XprimeX(3, 3) * XprimeX(2, 1)
XprimeXinv(1, 3) = XprimeX(2, 1) * XprimeX(3, 2) - XprimeX(2, 2) * XprimeX(3, 2)
XprimeXinv(2, 1) = XprimeXinv(1, 2)
XprimeXinv(2, 2) = XprimeX(1, 1) * XprimeX(3, 3) - XprimeX(1, 3) ^ 2
XprimeXinv(2, 3) = XprimeX(1, 1) * XprimeX(3, 2) - XprimeX(1, 2) * XprimeX(3, 1)
XprimeXinv(3, 1) = XprimeXinv(1, 3)
XprimeXinv(3, 2) = XprimeXinv(2, 3)
XprimeXinv(3, 3) = XprimeX(1, 1) * XprimeX(2, 2) - XprimeX(1, 2) ^ 2

' next calculate the determinant (cheating a little - actually calculating the 1,1 entry
' of X times adj(X) but this should be the same thing)
XprimeXdet = 0
For i = 1 To 3
    XprimeXdet = XprimeXdet + XprimeX(1, i) * XprimeXinv(1, i)
Next i

' next divide each entry of the inverse by the determinant
For i = 1 To 3
    For j = 1 To 3
        XprimeXinv(i, j) = XprimeXinv(i, j) / XprimeXdet
    Next j
Next i

' now multiply each entry in this matrix by RSS and divide by n-p to get the standard error
' n is UBound(sngOURData,2) and p is fixed at 3
For i = 1 To 3
    For j = 1 To 3
        XprimeXinv(i, j) = XprimeXinv(i, j) * LowSSE / (sngN - 3)
        XprimeXinv(i, j) = XprimeXinv(i, j) * TotalVolume ^ 2 / SeedAmount ^ 2
    Next j
Next i

LblCV1.Visible = True
lblCV2.Visible = True

lblCV3.Caption = Format(XprimeXinv(1, 1), "0.0") & vbCr & Format(XprimeXinv(2, 1), "0.0") & vbCr & _
    Format(XprimeXinv(3, 1), "0.0")
lblCV4.Caption = Format(XprimeXinv(1, 2), "0.0") & vbCr & Format(XprimeXinv(2, 2), "0.0") & vbCr & _
    Format(XprimeXinv(3, 2), "0.0")
lblCV5.Caption = Format(XprimeXinv(1, 3), "0.0") & vbCr & Format(XprimeXinv(2, 3), "0.0") & vbCr & _
    Format(XprimeXinv(3, 3), "0.0")

'plot best solution

Call OURPlot
Label23.Caption = "Completed all " & Format(sngCounter - 1, "###0") & " trials" & vbCr & _
    "Minimum error found was " & Format(LowSSE, "#.#e###")
lblCurrentSeedActive.Caption = ""
lblCurrentSeedSlowly.Caption = ""
lblCurrentSeedReadily.Caption = ""

For inI = 1 To 8
    chkCellOn(inI).Enabled = True
    txtSeed(inI).Enabled = True
    txtVolume(inI).Enabled = True
Next inI

' return priority to normal
RetVal = SetPriorityClass(CurrentProcessHandle, Normal)

End Sub

```

```

Private Sub btnBrowse_Click()

On Error Resume Next

FileOpenDialog.ShowOpen
txtInputFile.Text = FileOpenDialog.FileName
txtInputFile.Refresh
btnLoad.Enabled = True

End Sub

Public Sub btnLoad_Click()

Dim i As Integer
Dim j As Byte
Dim k As Integer
Dim l As Byte
Const intHeaderLines As Byte = 16
Dim strHeader(1 To intHeaderLines) As String
Dim strInputFile As String
Dim strDummy As String
Dim sngMinAC As Single
Dim sngAC As Single
Dim sngAvg(1) As Single

' *****
' Read input file into sngRawData array as follows:
' Time goes into sngRawData(0,XXX)
' Cell 'i' goes into sngRawData(i,XXX)
' with XXX as the data point number
' *****

Open txtInputFile.Text For Input As #1
ReDim sngRawData(8, 0) ' for first index, 0 = time, 1 through 8 are data

' Load header into array "strHeader". This array is not used.

For i = 1 To intHeaderLines
    Line Input #1, strHeader(i)
Next i

' load remainder of file into "strRawData"

i = -1
Do
    i = i + 1
    ReDim Preserve sngRawData(8, i) 'counter for second sngRawData dimension
    Input #1, strDummy 'increase size of sngRawData
    For j = 0 To 8 'step past leading comma
        Input #1, sngRawData(j, i) 'counter for first sngRawData dimension
    Next j 'read and keep these data
    Input #1, strDummy, strDummy 'discard last two columns (raw time and date information)
Loop Until EOF(1)
Close #1 'close input file

' displays number of data points in the file
txtNumPoints = "Data file contains " & UBound(sngRawData, 2) & " points per sample, ending at " & _
    Format(sngRawData(0, UBound(sngRawData, 2)), "0") & " hours."
txtNumPoints.Visible = True
txtNumPoints.Refresh

If txtEndTime.Text <> "" Then
If Val(txtEndTime.Text) < sngRawData(0, UBound(sngRawData, 2)) + 1 Then
    Do
        ReDim Preserve sngRawData(8, UBound(sngRawData, 2) - 1)
        If UBound(sngRawData, 2) < 5 Then Exit Do
        Loop Until txtEndTime.Text > sngRawData(0, UBound(sngRawData, 2))
    End If
End If

txtEndTime.Text = Format(sngRawData(0, UBound(sngRawData, 2)), "0")

Call ConvertToOUR

sngOHO = txtBestSeedActive.Text
sngSlowly = txtBestSeedSlowly.Text
sngReadily = txtBestSeedReadily.Text

```

```

For i = 1 To 8
    If chkCellOn(i) Then Call ASM(i)
Next i

Call OURPlot
btnOptimize.Enabled = True
btnBrowse.Enabled = False
txtInputFile.Enabled = False

End Sub

' size and fill sngOURData array
Private Sub ConvertToOUR()

Dim i As Byte
Dim j As Integer
Dim k As Integer
Dim sngSampleSize As Single
Dim inIgnorePoints As Integer

' sngOURData contains the following:
' First index      Second Index
'      0           Time data
'      1-8         Measured OUR data
'      9-16        Estimated OUR data (decay, hydrolysis, growth processes)
'      17-40       dOUR values used for variance and covariance estimation
' reset the array first to clear any values in it
ReDim sngOURData(0, 0)
ReDim sngOURData(40, UBound(sngRawData, 2) - 1)

sngMaxOUR = 0
k = 0

inIgnorePoints = UBound(sngRawData, 2) \ 30 ' sets a number of points which may be over "MaxOUR" - used for
setting the scale of plots

' move time data into the OUR array
For j = 0 To (UBound(sngOURData, 2))
    sngOURData(0, j) = sngRawData(0, j)
Next j

' Raw data gets converted to OUR data
For i = 1 To 8
    sngSampleSize = txtVolume(i).Text / 1000
    ' convert raw data to OUR data
    For j = 0 To UBound(sngRawData, 2) - 1
        sngOURData(i, j) = ((sngRawData(i, (j + 1)) - sngRawData(i, j)) / _
            (sngSampleSize * (sngRawData(0, (j + 1)) - sngRawData(0, j)))) / 60
        ' keep track of the maximum OUR for plotting
        If sngOURData(i, j) > sngMaxOUR Then
            If k > inIgnorePoints Then
                sngMaxOUR = sngOURData(i, j)
                k = 0
            Else: k = k + 1
            End If
        End If
    Next j
Next i

' pick appropriate scale for y axis plots (moved from loadbutton_click procedure)
k = 0
If sngMaxOUR > 10 Then
    Do
        k = k + 1
        sngMaxOUR = sngMaxOUR / 10
    Loop Until sngMaxOUR < 10
Elseif sngMaxOUR < 1 Then
    Do
        k = k - 1
        sngMaxOUR = sngMaxOUR * 10
    Loop Until sngMaxOUR > 1
End If
If Int(sngMaxOUR) < sngMaxOUR Then sngMaxOUR = (Int(sngMaxOUR) + 1) * 10 ^ k

End Sub

```

```

Private Sub ASM(intSample As Integer)
' this subroutine estimates synthetic OUR according to ASMI - aerobic processes only.
' intSample should be 1 through 8 only during the least squares estimation of parameters

Dim Ss() As Single
Dim Xs() As Single
Dim Xbh() As Single
Dim So() As Single

Dim Growth As Single
Dim Decay As Single
Dim Hydrolysis As Single
Dim TimeStep As Single
Dim subTimeStep As Single
Const inDiv As Integer = 20

Dim inTime As Integer
Dim SeedAmt As Single
Dim TreatAmount As Single
Dim FiltTreatAmount As Single
Dim TotalVolume As Single
Dim inMaxTime As Integer 'the last time in minutes...
Dim inCounter As Integer

inMaxTime = sngOURData(0, UBound(sngOURData, 2)) * 60

ReDim Ss(inMaxTime)
ReDim Xs(inMaxTime)
ReDim Xbh(inMaxTime)
ReDim So(inMaxTime)

' for least squares estimation, intSample is 1-8
' for error estimation, it is 9-32
If intSample Mod 8 > 0 Then
SeedAmt = txtSeed(intSample Mod 8).Text
TotalVolume = txtVolume(intSample Mod 8).Text
Else
SeedAmt = txtSeed(8).Text
TotalVolume = txtVolume(8).Text
End If

inCounter = 0

Do While sngOURData(0, inCounter) < 1 / 60
inCounter = inCounter + 1
Loop

' No oxygen modeling (two other places as well):
So(0) = 3

'Seed samples based on input:
Ss(0) = (sngReadily * SeedAmt) / TotalVolume
Xs(0) = (sngSlowly * SeedAmt) / TotalVolume
Xbh(0) = (sngOHO * SeedAmt) / TotalVolume

' for error estimation, perturb the appropriate parameter
If intSample \ 8 = 1 Then Xbh(0) = Xbh(0) + 0.01
If intSample \ 8 = 2 Then Xs(0) = Xs(0) + 0.01
If intSample \ 8 = 3 Then Ss(0) = Ss(0) + 0.01

For inTime = 1 To inMaxTime

'Calculate growth, decay, and hydrolysis rates for this time step, based on last time step
' values. Rates are in terms of Xbh
' all in a one minute time step now. Saving only the ones that match with sngourdata time steps
Growth = sngMuh *
(Ss(inTime - 1) / (Ss(inTime - 1) + sngKs)) *
(So(inTime - 1) / (So(inTime - 1) + sngKoh)) * Xbh(inTime - 1)
Decay = sngBh * Xbh(inTime - 1)
Hydrolysis = sngKh * (Xs(inTime - 1) / Xbh(inTime - 1)) /
(sngKx + (Xs(inTime - 1) / Xbh(inTime - 1))) *
(So(inTime - 1) / (sngKoh + So(inTime - 1))) * Xbh(inTime - 1)
Ss(inTime) = Ss(inTime - 1) - Growth / sngYh + Hydrolysis
Xs(inTime) = Xs(inTime - 1) + Decay * (1 - sngFp) - Hydrolysis
Xbh(inTime) = Xbh(inTime - 1) + Growth - Decay
So(inTime) = 3

```

```

'if the time on the ASM model and the time on the OUR data are within one minute then put this
'value in the array
If Abs(sngOURData(0, inCounter) * 60 - inTime) < 1 Then
    sngOURData(8 + intSample, inCounter - 1) = ((1 - sngYh) / sngYh) * Growth
    inCounter = inCounter + 1
End If
If inCounter > UBound(sngOURData, 2) Then Exit For

Next inTime

sngOURData(8 + intSample, inCounter - 1) = 2 * sngOURData(8 + intSample, inCounter - 2) - sngOURData(8 +
intSample, inCounter - 3)

End Sub

Private Sub OURPlot()

Dim i As Byte
Dim j As Integer
Dim k As Byte
Dim sngxMax As Single
Const inNumlabels As Integer = 5

' pick appropriate scale for x axis (same scale for all eight output boxes)

sngxMax = (sngOURData(0, UBound(sngOURData, 2)))
j = 0
If sngxMax > 10 Then
    Do
        j = j + 1
        sngxMax = sngxMax / 10
    Loop Until sngxMax < 10
ElseIf sngxMax < 1 Then
    Do
        j = j - 1
        sngxMax = sngxMax * 10
    Loop Until sngxMax > 1
End If
If Int(sngxMax) < sngxMax Then sngxMax = (Int(sngxMax) + 1) * 10 ^ j

For k = 1 To 8

    ' scale output box
    picPlot(k).Cls
    picPlot(k).Scale (-0.45 * sngxMax, 1.05 * sngMaxOUR)-(1.05 * sngxMax, -0.25 * sngMaxOUR)

    ' plot and label axes
    ' x axis
    picPlot(k).Line (0, 0)-(sngxMax, 0)
    For i = 1 To inNumlabels + 1
        picPlot(k).Line ((i - 1) * sngxMax / inNumlabels, -0.01 * sngMaxOUR)-(sngxMax * (i - 1) /
inNumlabels, 0)
        picPlot(k).CurrentX = (i - 1.2) * sngxMax / inNumlabels
        picPlot(k).CurrentY = -0.03 * sngMaxOUR
        picPlot(k).Print (i - 1) * sngxMax / inNumlabels
    Next i
    picPlot(k).CurrentX = 0.4 * sngxMax
    picPlot(k).CurrentY = -0.12 * sngMaxOUR
    picPlot(k).Print "Time (hours)"

    ' y axis
    picPlot(k).Line (0, 0)-(0, sngMaxOUR)
    For i = 1 To inNumlabels + 1
        picPlot(k).Line (-0.01 * sngxMax, (i - 1) * sngMaxOUR / inNumlabels)-(0, (i - 1) * sngMaxOUR /
inNumlabels)
        picPlot(k).CurrentX = -0.15 * sngxMax
        picPlot(k).CurrentY = (i - 0.9) * sngMaxOUR / inNumlabels
        picPlot(k).Print (i - 1) * sngMaxOUR / inNumlabels
    Next i
    picPlot(k).CurrentX = -0.38 * sngxMax
    picPlot(k).CurrentY = 0.52 * sngMaxOUR
    picPlot(k).Print " OUR"
    picPlot(k).CurrentX = -0.43 * sngxMax
    picPlot(k).CurrentY = 0.45 * sngMaxOUR
    picPlot(k).Print "(mg/L/min)"

```

```

' plot the actual OUR data (not the most efficient way but easy to follow and fast enough)

If chkCellOn(k) Then
    For j = 0 To UBound(sngOURData, 2) - 1
        picPlot(k).Line (sngOURData(0, j), sngOURData(k, j))-(sngOURData(0, j + 1), sngOURData(k, j +
1))
        picPlot(k).Line (sngOURData(0, j), sngOURData(k + 8, j))-(sngOURData(0, j + 1), sngOURData(k +
8, j + 1)), vbRed
    Next j
Else
    For j = 0 To UBound(sngOURData, 2) - 1
        picPlot(k).Line (sngOURData(0, j), sngOURData(k, j))-(sngOURData(0, j + 1), sngOURData(k, j +
1)), vbGrayText
    Next j
End If

Next k

End Sub

Private Sub chkCellOn_Click(Index As Integer)

Call ASM(Index)
Call OURPlot

End Sub

Private Sub chkCellOff_Click(Index As Integer)

Call OURPlot

End Sub

Private Sub Form_Load()

txtInputFile.Text = "C:\\"

ReDim sngRawData(0, 0)
lblCurrentSeedActive = txtBestSeedActive.Text & " mg COD/L"
lblCurrentSeedReadily = txtBestSeedReadily.Text & " mg COD/L"
lblCurrentSeedSlowly = txtBestSeedSlowly.Text & " mg COD/L"

Label23.Caption = ""
Label23.ForeColor = vbBlue
lblCV3.Caption = ""
lblCV4.Caption = ""
lblCV5.Caption = ""
btnOptimize.Enabled = False
btnLoad.Enabled = False
btnInterrupt.Visible = False

CurrentProcessHandle = GetCurrentProcess

End Sub

Private Sub ValidateChkCell(SeedAmt As Single, TotalVol As Single, Quit As Boolean)

Dim inI As Integer
Dim inJ As Integer
Dim Qty(1 To 8) As Single
Dim Total(1 To 8) As Single
Dim NumCellsOn As Integer

NumCellsOn = 0
Quit = False
For inI = 1 To 8
    chkCellOn(inI).Enabled = False
    txtSeed(inI).Enabled = False
    txtVolume(inI).Enabled = False
    If chkCellOn(inI) Then
        NumCellsOn = NumCellsOn + 1
        Qty(inI) = txtSeed(inI).Text
        Total(inI) = txtSeed(inI).Text
        SeedAmt = Qty(inI)
        TotalVol = Total(inI)
    End If
Next inI

```

```

For inI = 1 To 8
  If chkCellOn(inI) Then
    For inJ = 1 To 8
      If chkCellOn(inJ) Then
        If Qty(inI) <> Qty(inJ) Then
          Call MsgBox("Selected cells must have the same seed volume", vbCritical, "Volume error")
          Quit = True
        End If
        If Total(inI) <> Total(inJ) Then
          Call MsgBox("Selected cells must have the same total volume", vbCritical, "Volume
error")
          Quit = True
        End If
      End If
    Next inJ
  End If
Next inI

If NumCellsOn = 0 Then
  Call MsgBox("You must select at least one cell to analyze", vbOKOnly, "No cell selected")
  Quit = True
End If

If Quit = True Then
  For inI = 1 To 8
    chkCellOn(inI).Enabled = True
    txtSeed(inI).Enabled = True
    txtVolume(inI).Enabled = True
  Next inI
End If

End Sub

Private Sub txtVolume_Validate(Index As Integer, Cancel As Boolean)

Call ConvertToOUR
Call OURPlot

End Sub

```

Appendix D – Measured data

Ultrasound treatment summary		Dose kJ/g TS	Solids (mg/L)						pH
Date	Source/notes		VSS	ISS	TSS	VS	IS	TS	
11-Feb-09	SBR3 sludge		11,800	2,467	14,267	12025	3225	15250	6.9
	Treated (20)	4.6	8,633	2,033	10,667	10950	3900	14850	6.6
	Treated (30)	6.6	7,286	1,998	9,283	11825	3425	15250	6.7
19-Feb-09	SBR3 sludge		9,850	4,400	14,250	8,025	7,475	15,500	7.1
	Treated (10)	2.1	8,667	3,800	12,467	4,475	9,375	13,850	7.3
	Treated (40)	7.7	6,950	3,050	10,000	4,250	8,700	12,950	7.3
26-Feb-09	SBR3 sludge (very poor settling)		8,700	2,317	11,017	7,775	4,700	12,475	
	Treated (8)	2.1	7,900	2,233	10,133	8,175	3,875	12,050	
	Treated (16)	4.4	6,700	2,000	8,700	7,700	4,725	12,425	
5-Mar-09	SBR3 sludge (poor settling)		7,300	2,483	9,783	6,525	4,750	11,275	
	Treated (15)	4.8	6,267	2,233	8,500	5,250	5,650	10,900	
	Treated (30)	9.6	4,450	1,817	6,267	4,350	5,475	9,825	
10-Mar-09	SBR2 sludge		4,500	1,225	5,725	4,100	3,225	7,325	
	Treated (15)	7.4	3,350	983	4,333	3,725	3,550	7,275	
	Treated (25)	12.1	2,817	1,000	3,817	3,600	3,800	7,400	
19-Mar-09	SBR3 sludge		11,467	2,900	14,367	10,800	4,750	15,550	7.0
	Treated (20)	4.2	8,767	2,667	11,433	10,525	4,600	15,125	7.2
	Treated (40)	8.5	7,100	2,200	9,300	10,450	4,975	15,425	7.3
23-Mar-09	SBR3 sludge		11,167	2,800	13,967	10,525	3,750	14,275	
	Treated (15)	3.7	9,533	2,167	11,700	10,600	4,000	14,600	
	Treated (60)	14.6	4,600	1,700	6,300	10,050	4,300	14,350	
30-Mar-09	SBR3 sludge		10,767	2,433	13,200	10,275	3,900	14,175	
	Treated (30)	7.4	6,467	1,800	8,267	10,100	4,225	14,325	
	Treated (45)	10.9	5,067	1,567	6,633	10,475	2,675	13,150	
7-Apr-09	SBR3 sludge (decant issue?)		9,300	2,567	11,867	8,550	4,250	12,800	
	Treated (30)	8.0	5,400	2,033	7,433	7,575	5,250	12,825	
	Treated (45)	12.0	4,767	1,767	6,533	7,525	5,200	12,725	
14-Apr-09	SBR1 sludge		10,900	4,100	15,000	11,350	5,625	16,975	6.8
	Treated (15)	2.9	9,750	4,350	14,100	11,275	5,325	16,600	6.7
	Treated (30)	5.8	7,827	3,207	11,033	10,425	5,725	16,150	6.7
20-Apr-09	SBR1 sludge		6,767	1,967	8,733	8,325	3,150	11,475	7.6
	Treated (15)	4.7	4,733	1,733	6,467	7,250	4,400	11,650	7.2
	Treated (30)	9.6	4,533	1,867	6,400	7,525	3,900	11,425	7.2
24-Apr-09	SBR4 sludge		6,267	1,533	7,800	5,925	2,525	8,450	7.2
	Treated (30)	11.3	3,967	1,233	5,200	5,375	3,025	8,400	6.9
	Treated (45)	18.9	2,933	1,133	4,067	5,400	3,625	9,025	7.1
29-Apr-09	SBR3 Sludge		11,200	4,067	15,267	9,575	4,675	14,250	6.9
	Treated (45)	12.7	5,567	3,067	8,633	9,325	4,400	13,725	6.8
	Treated (60)	15.7	5,567	3,033	8,600	11,300	4,900	16,200	7.1
6-May-09	SBR 4 Sludge		11,533	4,033	15,567	11,275	5,225	16,500	6.9
	Treated (15)	3	9,133	3,617	12,750	10,275	5,900	16,175	6.8
	treated (30)	7	7,200	3,333	10,533	10,325	5,350	15,675	7.0

Date	Dose kJ/g TS	COD mg/L			Respirometry mg COD/L		
		tCOD	sCOD	ffCOD	Heterotrophs (Z _h)	Slowly degradable (X _s)	Readily degradable (S _s)
11-Feb-09		20159	158	256	13310	899	337
	4.6	17784	2948	1565			
	6.6	21255	4659	2637	5503	5286	282
19-Feb-09		17,968	260	306			
	2.1	14,974	2,669	990			
	7.7	14,518	6,575	2,799			
26-Feb-09		19,335	254	195	2640	7009	234
	2.1	15,494	2,116	996			
	4.4	14,778	4,394	1,888	2246	5648	1011
5-Mar-09		11,523	120	88			
	4.8	11,334	2,613	1,001			
	9.6	12,152	4,219	2,015			
10-Mar-09		6,171	220	183			
	7.4	8,563	2,707	466			
	12.1	8,060	3,243	1,102			
19-Mar-09		16,371	183	233	15733	679	166
	4.2	17,378	3,935	1,058	5706	5038	1
	8.5	17,756	7,115	1,920			
23-Mar-09		17,001	201	227	12050	644	0
	3.7	17,882	5,446	1,240	7066	3509	0
	14.6	18,827	11,334	4,030			
30-Mar-09		17,882	183	201	11263	1123	206
	7.4	16,812	7,335	1,568			
	10.9	18,008	9,319	2,959	1284	4741	3060
7-Apr-09		14,480	99	124	8535	895	83
	8.0	14,542	6,497	2,005	1268	3737	2219
	12.0	14,975	7,364	1,299			
14-Apr-09		17,883	452	248	8657	1512	0
	2.9	22,153	2,908	650	2843	3767	1589
	5.8	17,945	5,043	928			
20-Apr-09		15,222	37	149	10688	1350	327
	4.7	8,539	4,486	1,473			
	9.6	4,889	6,497	7,240	1405	3621	2383
24-Apr-09		8,725	50	31	7260	535	288
	11.3	9,591	3,372	545	3239	2548	199
	18.9	10,458	5,291	588			
29-Apr-09		16,786	153	201	9802	9984	0
	12.7	18,312	8,179	2,442	2101	9348	6285
	15.7	18,556	9,583	2,808	1507	10011	4912
6-May-09		11,170	67	37	15003	5436	412
	3	12,513	4,059	507	7304	10117	188
	7	11,659	5,860	885	1750	9157	3803

Date	Dose kJ/g TS	Nitrogen mg/L (all as nitrogen)				
		NO ₃ -N	NO ₂ -N	TKN	sTKN	NH ₃ -N
11-Feb-09		2.5	8.4	202		4
	4.6	4.4	13.5	195		12
	6.6	6.8	23.7	200	0	17
19-Feb-09		4.4	0.9	215		0
	2.1			200	0	25
	7.7			195		39
26-Feb-09		2.8	2.7	249	135	23
	2.1	0.2	2.7	276	174	140
	4.4	0.3	2.9	339	296	392
5-Mar-09		0.6	0.0	126	24	17
	4.8	0.4	2.7	135	32	8
	9.6	0.8	3.2	147	18	8
10-Mar-09		4.6	1.6	305	68	74
	7.4	0.6	2.3	276	25	28
	12.1	0.5	2.1	275	22	72
19-Mar-09		24.7	6.0	409	38	7
	4.2	0.6	0.0	444	164	6
	8.5	2.8	0.0	219	129	10
23-Mar-09		112.5	1.9	428	20	5
	3.7	1.3	5.8	312	39	5
	14.6	0.9	0.0	295	108	17
30-Mar-09		57.9	4.1	432	23	0.2
	7.4	0.3	0.0	487	86	5
	10.9	1.5	0.0	188	70	10
7-Apr-09		0.0	0.0	330	8	0
	8.0	0.9	0.0	232	74	4
	12.0	0.5	0.0	225	61	3
14-Apr-09		0.0	0.0	370	56	22
	2.9	0.3	0.0	347	49	6
	5.8	0.0	0.0	314	49	7
20-Apr-09		0.2	0.0	304	13	4
	4.7	0.3	0.0	163	34	9
	9.6	0.5	1.5	181	53	6
24-Apr-09		42.2	16.8	327	52	6
	11.3	0.8	7.0	293	84	2
	18.9	0.8	3.5	296	88	3
29-Apr-09		15.6	5.2	399	7	
	12.7	0.0	0.0	345	112	
	15.7	0.1	0.0	365	126	
6-May-09		3.8	4.8	388	30	4
	3	0.0	0.0	545	246	21
	7	0.0	3.1	571	463	22

Ozone treatment summary		O₃ consumed mg	Solids mg/L					
Date	Source/treatment		VSS	ISS	TSS	VS	IS	TS
21-May-09	SBR 3 Sludge		4,510	1,580	6,090	3,695	3,155	6,850
	Treatment A		4,020	1,440	5,460	3,335	3,240	6,575
	Treatment B		4,120	1,450	5,570	3,210	3,430	6,640
9-Jun-09	SBR 3 Sludge		4,847	1,427	6,273	4,775	2,195	6,970
	Treatment C	448.1	1,700	613	2,313	2,430	1,505	3,935
	Treatment D	342.5	4,204	1,211	5,416	4,485	2,160	6,645
11-Jun-09	SBR 3 Sludge		5,320	3,293	8,613	5,275	4,490	9,765
	Treatment E	359.6	4,350	1,850	6,200	4,695	2,665	7,360
	Treatment F	280.8	4,233	2,633	6,867	4,565	3,265	7,830
24-Jun-09	Waterloo Sludge		4,942	1,163	6,105	5,170	1,615	6,785
	Treatment G	363.7	4,550	1,067	5,617	5,365	1,735	7,100
	Treatment H	69.6	4,944	1,008	5,953	5,460	1,715	7,175
30-Jun-09	SBR 3 Sludge		6,140	1,787	7,927	6,550	2,450	9,000
	Treatment I	233.2	5,267	1,587	6,853	5,935	2,345	8,280
	Treatment J	87.0	6,027	1,833	7,860	5,755	2,385	8,140
9-Jul-09	SBR 3 Sludge		7,467	2,040	9,507	8,070	2,880	10,950
	Treatment K	104.0	6,847	1,913	8,760	7,175	2,705	9,880
	Treatment L	57.3	7,233	1,967	9,200	7,505	2,670	10,175
14-Jul-09	SBR 3 Sludge		7,173	2,480	9,653	6,465	2,695	9,160
	Treatment M	235.6	6,033	2,156	8,189	5,245	3,165	8,410
	Treatment N	158.6	6,533	2,073	8,607	5,670	2,945	8,615
21-Jul-09	SBR 3 Sludge		4,360	947	5,307	4,240	1,680	5,920
	Treatment O	517.7	2,907	713	3,620	3,840	1,640	5,480
	Treatment P	222.6	3,440	793	4,233	3,930	1,590	5,520
28-Jul-09	SBR 3 Sludge		2,007	1,660	3,667	1,890	2,065	3,955
	Treatment Q	369.9	1,060	1,500	2,560	1,505	2,060	3,565
	Treatment R	240.3	1,147	1,407	2,553	1,475	2,025	3,500
6-Aug-09	SBR 3 Sludge		2,693	913	3,607	2,960	1,885	4,845
	Treatment S	184.8	1,240	500	1,740	1,745	1,520	3,265
	Treatment T	168.7	2,160	813	2,973	2,290	1,750	4,040
11-Aug-09	SBR 3 Sludge		3,513	947	4,460	3,545	1,615	5,160
	Treatment U		1,887	560	2,447	2,230	1,250	3,480
	Treatment V		3,060	900	3,960	3,135	1,530	4,665
20-Aug-09	SBR 3 Sludge		4,560	1,000	5,560	4,350	1,620	5,970
	Treatment W	61.9	4,140	873	5,013	4,460	1,610	6,070
	Treatment X	64.6	4,187	733	4,920	4,420	1,570	5,990
27-Aug-09	SBR 3 Sludge		2,280	413	2,693	2,420	980	3,400
	Treatment Y	41.5	1,847	400	2,247	2,010	1,020	3,030
	Treatment Z	34.6	1,660	340	2,000	1,850	970	2,820

Date	O ₃ consumed mg	COD mg/L			Respirometry mg COD/L		
		tCOD	sCOD	ffCOD	Z _h	X _s	S _s
21-May-09		6,045	13	13			
		6,568	437	396			
		6,594	720	769			
9-Jun-09	448.1						
	342.5						
11-Jun-09		6,378	186	199			
	359.6	6,902	216	157			
	280.8	6,738	1,439	1,086			
24-Jun-09		10,047	645	695			
	363.7	10,523	1,287	1,067			
	69.6	10,206	925	858			
30-Jun-09		9,794	33	33			
	233.2	9,952	1,002	771			
	87.0	9,857	425	359			
9-Jul-09		9,667	93	95	1258	186.9	0
	104.0	9,984	628	346	1801	234.7	0
	57.3	11,474	609	666	1383	166.6	0
14-Jul-09		11,854	62	117			
	235.6	12,900	1,388	1,204			
	158.6	11,410	1,078	958			
21-Jul-09		6,814	37	47	2426	0	46
	517.7	6,593	1,826	957	19	2241	652.8
	222.6	7,068	932	583	112	2090	678
28-Jul-09		3,486	35	23	2053	7.2	8.6
	369.9	2,567	1,090	475	14	865.8	273
	240.3	2,662	856	406	22.6	849.6	341.2
6-Aug-09		4,184	58	49	1108	1147	0
	184.8	2,789	761	330	30	767	485
	168.7	3,930	691	363	64	1129	637
11-Aug-09		7,226	29	0	3083	32	59
		3,645	197	266	2244	69	2
		5,198	387	203	2972	43	54
20-Aug-09		9,192	70	81			
	61.9	9,350	697	482			
	64.6	8,051	666	408			
27-Aug-09		3,455	22	28	1834	150.1	0.1
	41.5	2,948	311	177	529.2	1024	40.6
	34.6	2,726	304	147	423.8	941.7	46.4

Date	O ₃ consumed mg	Nitrogen mg/L					pH
		NO ₃ -N	NO ₂ -N	TKN	sTKN	NH ₃ -N	
21-May-09		0.1	0.0	352	12	4	
		0.0	0.5	359	57	31	
		0.0	0.0	379	83	43	
9-Jun-09		0.0	3.4		11	0	7.0
	448.1	36.5	1.8	222	102	8	6.6
	342.5	0.0	0.0	442	73	23	6.3
11-Jun-09		0.2	0.0		17	3	
	359.6	0.0	0.0	453	90	14	
	280.8	0.1	0.0	494	89	23	
24-Jun-09		0.1	0.0	347	44	18	5.1
	363.7	3.1	1.9	335	69	15	4.6
	69.6	0.1	0.0	332	51	17	5.3
30-Jun-09		0.2	0.0	625	31	3	7.4
	233.2	0.2	0.0	588	76	3	6.9
	87.0	0.2	0.0	635	59	4	7.3
9-Jul-09		0.2	0.0	749	31	21	7.3
	104.0	0.1	0.0	714	87	26	7.3
	57.3	0.3	0.0	749	61	25	7.5
14-Jul-09		0.3	0.0	677	66	11	7.4
	235.6	6.3	1.4	693	145	12	6.7
	158.6	0.3	0.0	693	133	18	6.9
21-Jul-09		3.4	4.9	385	48	2	7.4
	517.7	50.8	2.4	390	120	4	6.9
	222.6	26.9	1.8	378	75	4	7.2
28-Jul-09		11.8	2.6	202	35	2	7.5
	369.9	49.5	3.3	198	74	3	6.9
	240.3	39.9	1.9	186	63	3	7.1
6-Aug-09		13.6	17.3	292	48	5	7.5
	184.8	60.6	2.6	209	74	4	7.0
	168.7	56.2	3.8	266	61	4	7.2
11-Aug-09		12.6	4.7	332	31	2	7.3
		16.0	6.2	203	47	3	7.2
		0.3	8.2	322	52	4	7.2
20-Aug-09		0.2	0.0	455	76	14	7.5
	61.9	0.2	0.0	427	91	15	7.5
	64.6	0.1	0.0	421	95	13	7.5
27-Aug-09		38.4	6.4	242	60	2	7.4
	41.5	45.6	4.1	215	67	3	7.5
	34.6	44.7	4.3	198	66	2	7.7